Award Number: W81XWH-10-1-0461

TITLE: Characterization and targeting of the aldehyde dehydrogenase subpopulation in ovarian cancer

PRINCIPAL INVESTIGATOR: Charles N. Landen, Jr., M.D., M.S.

CONTRACTING ORGANIZATION: University of Alabama at Birmingham
Birmingham, AL 35249

REPORT DATE: July 2013

TYPE OF REPORT: Annual

PREPARED FOR: U.S. Army Medical Research and Materiel Command
Fort Detrick, Maryland 21702-5012

REPORT DOCUMENTATION PAGE

Form Approved
OMB No. 0704-0188

1. REPORT DATE	2. REPORT TYPE	3. DATES COVERED
July 2013	Annual	1 July 2012 – 30 June 2013

4. TITLE AND SUBTITLE
Characterization and targeting of the aldehyde dehydrogenase subpopulation in ovarian cancer

5a. CONTRACT NUMBER

5b. GRANT NUMBER
W81XWH-10-1-0461

5c. PROGRAM ELEMENT NUMBER

6. AUTHOR(S)
Charles N. Landen, Jr., M.D., M.S.

E-Mail: clanden@uab.edu

5d. PROJECT NUMBER

5e. TASK NUMBER

5f. WORK UNIT NUMBER

7. PERFORMING ORGANIZATION NAME(S) AND ADDRESS(ES)
University of Alabama at Birmingham
Birmingham, AL 35249

8. PERFORMING ORGANIZATION REPORT NUMBER

9. SPONSORING / MONITORING AGENCY NAME(S) AND ADDRESS(ES)
U.S. Army Medical Research and Materiel Command
Fort Detrick, Maryland 21702-5012

10. SPONSOR/MONITOR'S ACRONYM(S)

11. SPONSOR/MONITOR'S REPORT NUMBER(S)

12. DISTRIBUTION / AVAILABILITY STATEMENT
Approved for Public Release; Distribution Unlimited

13. SUPPLEMENTARY NOTES

14. ABSTRACT

Despite a common outstanding response to primary therapy, most ovarian cancer patients will experience recurrence due to what is often microscopic undetectable disease. One possible cause of this is a chemoresistant population of cells with stem cell characteristics. We have examined one potential population in particular, the ALDH-positive population. We have shown that ALDH1A1-positive cells are more tumorigenic than ALDH1A1-negative cells, contribute to poor patient outcomes, and contribute to chemoresistance. These effects can be reversed by downregulating ALDH1A1 expression with nanoparticle-delivered siRNA. Additionally, we have shown that CSCs are clinically significant, in that chemoresistant tumors have increased density of ALDH and CD133 cells. Importantly, they do not seem to explain the entire story, as there are still many CSC-negative cells present at the conclusion of treatment. Specifically, endoglin (CD105) and hedgehog family members (Gli1 and Gli2) appear to play important roles in chemotherapy resistance, and when targeted enhance response to chemotherapy. To further identify other important players, we have further developed the patient-derived xenograft (PDX) model where patient samples are directly implanted into mice, and when formed, treated with chemotherapy. The treated tumors, like patient specimens, are enriched with ALDH1-positive cells. Further characterization of the surviving population is underway, in conjunction with separately-funded protocols.

15. SUBJECT TERMS
Ovarian Cancer, aldehyde dehydrogenase, ALDH1A1, cancer stem cell

16. SECURITY CLASSIFICATION OF:			17. LIMITATION OF ABSTRACT	18. NUMBER OF PAGES	19a. NAME OF RESPONSIBLE PERSON
a. REPORT	b. ABSTRACT	c. THIS PAGE			USAMRMC
U	U	U	UU	69	19b. TELEPHONE NUMBER *(include area code)*

Table of Contents

	Page
Introduction……..	**1**
Body……..	**1**
Key Research Accomplishments……..	**6**
Reportable Outcomes……	**7**
Conclusions……	**11**
References……	**12**
Appendices……	**12**

Characterization and targeting of the ALDH subpopulation in ovarian cancer

Charles N. Landen, Jr., MD, MS
University of Alabama at Birmingham, Birmingham, AL
Ovarian Cancer Academy OC093443 July 2012- June 2013 Annual Report

INTRODUCTION:

While most ovarian cancer patients initially respond to chemotherapy, most will ultimately recur and succumb to disease, suggesting that there is a subpopulation of cells within a heterogeneous tumor that has either inherent or acquired resistance to chemotherapy[1]. Recently subpopulations of cancer cells in solid tumors have been observed to have properties of stem cells, and therefore designated as "cancer stem cells" (CSC's) or tumor initiating cells (TIC's)[2,3]. The intent of this project is to characterize whether ovarian cells that express aldehyde dehydrogenase (ALDH1A1) have cancer stem cell properties, and if targeting ALDH1A1 would lead to a reversal of the chemoresistant properties. Characteristics of cancer stem cell that will be assessed include tumorigenicity experiments, evidence of multipotentiality, and enhanced resistance to chemotherapeutics. The effects of ALDH1A1 downregulation will be determined both *in vitro* and *in vivo*, using small interfering RNA (siRNA) encapsulated in nanoparticles that allow efficient *in vivo* delivery. If our hypotheses are confirmed, we will have identified a subpopulation of ovarian cancer cells that might survive initial chemotherapy and contribute to resistance, and furthermore may find a clinically feasible novel methodology to target these cells to improve outcomes in this devastating disease. If ALDH1 cells are not explaining the full population of chemoresistant cells, these studies will provide the opportunity to more fully characterize which cells are mediating survival of primary therapy.

BODY:

Task 1: Determine tumorigenicity of ALDH1A1 subpopulations

The goal of task 1 was to determine the tumorigenicity of ALDH1A1 subpopulations. In a prior annual report, we described results published in Molecular Cancer Therapeutics[4] showing tumorigenicity of ALDH1A1-positive cells compared to ALDH1A1-negative cells from the A2780cp20 cell line.

Task 2: Determine if ALDH1-positive cells survive chemotherapy in the tumor microenvironment.

We have previously reported on performed IHC on these for ALDH1, CD44, and CD133 to determine whether recurrent tumors, which are generally more chemoresistant, are predominantly composed of these populations. We found that tumors collected immediate after receiving primary therapy, the time at which cells surviving would ultimately cause recurrent disease, were higher in both ALDH1 (2-fold) and CD133 (24-fold) cells.

To examine whether this is also noted in a setting where chemotherapy administration and tumor collection is more controlled, we have established protocols for development of primary xenografts in SCID mice, termed "patient-derived xenografts" (PDX). We previously reported that growth in the subcutaneous site was most efficient. We have continued to establish

PDX tumors, and now have approximately 42 patients in whom PDX tumors have been established, propagated, and stored. Previously we reported that they are histologically similar and respond to chemotherapy similar to patients. In the last year we have further evaluated whether these PDX tumors have similar expression profiles as the tumor from which they were derived. We performed a quantitative PCR array for 84 oncogenes that are recognized targets for therapy, on 4 pair of PDX tumors and patient tumors. There was not a significant difference in gene expression in 79 of the cancer drug target genes, with an overall R^2-value of .7441 (Figure 1). 5 genes had a decrease in expression in the PDX sample when compared to the patient specimen. These genes were PDGFRA, PDGFRB, FLT1, KDR and FLT4. All of these genes would be expected to be decreased in the PDX tumor, since they are genes produced by the host, and the primers for qPCR are human-specific. If these genes are removed from the analysis and only tumor cell-specific gene expression is considered, the R^2-value increases to 0.8891. Therefore, while the PDX model may not be ideal for targeting proteins expressed by stromal cells, overall there is consistency in expression of targetable oncogenes, supporting use of the model for drug development.

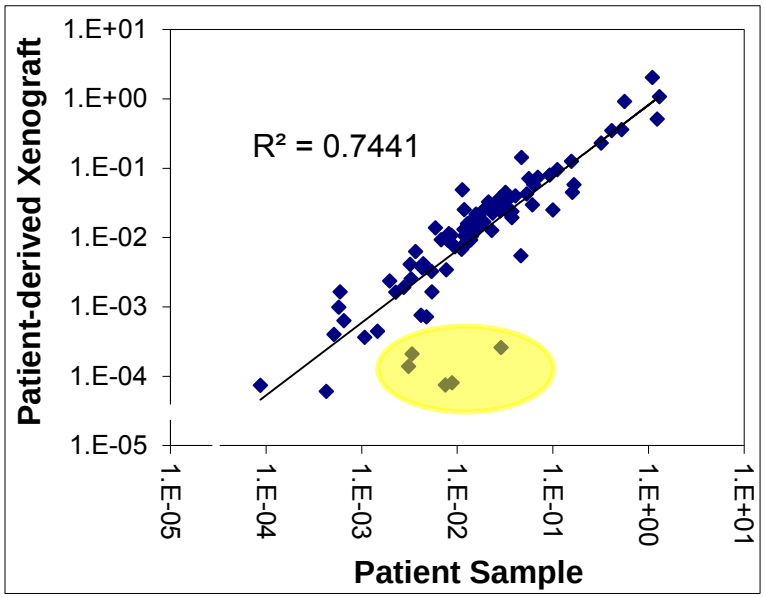

Figure 1. Quantitative PCR array comparing PDX tumors and human samples

With the model validated, we turned our attention to changes in tumors with chemotherapy treatment, in an effort to identify pathways contributing to chemoresistance. In order to determine whether putative cancer stem cells are enriched in treated samples, we previously reported that on average, there was a significant increase in ALDH1 and CD133-positive CSCs comprising treated tumors. CD44 was only increased in two tumors, and not significant overall. These are consistent with findings from patient tumors. However, it is important to note that treated tumors are not composed of ONLY these cells. Therefore in the last year we have subjected untreated and treated PDX tumors to RNASeq analysis, and in pairwise fashion examined the genes and pathways changing with chemotherapy treatment, either by enrichment of the surviving population, or induced by chemotherapy exposure. Initially

6 pair of tumors have been sequenced and analyzed (support for sequencing provided in a separate grant, not funded by this grant, but work is related).

Initially, analysis of all 6 tumor pairs together only found 85 genes that were, on average, significantly different when comparing the 6 treated and untreated tumors. However, when subjected to pathway analysis with IPA software, some very interesting trends are apparent (Table 1). Several pathways are indeed significant altered among several tumors. These include EIF2 signaling (the #1 pathway in 4 of the 6 pair), mTOR signaling, antigen presentation, protein ubiquitination, mitochondrial dysfunction, glycolysis, and remodeling of epithelial adherens junctions.

Table 1. Pathways significantly altered in PDX tumors treated with chemotherapy.

Tumor 106	
Ingenuity Canonical Pathways	**fold increase**
EIF2 Signaling	47.40
Regulation of eIF4 and p70S6K Signaling	15.40
mTOR Signaling	15.20
Antigen Presentation Pathway	9.85
Protein Ubiquitination Pathway	6.44
Mitochondrial Dysfunction	5.20
Remodeling of Epithelial Adherens Junctions	5.11
Atherosclerosis Signaling	4.92
RhoGDI Signaling	3.66
Clathrin-mediated Endocytosis Signaling	3.64

Tumor 108	
Ingenuity Canonical Pathways	**fold increase**
EIF2 Signaling	7.75
Mitochondrial Dysfunction	6.85
Protein Ubiquitination Pathway	6.12
Glycolysis I	5.69
mTOR Signaling	3.45
Aryl Hydrocarbon Receptor Signaling	2.95
Regulation of eIF4 and p70S6K Signaling	2.69
Superpathway of Serine and Glycine Biosynthesis I	2.69
4-hydroxyproline Degradation I	2.63
Cell Cycle: G1/S Checkpoint Regulation	2.60

Tumor 115	
Ingenuity Canonical Pathways	**fold increase**
Role of NFAT in Regulation of the Immune Response	3.26
Ephrin A Signaling	3.20
PKCθ Signaling in T Lymphocytes	2.59
Systemic Lupus Erythematosus Signaling	2.08
Axonal Guidance Signaling	2.08
Pentose Phosphate Pathway (Oxidative Branch)	2.03
G Protein Signaling Mediated by Tubby	2.00
Complement System	2.00
Calcium-induced T Lymphocyte Apoptosis	1.91
Antiproliferative Role of Somatostatin Receptor 2	1.87

Tumor 116	
Ingenuity Canonical Pathways	**fold increase**
EIF2 Signaling	70.90
mTOR Signaling	24.80
Regulation of eIF4 and p70S6K Signaling	23.90
Mitochondrial Dysfunction	9.90
Antigen Presentation Pathway	5.92
Complement System	4.61
Remodeling of Epithelial Adherens Junctions	4.56
Glutathione Redox Reactions I	4.10
Crosstalk between Dendritic Cells and Natural Killer Cells	3.89
Regulation of Actin-based Motility by Rho	3.69

Tumor 121	
Ingenuity Canonical Pathways	**fold increase**
EIF2 Signaling	64.90
Regulation of eIF4 and p70S6K Signaling	24.50
mTOR Signaling	21.00
Mitochondrial Dysfunction	7.67
RhoGDI Signaling	5.66
Protein Ubiquitination Pathway	5.62
Epithelial Adherens Junction Signaling	5.36
Remodeling of Epithelial Adherens Junctions	5.16
Glycolysis I	4.51
Antigen Presentation Pathway	4.11

Tumor 136	
Ingenuity Canonical Pathways	**fold increase**
Atherosclerosis Signaling	13.00
LXR/RXR Activation	12.10
Altered T Cell and B Cell Signaling in Rheumatoid Arthritis	8.83
Hepatic Fibrosis / Hepatic Stellate Cell Activation	8.37
Crosstalk between Dendritic Cells and Natural Killer Cells	7.76
Coagulation System	7.58
Dendritic Cell Maturation	7.45
B Cell Development	7.01
Inhibition of Matrix Metalloproteases	6.99
T Helper Cell Differentiation	6.37

Intriguingly, it was the same 4 tumors in which these pathways were altered, suggesting either a link between them, or duplication of family members leading to their reveal as important. In the other two pair, most of the pathways significantly altered were participants in the immune system. Therefore, not only are several pathways in common among the multiple pair, there appears to be a dichotomy, whereby one family of tumors may respond to chemo with one set of pathways relating to metabolism and controls on translation/transcription/protein turnover, and the other through the immune system. Additional work is required to validate these findings, and identify ways to target the system to enhance chemotherapy response.

Task 3: Target ALDH1 with siRNA *in vivo*

We previously reported use of a method for delivery of siRNA *in vivo* using DOPC nanoparticles to target ALDH1A1 in vivo. Immunohistochemical analysis confirmed reduced ALDH1A1 expression with ALDH1A1-siRNA/DOPC treatment compared to controls but not with chemotherapy alone. The combination of ALDH1A1 siRNA and docetaxel resulted in significantly reduced growth, by 93.6% compared to control siRNA ($p<0.001$), by 89.8% compared to docetaxel plus control siRNA ($p=0.003$), and by 91.4% compared to ALDH1A1 siRNA ($p=0.002$).

Task 4: Evaluate mechanisms of ALDH1-mediated chemoresistance

We previously reported completion of microarray studies performed on ALDH1-positive and negative populations in order to identify which pathways may be overexpressed and targetable. In conjunction with this list, as well as genes identified in stem cell pathway analysis of patient primary/recurrent pair, two genes have been further characterized for their contribution to chemotherapy resistance.

First, the endoglin pathway was evaluated. Endoglin expression was intriguing, as it had previously only been known to be expressed in developing endothelial cells. Therefore, Western blot and qPCR were used to evaluate endoglin expression in multiple ovarian cancer lines. Anti-endoglin siRNAs were used to downregulate expression in ES2 and HeyA8MDR. In vitro, the effects of endoglin-knockdown individually and with chemotherapy were evaluated by MTT assay, cell-cycle analysis, alkaline comet assay, and γ-H2AX foci formation. In vivo, mice inoculated with ES2 or HeyA8MDR cell lines were administered chitosan-encapsulated anti-ENG siRNA or control siRNA with and without carboplatin.

As described in the accompanying manuscript, endoglin was indeed highly expressed in at least 4 ovarian cancer cell lines (Figure 2). Inhibition of endoglin expression with siRNA significantly decreased cell viability (by 50%, $p<0.001$, and 84%, $p<0.001$, respectively), increased apoptosis, induced double-stranded DNA damage, and increased cisplatin sensitivity. In an orthotopic mouse model, anti-endoglin treatment decreased tumor weight in both ES2 and HeyA8MDR models when compared to control (41.2% reduction, $p=0.001$; and 35.6% reduction, $p=0.014$; respectively, Figure 3). Endoglin inhibition with carboplatin administration was associated with even greater response when compared to control (61.2% and 57.7% reduction, $p<0.001$ for both).

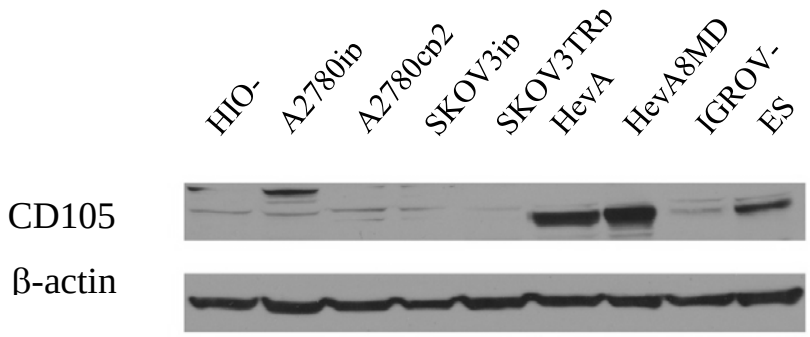

Figure 2. Expression of CD105 (endoglin) in ovarian cancer cell lines.

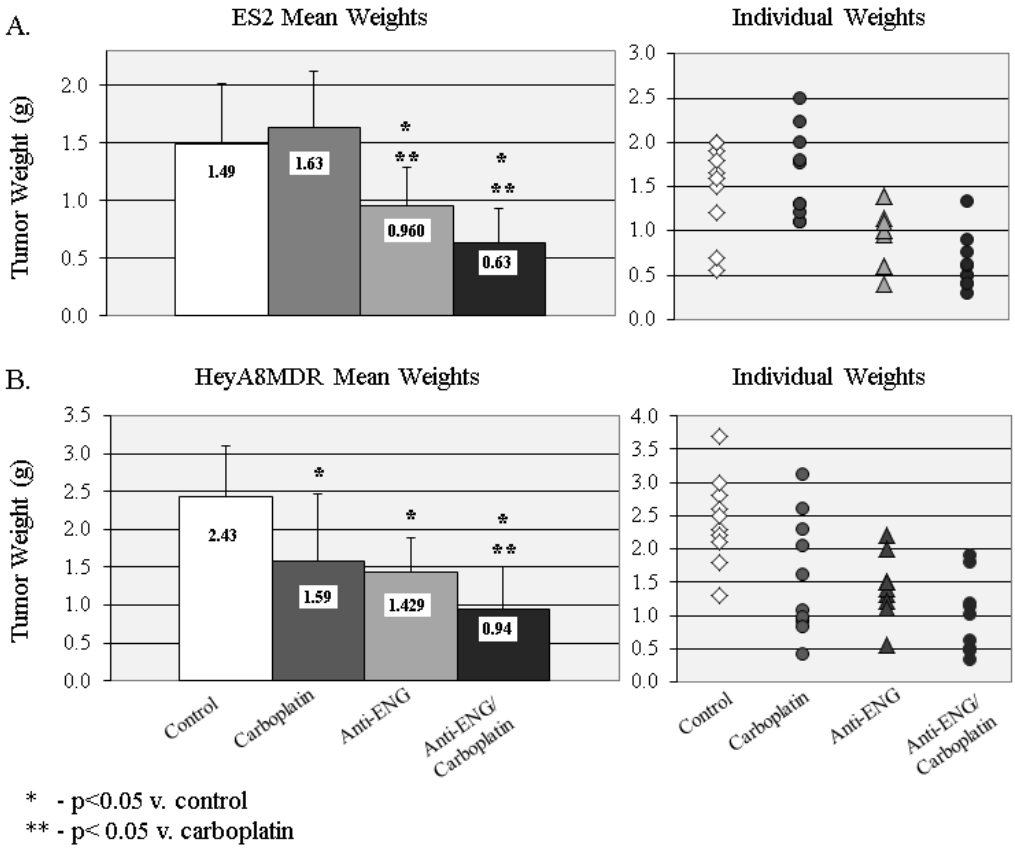

Figure 3. SiRNA-mediated downregulation of CD105 (endoglin) in orthotopic models of ovarian cancer – ES2 (A) and HeyA8MDR (B).

In parallel, the Hedgehog pathway was examined for its potential in chemotherapy resistance. The hedgehog (HH) pathway has been implicated in the formation and maintenance of a variety of malignancies, including ovarian cancer; however, it is unknown whether HH signaling is involved in ovarian cancer chemoresistance. The goal of this investigation was to determine the effects of antagonizing the HH receptor, Smoothened (Smo), on chemotherapy response in ovarian cancer. As reported in the accompanying manuscript, expression of HH pathway

members was assessed in 3 pairs of parental and chemotherapy-resistant ovarian cancer cell lines (A2780ip2/A2780cp20, SKOV3ip1/SKOV3TRip2, HeyA8/HeyA8MDR) using qPCR and Western blot. Cell lines were exposed to increasing concentrations of two different Smo antagonists (cyclopamine, LDE225) alone and in combination with carboplatin or paclitaxel. Selective knockdown of Smo, Gli1 or Gli2 was achieved using siRNA constructs. Cell viability was assessed by MTT assay. A2780cp20 and SKOV3TRip2 orthotopic xenografts were treated with vehicle, LDE225, paclitaxel or combination therapy. Chemoresistant cell lines demonstrated higher expression (>2-fold, $p<0.05$) of HH signaling components compared to their respective parental lines. Smo antagonists sensitized chemotherapy-resistant cell lines to paclitaxel (Figure 4A), but not to carboplatin (data not shown). With treatment, cells had a profound G2 phase arrest (Figure 4B-C). LDE225 treatment also increased sensitivity of ALDH-positive cells to paclitaxel. A2780cp20 and SKOV3TRip2 xenografts treated with combined LDE225 and paclitaxel had significantly less tumor burden than those treated with vehicle or either agent alone. Increased taxane sensitivity appeared to be mediated by a decrease in P-glycoprotein (MDR1) expression. Selective knockdown of Smo, Gli1 or Gli2 all increased taxane sensitivity. Smo antagonists reverse taxane resistance in chemoresistant ovarian cancer models, suggesting combined anti-HH and chemotherapies could provide a useful therapeutic strategy for ovarian cancer

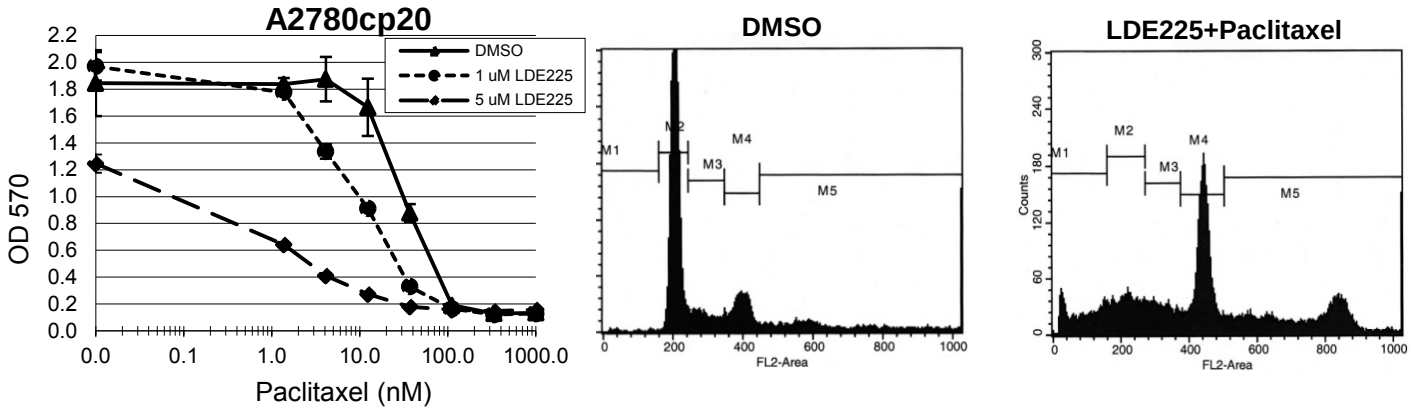

Figure 4. (A) Treatment of the chemoresistant cell line A2780cp20 with LDE225 sensitized cells to paclitaxel, and (B,C) led to a dramatic phase G2 arrest

KEY RESEARCH ACCOMPLISHMENTS:

- ALDH-positive cells from the A2780cp20 and SKOV3TRip2 cell lines have approximately 50-fold increased tumorigenicity compared to ALDH-negative cells.
- Tumors treated with chemotherapy are enriched in the ALDH1 And CD133 CSC population, compared to matched samples collected prior to therapy.
- Efficient establishment of primary xenografts directly from patient tumors is feasible, and mimic patient tumors in histologic make-up, CSC density, and response to chemotherapy.
- Xenograft tumors from mice treated with chemotherapy are similarly enriched in ALDH1 and CD133 CSCs.

- Treatment of tumor-bearing mice with ALDH1A1-targeting siRNA in DOPC sensitized normally-resistant cell lines to cisplatin or paclitaxel.
- Stem cell pathway genes endoglin and hedgehog mediators Gli1 and Gli2 contribute to chemotherapy resistance, and targeting these genes restores sensitivity to chemotherapy.

REPORTABLE OUTCOMES:

- Publications:

1. Steg AS, Bevis KS, Katre AA, Ziebarth A, Alvarez RD, Zhang K, Conner M, **Landen CN**. Stem cell pathways contribute to clinical chemoresistance in ovarian cancer. *Clin Can Res*, 18(3):869-81, 2012.
2. Stone RL, Nick AM, McNeish IA, Balkwill F, Han HD, Bottsford-Miller J, Rupaimoole R, Armaiz-Pena GN, Pecot CV, Coward J, Deavers MT, Vasquez HG, Urbauer D, **Landen CN**, Wei H, Gershenson H, Matsuo K, Shahzad MMK, King ER, Tekedereli I, Ozpolat B, Ahn EH, Bond VK, Wang R, Drew AF, Gushiken F, Collins K, DeGeest K, Lutgendorf SK, Chiu W, Lopez-Berestein G, Afshar-Kharghan V, Sood AK. Paraneoplastic Thrombocytosis in Ovarian Cancer. *NEJM*, 366(7): 610-8, 2012.
3. Ziebarth AJ, **Landen CN** Jr, Alvarez RD. Molecular/genetic therapies in ovarian cancer: future opportunities and challenges. *Clin Obstet Gynecol*, 55(1):156-72, 2012.
4. Kim KK, Zsebik GN, Straughn JM, **Landen CN**. Management of Complex Pelvic Masses Using a Multivariate Index Assay: A Decision Analysis. *Gyn Onc*, 126(3): 364-8, 2012.
5. Steg AS, Katre AA, Bevis KS, Ziebarth A, Dobbin ZC, Shah MS, Alvarez RD, **Landen CN**. Smoothened Antagonists Reverse Taxane Resistance in Ovarian Cancer. *Mol Cancer Ther*, 11(7): 1587-97, 2012. †
6. Qin Y, Xu J, Aysola K, Oprea G, Reddy A, Matthews R, Okoli J, Cantor A, Grizzle WE, Partridge EE, Reddy ESP, **Landen CN**, and Rao VN. BRCA1 Proteins Regulate Growth of Ovarian Cancer Cells by Tethering Ubc9. *Am J Can Res*, 2(5): 540-8, 2012.
7. Li H, Cai Q, Wu H, Vathipadiekal V, Dobbin ZC, Li T, Hua X, **Landen CN**, Birrer MJ, Sánchez-Beato M, Zhang R. SUZ12 promotes human epithelial ovarian cancer by suppressing apoptosis via silencing HRK. *Mol Can Res*, 10(11): 1462-72, 2012.
8. Ziebarth AJ, Nowsheen S, Steg AS, Shah MM, Katre AA, Dobbin ZC, Han HD, Lopez-Berestein G, Sood AK, Conner MG, Yang ES, **Landen CN**. Endoglin (CD105) contributes to platinum resistance and is a target for tumor-specific therapy in epithelial ovarian cancer. *Clin Can Res*, 19(1): 170-82, 2013.
9. Chen H, **Landen CN**, Li Y, Alvarez RD, Tollefsbol TO. Epigallocatechin Gallate and Sulforaphane Combination Treatment Induce Apoptosis in Paclitaxel-Resistant Ovarian Cancer Cells through hTERT and Bcl-2 Down-regulation. *Exp Cell Res*, 319(5): 697-706, 2013.

10. Chen H, **Landen CN**, Li Y, Alvarez RD, Tollefsbol TO. Enhancement of Cisplatin-mediated Apoptosis in Ovarian Cancer Cells through Potentiating G2/M Arrest and p21 Upregulation by Combinatorial Epigallocatechin Gallate and Sulforaphane. *J Oncol,* 2013: 872957, 2013.
11. Schultz MJ, Swindall AF, Wright JW, Sztul ES, **Landen CN**, Bellis SL. ST6Gal-I sialyltransferase confers cisplatin resistance in ovarian tumor cells. *J Ovar Res,* 6(1): 25, 2013.
12. Erickson BK, Conner MG, **Landen CN Jr**. The Role of the Fallopian Tube in the Origin of Ovarian Cancer. *Am J Obstet Gynecol, in press*.
13. Dobbin ZA, **Landen CN**. The importance of the PI3K/AKT/mTOR pathway in the progression of ovarian cancer. *Int J Mol Sciences*, *in press*.
14. **Landen CN** and Lengyl E. Summary of the 2013 American Association for Cancer Research (AACR) Annual Meeting. *Gyn Onc, in press*.

- Abstracts presented:

1. Ziebarth A, Steg AD, Katre AA, Zhang K, Nowsheen S, Yang HS, Connor M, Lopez-Berestein G, Sood AK, and **Landen CN**. Targeting Endoglin (CD105) induces apoptosis, improves platinum sensitivity both in vivo and in vitro, and is a potential therapeutic target in epithelial ovarian cancer. *9th International Conference on Ovarian Cancer*, MD Anderson Cancer Center, Houston, TX, 2011. Oral presentation.
2. Ziebarth A, Steg AD, Katre AA, Zhang K, Nowsheen S, Yang SH, Connor MG, Lopez-Berestein G, Sood AK, **Landen CN**. A novel role for the TGF-β co-receptor endoglin (CD105) in platinum resistant epithelial ovarian cancer. *43rd Annual Society of Gynecologic Oncologists Meeting*, 2012.
3. Ziebarth A, Dobbin ZC, Katre AA, Steg AD, Alvarez RD, Conner MG, and **Landen CN**. Primary ovarian cancer murine xenografts maintain tumor heterogeneity and biologically correlate with patient response to primary chemotherapy. *43rd Annual Society of Gynecologic Oncologists Meeting*, 2012.
4. Yang E, Nowsheen S, Cooper T, **Landen CN**, Bonner J. Poly (ADP-Ribose) Polymerase Inhibition Attenuates Radiation-Induced Non-Homologous End-Joining Repair and Augments Cervical Cancer Response to Radiation. *43rd Annual Society of Gynecologic Oncologists Meeting*, 2012.
5. Kim KH, Bevis KS, Walsh-Covarrubias J, Alvarez RD, Straughn JM, **Landen CN**. Optimizing the Research Experience in Gynecologic Oncology Fellowships. *43rd Annual Society of Gynecologic Oncologists Meeting*, 2012.
6. Dobbin ZC, Katre AA, Ziebarth A, Shah MM, Steg AD, Alvarez RD, Conner MG, **Landen** CN. An Optimized Primary Ovarian Cancer Xenograft Model Mimics Patient Tumor Biology and Heterogeneity. *Ovarian Cancer: Prevention, Detection and Treatment of the Disease and its Recurrence*, Pittsburg, PA, 2012. §

7. Zimmerman J, Crittenden F, **Landen CN**, Alvarez RD, Brezovich I, Kuster N, Costa F, Barbault A, Pasche B. Amplitude Modulated Radiofrequency Electromagnetic Fields as a Novel Treatment for Ovarian Cancer. *34th Annual Meeting of the Bioelectromagnetics Society*, Brisbane, Australia, 2012.
8. Dobbin ZC, Katre AA, Ziebarth A, Shah MM, Steg AD, Alvarez RD, Conner MG, **Landen CN**. Use of an optimized primary ovarian cancer xenograft model to mimic patient tumor biology and heterogeneity. *American Society of Clinical Oncology*, 2012.
9. Leath CA, Alvarez RA, **Landen CN**. Determination of Potential Ovarian Cancer Stem Cells in Patients with High Grade Serous Cancer Undergoing Neoadjuvant Chemotherapy. *WRHR Scholars Research Symposium*, Philadelphia, PA, 2012.
10. Walters C, Straughn J, Landen C, Estes J, Huh W, Kim K. Port-Site Metastases after Robotic Surgery for Gynecologic Malignancy. *43rd Annual Society of Gynecologic Oncologists Meeting*, 2013.
11. Shah M, Nowsheen S, Katre A, Dobbin Z, Erickson B, Alvarez R, Konstantinopoulos P, Yang E, Landen C. Towards personalized PARP therapy: XRT-induced Rad51 predicts response to ABT-888 in ovarian cancer. *43rd Annual Society of Gynecologic Oncologists Meeting*, 2013.
12. Ziebarth AJ, Nowsheen S, Steg AD, Shah MM, Katre AA, Dobbin ZC, Sood AK, Conner MG, Yang ES, and **Landen CN**. Endoglin (CD105) is a target for ovarian cancer cell-specific therapy through induction of DNA damage *Proceedings of the American Association of Cancer Research,* 2013.
13. Erickson BK, Steg AD, Dobbin ZC, Katre AA, Alvarez RD, **Landen CN**. Examination of the chemoresistant subpopulation in ovarian cancer identifies DNA repair genes contributing to survival after primary therapy. *Proceedings of the American Association of Cancer Research,* 2013.
14. Erickson BK, Dobbin ZC, Shim E, Alvarez RD, Conner MG, **Landen CN**. Identical TP53 mutations support a common origin for mixed histology epithelial ovarian cancer. *Proceedings of the American Association of Cancer Research*, 2013.
15. Burke MR, Steg AD, Jeong DH, Dobbin ZC, **Landen CN.** GSI-1 synergizes with LDE225 in ovarian cancer cells by inhibiting the proteasome *Proceedings of the American Association of Cancer Research,* 2013.
16. Jackson WP, Katre AA, Dobbin ZC, Steg AD, **Landen CN**. Pathway analysis of chemoresistance in ovarian cancer cell lines. Proceedings of the American Association of Cancer Research, 2013.
17. Jimenez H, Zimmerman JW, **Landen CN**, Brezovich I, Chen D, Kuster N, Capstick M, Gong Y, Barbault A, Pasche B. Amplitude-Modulated Radiofrequency Electromagnetic Fields Inhibit Ovarian Cancer cell Growth has been accepted for Platform presentation. Bioeletromagnetics Society, 2013.

- Grants awarded for which data generated by this work contributed preliminary data:

- Principle Investigator. *Identifying mediators of chemoresistance in ovarian cancer*. The Norma Livingston Foundation. 50,000, 5/1/2012-4/30/2014.
- Principle Investigator. *Development of a Personalized Therapy Model in Cervical Cancer*. Pilot Project, SPORE in Cervical Cancer. 9/1/2012 – 8/31/2013. $30,000.
- Co-Principle Investigator. Predicting response of ovarian cancers to PARP Inhibitors. The ROAR Foundation. 12/14/2012 – 12/13/2014.

- Funding applied for with decision pending:

AACR Basic Cancer Research Fellowship Role: Mentor
Sponsor: American Association of Cancer Research
BARD1 and chemoresistance in epithelial ovarian cancer
Major Goals of Project: The purpose of this proposal is to explore the potential of targeting BARD1 in such a fashion, as our preliminary studies suggest it plays a prominent role in chemotherapy-resistant ovarian cancer.

Multi-Investigator Grant Role: Co-PI (Tollefsbol)
Sponsor: UAB Comprehensive Cancer Center
Novel Dietary Epigenetic Approaches for Chemosensitization of Ovarian Cancer
Major Goals of Project: In this proposal we hypothesize that green tea combined with cruciferous vegetables, such as broccoli sprouts, as sources of the epigenetic-modifying compounds SFN and EGCG, will reduce the growth of chemoresistant ovarian tumors in mice. We will also determine the epigenetic mechanisms for decreased expression of key tumor-related genes such as telomerase and determine the genome-wide impact of these compounds on epigenetics in chemoresistant ovarian cancers.

Multi-Investigator Grant Role: Co-PI (Prevelige)
Sponsor: UAB Comprehensive Cancer Center
Overcoming Chemoresistance with Protein Cage Nanoparticle-Mediated SiRNA Therapeutics
Major Goals of Project: This proposal intends to determine the ability of modified PCN nanoparticles to delivery siRNA to ovarian cancer cells in vivo, to be used as a therapeutic modality in overcoming taxane chemoresistance. PCNs will be further modified to avoid detection and destruction by the adaptive immune system, and to enhance tumor uptake through ligand/receptor interactions

R01 Role: Co-I (van Waardenburg)
Sponsor: NIH/NCI
The DNA repair enzyme tyrosyl-DNA phosphodiesterase I as therapeutic target
Major Goals of Project: The hypothesis of this proposal is that alterations in the catalytic mechanism of Tdp1 that stabilize the covalent Tdp1-DNA intermediate may be exploited in the development of novel cancer therapeutics. The project seeks to determine the frequency and clinical significance of Tdp1 expression in ovarian cancer, as well as the potential of newly-developed inhibitors as effective therapeutics.

OCRP Resource Development Award Role: PI

Sponsor: Department of Defence
Characterization and Distribution of Ovarian Patient-Derived Xenografts
Major Goals of Project: To characterize and make available a patient-derived xenograft model that may improve understanding of the significance of ovarian cancer heterogeneity and more accurately predict response to therapies.

Program Project Development Grant Role: PI
Sponsor: Ovarian Cancer Research Fund
New strategies to address chemotherapy resistance in ovarian cancer
Major Goals of Project: to define novel mechanisms of acquired and intrinsic resistance to therapy and to develop new technologies to target ovarian cancer cells in a manner that will provide successful strategies to circumvent chemoresistance in this disease context.

CONCLUSIONS:

Our data demonstrate that ALDH1A1-positive cells are more tumorigenic than ALDH1A1-negative cells, contribute to poor patient outcomes, and contribute to chemoresistance. Importantly, these effects can be reversed by downregulating ALDH1A1 expression with nanoparticle-delivered siRNA. Additionally, we have shown that increased tumorigenicity is not only an important ex vivo assessment of CSCs, but that they are clinically significant as well, in that chemoresistant tumors have increased density of ALDH and CD133 cells. This suggests that they represent at least part of the chemoresistant population within a heterogeneous tumor. Importantly, they do not seem to explain the entire story, as there are still many CSC-negative cells present at the conclusion of treatment. Further evaluation of the mechanism stem cell pathways have on chemotherapy resistance have found that endoglin (CD105) and hedgehog mediators Gli1 and Gli2 are strongly associated with resistance. Targeted either of these pathways restored sensitive to paclitaxel or carboplatin *in vitro* and *in vivo*. Although response to chemotherapy in PDX models is highly variable at the individual gene level, pathway analysis reveals multiple pathways that commonly altered in many tumors. The immune system also appears to mediate a robust response in some tumors. Future work will attempt to delineate which of these pathways is most contributory, and how they may be best targeted to kill the final chemotherapy resistant population in ovarian cancer.

REFERENCES:

1. Bast RC, Jr., Hennessy B, Mills GB. The biology of ovarian cancer: new opportunities for translation. Nat Rev Cancer 2009;9(6):415-28.
2. Dalerba P, Cho RW, Clarke MF. Cancer stem cells: models and concepts. Annu Rev Med 2007;58:267-84.
3. Rosen JM, Jordan CT. The increasing complexity of the cancer stem cell paradigm. Science 2009;324(5935):1670-3.

4. Landen CN, Jr., Goodman B, Katre AA, *et al.* Targeting aldehyde dehydrogenase cancer stem cells in ovarian cancer. Mol Cancer Ther 2010;9(12):3186-99.
5. Steg AD, Bevis KS, Katre AA, *et al.* Stem cell pathways contribute to clinical chemoresistance in ovarian cancer. Clin Cancer Res 2012;18(3):869-81.

APPENDICES:

- Appendix 1: Publications
    - Steg AS, Katre AA, Bevis KS, Ziebarth A, Dobbin ZC, Shah MS, Alvarez RD, **Landen CN**. Smoothened Antagonists Reverse Taxane Resistance in Ovarian Cancer. *Mol Cancer Ther*, 11(7): 1587-97, 2012.
    - Ziebarth AJ, Nowsheen S, Steg AS, Shah MM, Katre AA, Dobbin ZC, Han HD, Lopez-Berestein G, Sood AK, Conner MG, Yang ES, **Landen CN**. Endoglin (CD105) contributes to platinum resistance and is a target for tumor-specific therapy in epithelial ovarian cancer. *Clin Can Res*, 19(1): 170-82, 2013.
    - Erickson BK, Conner MG, **Landen CN Jr**. The Role of the Fallopian Tube in the Origin of Ovarian Cancer. *Am J Obstet Gynecol, in press*.
- Appendix 2: Curriculum Vitae, Charles N. Landen, Jr.

Endoglin (CD105) contributes to platinum resistance and is a target for tumor-specific therapy in epithelial ovarian cancer

Angela J. Ziebarth[1], Somaira Nowsheen[2], Adam D. Steg[1], Monjri M. Shah[1], Ashwini A. Katre[1], Zachary C. Dobbin[1], Hee-Dong Han[3], Gabriel Lopez-Berestein[3,4,5], Anil K. Sood[4,5,6], Michael Conner[7], Eddy S. Yang[2], and Charles N. Landen[1*]

[1] Department of Obstetrics and Gynecology, University of Alabama at Birmingham, Birmingham, AL 35294
[2] Department of Radiation Oncology, University of Alabama at Birmingham, Birmingham, AL 35294
[3] Center for RNA Interference and Non-Coding RNA, [4]Departments of Experimental Therapeutics, [5]Cancer Biology, and [6]Gynecologic Oncology & Reproductive Medicine, U.T.M.D. Anderson Cancer Center, Houston, TX 77030
[7] Department of Pathology, University of Alabama at Birmingham, Birmingham, AL 35294

Running Title: Cytotoxic induction of DNA damage with endoglin targeting

Keywords: Endoglin, CD105, platinum resistance, ovarian cancer, siRNA, cancer stem cells

*Correspondence: Charles N. Landen, Jr., MD, MS
Associate Professor
Department of Obstetrics and Gynecology
The University of Alabama at Birmingham
176F RM 10250
619 19th Street South
Birmingham, AL 35249
Work: 205-934-4986
Fax: 205-975-6174
clanden@uab.edu

Acknowledgements: Funding support provided in part by the University of Alabama at Birmingham Center for Clinical and Translational Science (5UL1RR025777), the Reproductive Scientist Development Program through the Ovarian Cancer Research Fund and the National Institutes of Health (K12 HD00849), and the Department of Defense Ovarian Cancer Research Academy (OC093443), the Ovarian Cancer Research Fund, U54 CA151668, P50 CA083639, and the RGK Foundation.

Statement of Translational Relevance: Ovarian cancer remains the most lethal gynecologic malignancy, largely due to its high rate of chemoresistant recurrence. Endoglin (CD105) is overexpressed on tumor-associated endothelial cells and is a target for anti-angiogenic therapy, but expression on tumor cells has only been recently demonstrated. In the current study, we demonstrate that endoglin is actually predominantly expressed in the cytoplasm of malignant cells, and downregulating endoglin promotes apoptosis, induces DNA damage, and sensitizes cells to platinum therapy *in vitro* and *in vivo*. This occurs through effects on numerous DNA repair genes, most prominently BARD1. The novel demonstration of efficacy in targeting tumor cells themselves, in addition to the previously-recognized effects of targeting vasculature, make this therapeutic an attractive mechanism to target both compartments of the tumor microenvironment.

Abstract:

Purpose: Endoglin (ENG, CD105) is a membranous protein overexpressed in tumor-associated endothelial cells, chemoresistant populations of ovarian cancer cells, and potentially stem cells. Our objective was to evaluate the effects and mechanisms of targeting endoglin in ovarian cancer.

Experimental Design: Global and membranous endoglin expression was evaluated in multiple ovarian cancer lines. *In vitro,* the effects of siRNA-mediated endoglin knockdown with and without chemotherapy were evaluated by MTT assay, cell-cycle analysis, alkaline comet assay, γ-H2AX foci formation, and qPCR. In an orthotopic mouse model, endoglin was targeted with chitosan-encapsulated siRNA with and without carboplatin.

Results: Endoglin expression was surprisingly predominantly cytoplasmic, with a small population of surface-positive cells. Endoglin inhibition decreased cell viability, increased apoptosis, induced double-stranded DNA damage, and increased cisplatin sensitivity. Targeting endoglin downregulates expression of numerous DNA repair genes, including BARD1, H2AFX, NBN, NTHL1, and SIRT1. BARD1 was also associated with platinum resistance, and was induced by platinum exposure. *In vivo*, anti-endoglin treatment decreased tumor weight in both ES2 and HeyA8MDR models when compared to control (35-41% reduction, $p<0.05$). Endoglin inhibition with carboplatin was associated with even greater inhibitory effect when compared to control (58-62% reduction, $p<0.001$).

Conclusions: Endoglin downregulation promotes apoptosis, induces significant DNA damage through modulation of numerous DNA repair genes, and improves platinum sensitivity both *in vivo* and *in vitro.* Anti-endoglin therapy would allow dual treatment of both tumor angiogenesis

and a subset of aggressive tumor cells expressing endoglin and is being actively pursued as therapy in ovarian cancer.

Introduction

Epithelial ovarian carcinoma (EOC) remains the most lethal gynecologic malignancy.[1] While initial response to first-line therapy (consisting of surgical cytoreduction and combination platinum/taxane therapy) is usually effective, the majority of patients will ultimately recur with chemotherapy-resistant cancer and succumb to disease. This emphasizes the need for novel therapies aimed at targeting the population of cancer cells most resistant to initial therapy.

Endoglin (ENG) is a 180kDa disulfide-linked homodimer transmembrane protein most prominently expressed on proliferating endothelial cells. It is a well-characterized angiogenic marker that is upregulated during angiogenesis, and is overexpressed in vascular endothelium in malignancies including ovarian, leukemia, gastrointestinal stromal tumors (GIST), melanoma, and laryngeal cancers, but is rarely expressed in non-endothelial cells.[2-3] It is a co-receptor of TGFBR2 that binds TGF-B and is an important mediator of fetal vascular/endothelial development.[4] Recently, anti-angiogenic agents have received extensive attention as new therapeutic modalities, and CD105 has become an additional target by which intratumoral angiogenesis may be targeted.[5-6] However, endoglin may serve in a capacity beyond angiogenesis alone. Studies in GIST[7] and breast cancer[8] suggest that endoglin is upregulated not only in tumor endothelial cells, but also in actual tumor cells, and is associated with poor prognosis. Soluble endoglin has also been noted in ovarian cancer ascites,[9] and increased endoglin expression in ovarian cancer endothelial cells is associated with poor prognosis.[10] Additionally, we have recently shown that while endoglin is rarely expressed in primary ovarian cancer cells, it is frequently expressed in recurrent platinum-resistant tumor cells, as compared to the primary untreated tumor.[11] These findings suggest a broader role of endoglin in tumor cell biology beyond that of endothelial expression alone. The goal of our current study is to evaluate

the effects of targeting tumor-specific endoglin in ovarian cancer both *in vitro* and *in vivo* and explore the mechanisms by which endoglin may contribute to chemoresistance.

Methods and Materials

Evaluation of endoglin expression in ovarian cancer cell lines. Multiple ovarian cancer cell lines were evaluated for the presence of endoglin, including HeyA8, HeyA8MDR, ES2, A2780ip2, A2780cp20, A2780cp55, SKOV3ip1, SKOV3TRp2, IGROV-AF1, and HIO-180. Cells were maintained in RPMI-1640 medium with 10% fetal bovine serum (FBS) (Hyclone, Logan, UT). The taxane-resistant cell line HeyA8MDR was maintained in the same media with the addition of 150 ng/ml of paclitaxel. Cell lines were routinely screened for Mycoplasma (GenProbe detection kit; Fisher, Itasca, IL) and all experiments performed on 70-80% confluent cultures. Cells less than 20 passages from confirmation of genotype by STR analysis were used.

Cell lysates were collected in modified radioimmunoprecipitation assay lysis buffer with protease inhibitor cocktail (Roche, Manheim, Germany). Immunoblot analysis was performed using rabbit anti-endoglin antibody (Sigma, St. Louis, MO) at 1:500 dilution overnight at 4°C. A loading control was performed with mouse anti-β-actin antibody (Clone AC-15, Sigma) at 1:20,000 dilution for 1 hour at RT. After washing, membranes were incubated in HRP-conjugated goat anti-rabbit (for Endoglin) or goat anti-mouse (for β-actin) secondary antibodies (Bio-Rad, Hercules, CA). Visualization was performed by enhanced chemiluminescence (Pierce Thermo Scientific, Rockford, IL).

Immunohistochemistry. Cell lines in culture were washed with ice cold PBS twice, then fixed by applying 100% ice cold methanol for 10 min. Cells were rehydrated with PBS. Endogenous

peroxidase was blocked with 3% H2O2 in methanol for 15min at RT. The slides were incubated in 10% normal goat serum for 1 hr at RT. The primary anti-endoglin antibody (Sigma HPA011862) was diluted in 10% normal goat serum at 1:50. The slides were kept at 4°C overnight. Biotin-labeled secondary antibody was applied on cells at the concentration of 1:2000 for 1hr at RT, followed by avidin-biotin peroxidase buffer. DAB (3,3'-diaminobenzidine) was used as chromophore to detect the staining. To visualize endoglin expression in tumor sections, formalin-fixed paraffin-embedded tissue was cut in sections of 5uM thickness. Slides were warmed for 15 minutes and sequentially deparaffinized. Antigen retrieval was carried out in Citrate buffer (pH6.0) in a pressure cooker at high pressure for 5 min. Endogenous peroxidase was quenched by 3% H2O2 in methanol for 15 min. Slides were incubated in 10% normal goat serum for 1hr at RT. Slides were then incubated (4°C, Overnight) in antibody against endoglin (Sigma HPA011862) in 10% normal goat serum at 1:200 dilution. Detection was carried out using biotin labeled secondary antibody against rabbit at dilution of 1:2000 incubated at RT for 1 hr, followed by avidin-biotin peroxidase buffer. DAB (3,3'-diaminobenzidine) was used as chromophore.

Flow cytometry. After trypsinisation and centrifugation, the cell pellet was washed and resuspended in washing buffer (PBS containing 2% FBS and 0.1% sodium azide).$1x10^7$ cells were resuspended in 50µls of 10% goat buffer for 1hr kept on ice. Cells were incubated in antibody against endoglin 1:100 (Sigma HPA011862) in 10% goat serum for 1hr on ice. Alexa-488-conjugated anti rabbit antibody was applied on cells for 30 minutes and incubated on ice. The cells were washed twice in PBS and analyzed by FACS.

Endoglin Downregulation by siRNA transfection: In order to determine the effects of endoglin downregulation in ovarian cancer cells, transient knockdown was accomplished with anti-endoglin siRNA. Lipofectamine 2000 (Invitrogen) transfection was performed on Hey8MDR and ES2 cell lines using control siRNA (target sequence: 5'-UUCUCCGAACGUGUCACGU-3', Sigma) lacking known human or mouse targets, or one of two different Endoglin-targeting constructs (5'-CAAUGAGGCGGUGGCAAU-3' ["ENG_A"} or 5'-CAGAAACAGUCCAUUGUGA-3' ["ENG_B"], Sigma). These anti-human sequences have no more than 8 consecutive bp homology with murine CD105 (by BLASTN) and therefore should not affect murine endoglin expression. Lipofectamine was added to 5µg siRNA at a 3:1 v/v ratio (or as otherwise specified, as in Figure 1E) were incubated for 20 min at RT, added to cells in serum-free RPMI to incubate for 12 hours in 6- well plates, then maintained in 10% FBS/RPMI for an additional 12 hours, trypsinized and re-plated on a 96-well plate at a concentration of 2,000 cells per well. Cells were treated with vehicle or increasing doses of carboplatin or paclitaxel to generate an IC 50 curve. After 5 days, cells were washed and incubated with MTT reagent (Sigma) for 2 hours at 37°C. Media was then removed, cells dissolved in DMSO, and optical density measurements at 570 nm read with a spectrophotometer. The IC50 was the chemotherapy concentration giving the OD_{IC50} reading, calculated by the formula $OD_{IC50} = [(OD_{MAX} - OD_{MIN})/2 + OD_{MIN}]$. Assays were repeated in triplicate.

Apoptosis analysis. Analysis of apoptosis was performed with the Annexin V assay combined with propidium iodide (PI, eBiosciences #88-8005-74). ES2 and HeyA8MDR cells were transfected with either control siRNA or anti-endoglin siRNA in serum-free RPMI growth media for 12 hours, followed by maintenance in 10% FBS/RMPI. Cells were trypsinized 96 hours

following transfection, washed twice in PBS, and then resuspended in 200μL 1x binding buffer containing 5μL of Annexin V. 10μL of PI was added, cells were incubated for 10 minutes at RT in the dark. Fluorescent signal (FITC and PI) in cells were analyzed by FACS and data were analyzed with FlowJo v.7.6.1 (Ashland, OR).

Alkaline comet assay. ES2 cells (n=400,000 in 6-well plate) were transfected with endoglin and control siRNA. Twenty-four hours following transfection, cells were exposed to cisplatin without supplemental SVF at a concentration of 1μM (the approximate IC80 level for this line) for either 1 or 4 hours, carefully rinsed to remove the drug, and cultured in regular media. Vehicle or control siRNA were included in all experiments. At the indicated time points, cells were collected and subjected to alkaline comet assay according to the manufacturer's instructions (catalog # 4250-050-K; Trevigen). Briefly, cells were combined with low melting agarose onto CometSlides (Trevigen). After lysis, cells were subjected to electrophoresis and stained with SYBR green. Subsequently, cells were visualized using fluorescent microscopy (Carl Zeiss, Thornwood, NY). At least 200 comet images were analyzed for each time point using Comet Score software (version 1.5; TriTek Corp.). The number of tail-positive cells with small and large nuclei was manually counted by an examiner blinded to treatment group, and expressed as a percentage of all cells evaluated. Experiments were repeated in triplicate.

γ-H2AX foci formation. ES2 cell lines were cultured and seeded on sterile cover slips. Twenty-four hours following transfection with control or anti-endoglin siRNA, cells were exposed to 1μM cisplatin for either 1 or 4 hours, carefully rinsed to remove the drug, and cultured in regular media. Following the treatment period, IHC was performed as previously described[12-13] with

slight modification for foci staining. Briefly, cells were rinsed in phosphate buffered saline (PBS) and incubated for 5 minutes at 4°C in ice-cold cytoskeleton buffer (10mM Hepes/KOH, pH 7.4, 300mM sucrose, 100mM NaCl, 3mM MgCl2) supplemented with 1mM PMSF, 0.5mM sodium vanadate and proteasome inhibitor (Sigma, 1:100 dilution) followed by fixation in 70% ethanol for 15 minutes. The cells were blocked and incubated with primary antibody (1:500 dilution, anti-phosphoH2AX Ser139, Millipore, catalog # MI-07-164). The secondary antibody was anti-rabbit Alexa Fluor 488–conjugated antibody (1:2000 dilution; Invitrogen). DAPI (Invitrogen, catalog # D21490) was used for nuclear staining. The cover slips were subsequently mounted onto slides with mounting media (Aqua poly mount, Polysciences, Inc. catalog # 18606) and analyzed via fluorescence microscopy (Carl Zeiss, Thornwood, NY). Positive and negative controls were included on all experiments. A total of 500 cells were assessed. For foci quantification, cells with greater than 10 foci were counted as positive according to the standard procedure. Experiments were repeated in triplicate.

RNA extraction from cell lines. Total RNA was isolated from ovarian cancer cell lines using Trizol reagent (Invitrogen, Carlsbad, CA) per manufacturer's instructions. RNA was then DNase treated and purified using the RNeasy Mini Kit (QIAGEN, Hilden, Germany). RNA was eluted in 50 μL of RNase-free water and stored at -80°C. The concentration of all RNA samples was quantified by spectrophotometric absorbance at 260/280 nm using an Epoch Microplate Spectrophotometer (BioTek Instruments, Winooski, VT).

DNA repair qPCR array. ES2 and HeyA8 cells in culture were exposed to siRNA against endoglin in Lipofectamine 2000 as described above. After 48 hours, cells were collected and

mRNA extracted. Two replicates per cell line were performed. These four samples were then subjected to a quantitative PCR array consisting of 84 genes from DNA damage/repair pathways (plus additional housekeeping genes; the RT2 Profiler PCR Array Human DNA Damage Signaling Pathway, SA Biosciences Cat# PAHS-209Z, performed per manufacturer's instructions). Briefly, extracted RNA was converted to cDNA and amplified using the RT^2 FFPE PreAMP cDNA Synthesis Kit (SABiosciences, Frederick, MD). Quality of cDNA was confirmed with the Human RT^2 RNA QC PCR Array (SABiosciences). Gene expression was analyzed using the Human DNA Damage Signaling Pathway RT^2 Profiler PCR Array (SABiosciences), which profiles the expression of 84 genes involved in pluripotent cell maintenance and differentiation[14]. Functional gene groupings consist of the ATM/ATR signaling, nucleotide excision repair, base-excision repair, mismatch repair, double strand break repair, apoptosis, and cell cycle checkpoint regulators. PCR amplification was performed on an ABI Prism 7900HT sequence detection system and gene expression was calculated using the comparative C_T method[15].

Reverse transcription and quantitative PCR. Extracted RNA samples were diluted to 20 ng/μL using RNase-free water. cDNA was prepared using the High Capacity cDNA Reverse Transcription Kit (Applied Biosystems). The resulting cDNA samples were analyzed using quantitative PCR. Primer and probe sets for *ENG* (PPH01140F) *ATM* (PPH00325C), *BARD1* (PPH09451A), *DDIT3* (PPH00310A), *H2AFX* (PPH12636B), *NBN* (PPH00946C), *NTHL1* (PPH02720A), *PPP1R15A* (PPH02081E), *SIRT1* (PPH02188A), *ATP7B* (PPH06148A), and *RPLP0* (Hs99999902_m1, housekeeping gene) were obtained from SABiosciences and used according to manufacturer's instructions. PCR amplification was performed on an ABI Prism

7900HT sequence detection system and gene expression was calculated using the comparative C_T method.

Orthotopic Mouse Model. Female athymic nude mice (nu-nu) were obtained from the National Cancer Institute Frederick Cancer Research and Development Center (Frederick, MD). Mice were cared for in accordance with American Association for Accreditation of Laboratory Animal Care guidelines, the United States Health Services Commissioned Corps "Policy on Human Care and Use of Laboratory Animals," and University of Alabama at Birmingham Institutional Animal Care and Use Committee policies. ES2 tumors were established by intraperitoneal (IP) injection of $1x10^6$ cells suspended in 200μL of serum free RPMI media. Hey8MDR tumors were established in a similar way, using $5x10^5$ cells. To evaluate the effectiveness of endoglin-targeted therapy *in vivo,* siRNA was incorporated into chitosan nanoparticles as previously described.[16-17] Therapy was initiated 1 week after tumor cell injection. Mice were randomized to one of four treatments (n=10 per group): a) control siRNA alone (150 ug/kg twice weekly injected IV), b) control siRNA with IP carboplatin (160 mg), c) anti-endoglin siRNA (150 ug/kg twice weekly) alone, or d) anti-endoglin siRNA with carboplatin. All treatments were suspended in 100 μL 0.9% normal saline (NS). Mice were monitored for adverse effects, and all treatment groups sacrificed when control mice became uncomfortable with tumor burden. ES2 tumors behaved aggressively, and were harvested following 2 weeks of treatment. Hey8MDR tumors were harvested after 3 weeks of therapy. Mouse weight, ascites volume, tumor weight and distribution of tumor were recorded. Representative tumor samples were obtained from 5 mice in each treatment group, formalin-fixed, paraffin-embedded, and cut into 5 micron sections for evaluation of Proliferating Cell Nuclear Antigen (PCNA), Terminal deoxynucleotidyl transferase

mediated dUTP Nick End Labeling assay (TUNEL), γ H2AX (phosphorylation of Histone 2A protein) and 53BP1 (a mediator of the DNA damage checkpoint).

Tumor PCNA Immunohistochemistry and TUNEL. Sections were deparaffinized and re-hydrated, and antigen retrieval was performed with citrate buffer (pH 6.0) in pressure cooker for 5 minutes. Endogenous peroxidase activity was quenched with 3% hydrogen peroxide solution in methanol for 15 minutes. Sections were blocked with CytoQ immune diluent and block and probed with PCNA primary antibody (PCNA-PC10, Cell signaling Technology, 1:5000 dilution) at 4°C overnight. Sections were washed and incubated with the Mach 3 mouse HRP polymer system. After rinsing, the sections were incubated with DAB chromophoric solution (Scytek Labs, Utah, USA) for 5 min at room temperature, then counterstained with Gill's hematoxylin (Ricca chemicals). Four 40x microscopic fields were counted from each section, averaged over 5 mice in each treatment group, and expressed as a percentage of the total number of tumor cells. Apoptosis was determined by TUNEL assay with a colorimetric apoptotic cell detection kit (Promega), per manufacturer's instruction. As with PCNA IHC, 4 microscopic fields at 40x magnification were evaluated from each section. Stained cells were recorded as a percentage of the total number of tumor cells.

Tumor γH2AX and 53BP1 IHC. Formalin fixed tissues were heated at 60°C for 1hr and rehydrated according to standard protocol. Subsequently, the tissues were permeabilized in 0.5% Triton X-PBS for 10 min, blocked in 2% BSA-0.1% Triton-X-PBS for 1 hr, and incubated with primary antibodies (1:500 dilution, anti phospho H2AX Ser139, Millipore, catalog # MI-07-164; 1:500 dilution, anti-53BP1, Novus Biologicals, catalog # NB100-304). The secondary antibody

was anti-rabbit Alexa Fluor 488–conjugated antibody (1:2000 dilution; Invitrogen). DAPI (Invitrogen, catalog # D21490) was used for nuclear staining. The slides were subsequently mounted using mounting media (Aqua poly mount, Polysciences, Inc. catalog # 18606) and analyzed via fluorescence microscopy (Carl Zeiss, Thornwood, NY). Positive and negative controls were included on all experiments. A total of 500 cells were assessed. For foci quantification, cells with greater than 10 foci were counted as positive according to the standard procedure. Experiments were repeated in triplicate. Data show the mean and SEM.

Statistics. Analysis of normally distributed continuous variable was performed using a two-tailed Student's t-test. Those data with alternate distribution were examined using a nonparametric Mann-Whitney U test. A $p<0.05$ was considered statistically significant.

Results

Effects of endoglin downregulation on cell viability and platinum sensitivity. Endoglin is expressed by multiple ovarian cancer cell lines (Figure 1A), most prominently in HeyA8, HeyA8MDR, and ES2 cells. Weak expression was detected in the HIO-180, A2780ip2, A2780cp20, SKOV3ip1, SKOV3TRp2, and IGROV-AF1 cell lines. This was previously demonstrated at the mRNA level by quantitative PCR[11]. To confirm that expression was predominantly at the cell surface, consistent with its function as a co-receptor for TGFβ, we performed immunohistochemistry on the ES2 and HeyA8MDR cell lines. Surprisingly, the predominant staining was noted n the perinuclear cytoplasm (Figure 1B). This was confirmed by flow cytometry, where interestingly not only was membranous staining rare, but there was a very distinct separate population with 100-fold fluorescent intensity (rather than a global shift among

all cells), consistent with a separate small population of cells with strong endoglin surface expression (Figure 1C). This population represented 6.0% of HeyA8MDR and 5.4% of ES2 cells. On close examination of IHC on cultured cells, a minority of the cells could be seen to have strong membranous expression of CD105 (arrows, Figure 1B). A separate endoglin-positive population has previously been noted in renal cell carcinoma cells, which did exhibit stem-cell properties.[18] However, these data are conclusive that the majority of endoglin expression in ovarian cancer is cytoplasmic, suggesting a role other than just as a co-receptor for TGF-beta.

To determine whether siRNA-mediated downregulation of endoglin had significant effects on viability and chemosensitivity, two different siRNA constructs (ENG_A siRNA and ENG_B siRNA) were examined. Both effectively reduced endoglin expression at 48 hours at the mRNA (Figure 1D) and protein level[11]). Both were previously shown to reduce cell viability[11]. To determine the mechanism by which endoglin knockdown reduced viability, evaluation of apoptosis was performed by the TUNEL assay. Annexin V/PI co-fluorescent staining performed 48 hours following transfection indicated significantly fewer viable cells in those treated with anti-endoglin siRNA than those treated with control siRNA (47.2% vs. 65.1%, $p<0.05$). A sample flow cytometry plot and a graph of average over three experiments are shown in Figure 1D. Those treated with anti-endoglin siRNA had increased percentages of cells in both early apoptosis (21.5% vs. 17.9%, $p<0.05$) and late apoptosis (18.9% vs. 12.0%, $p<0.05$). Effects were more pronounced when combined with cisplatin. In order to determine whether Endoglin knockdown had an effect on viability in combination with chemotherapy, cells were exposed to siRNA, then re-plated after 24 hours, and incubated with increasing concentrations of cisplatin or paclitaxel. Because endoglin downregulation alone was associated with substantial cell death in the HeyA8MDR model, knockdown was performed with several dilutions of siRNA in an effort

to more clearly delineate effects on platinum sensitivity. In both ES2 (normal IC50 for cisplatin = 0.7μM) and HeyA8MDR (normal IC50 for cisplatin = 0.65μM) models, increased cisplatin chemosensitivity was noted (up to 4-fold and 2-fold reduction in IC50, respectively, Figure 1E). Similar experiments were performed with paclitaxel, which did not show an increased sensitization with endoglin downregulation (data not shown).

Downregulation of endoglin induces DNA damage *in vitro*. Because platinum toxicity is mediated primarily through induction of DNA damage, we evaluated whether the enhanced cisplatin sensitivity from endoglin knockdown was a result of increased DNA damage. DNA damaging agents can induce both single-stranded breaks (SSBs) and double stranded breaks (DSBs) which can lead to initiation of apoptotic pathways. DNA damage in the ES2 line was first assessed via an alkaline comet assay, which detects both SSB and DSB. As quantified in Figure 2A, increased DNA damage over 24 hours was observed with cisplatin, endoglin downregulation with siRNA, and the combination (although combination therapy was not significantly increased compared to either single-agent treatment). A representative section demonstrating common effects on nearly all cells is shown (Figure 2B). Because a long comet tail can be the result of either DNA damage without death or apoptosis-associated DNA release, the nucleus size was also quantified. A small nucleus would be associated with apoptosis, whereas a long comet tail associated with a normal (larger) nucleus would indicate just DNA damage. As shown in Figure 2C for cells treated for 24 hours, those cells with a long tail present predominantly still had a large nucleus. Because most toxic effects on viability noted previously were assessed at 48 hours or longer, this DNA damage may be a precursor to apoptosis

induction. But it does demonstrate that DNA damage is the inciting event, rather than a result of apoptosis triggered by other mechanisms.

To further characterize the specific nature of DNA damage, development of foci of activated γ-H2AX was performed (Figure 2D). ES2 cells were employed, due to the rapid toxicity and cell death noted with endoglin downregulation with HeyA8. Phosphorylation of the histone protein H2AX on serine 139 (γ-H2AX) occurs at sites flanking DNA DSBs. The phosphorylation of thousands of H2AX molecules forms a focus in the chromatin flanking the DSB site that can be detected *in situ*. A higher proportion of cells with persistent γ-H2AX foci was noted with endoglin downregulation, to an even greater extent than cisplatin alone. The combination of cisplatin and endoglin downregulation induced more DSB repair than either agent alone. Collectively, these data suggest that a primary mechanism of DNA damage after endoglin downregulation is through induction of double-strand breaks in DNA.

Endoglin-targeting DNA damage is through effects on multiple mediators of DNA repair. In order to determine the mechanism by which downregulation of endoglin induces DNA damage, we first subjected both ES2 and HeyA8MDR cells treated with control siRNA or endoglin-siRNA for 48 hours to a qPCR-based array of 84 genes participating in DNA damage and repair pathways. This exploratory analysis found multiple genes that were either downregulated or upregulated in response to decreased endoglin, some of which were only associated with changes in one cell line (Supplemental Table 1). Select genes were then chosen for confirmatory assessment with qPCR (Figure 3). Genes for these analyses were selected based on the degree to which they were altered, the associated p-value, and whether the change was noted in both cell lines. With endoglin downregulation, significant concurrent downregulation

was noted by qPCR in H2AFX (36-43%), BARD1 (47-71%), NBN (38-41%), NTHL1 (39-53%), and SIRT1 (34-49%). A significant induction of mRNA was noted in DDIT3 (1.9-2.6-fold) and PPP1R15A (1.27-1.74-fold). There was no single DNA repair pathway subclass that comprised all affected genes, but consistent with data from the γ-H2AX assay, most were participants in either the double stranded break repair (BARD1, H2AFX, NBN) or nucleotide excision repair (SIRT1, NTHL1).

The downregulation of BARD1 was particularly interesting. BARD1 is an oncogenic regulator of BRCA1, and downregulation would be expected to result in export of BRCA1 from the nucleus and impairment of DNA repair. Furthermore, BARD1 was noted to be significantly *upregulated* in chemoresistant tumor samples from patients, compared to their primary tumors.[11] BARD1 expression is prominent in ES2 and HeyA8MDR, which follows if it is under transcriptional regulation by endoglin. Therefore, we examined BARD1 induction in response to platinum treatment in a progressively platinum-resistant triad of cell lines derived from A2780: A2780ip2 (which generates IP tumors more consistently than the parental line but is chemosensitive), A2780cp20 (having a platinum IC50 of 20μM), and A2780cp55 (with an IC50 of 55μM). The A2780cp20 and cp55 lines are stably platinum-resistant, and not chronically maintained in platinum. BARD1 expression is minimal in the parental A2780ip2 line, but increases at baseline ("Untreated") with each degree of platinum resistance (Figure 3B). Additionally, when exposed to an IC50 concentration of carboplatin, BARD1 mRNA production is significant increased in both A2780ip2 and A2780cp20. Levels were unchanged with carboplatin exposure in A2780cp55, likely due to its high baseline expression. A significant reduction in BARD1 with endoglin downregulation and an induction of BARD1 in response to platinum exposure strongly implicate this gene and its control on BRCA1 as a major mechanism

through which endoglin downregulation may lead to DNA damage, apoptosis, and sensitivity to platinum.

In addition to enhanced DNA repair mechanisms, a major mechanism of platinum resistance is through increased export of platinum agents through copper transporters such as ATP7B.[19] Therefore we also examined the effects of endoglin downregulation on ATP7B by qPCR. SiRNA-mediated targeting of endoglin resulted in a significant downregulation of ATP7B (by 20-24%, $p<0.05$, Figure 3C). While significant, this was not to the same extent many DNA repair genes were induced or activated.

Evaluation of tumor growth with anti-endoglin treatment in an orthotopic murine model. In order to determine if endoglin downregulation was an effective therapy *in vivo*, an orthotopic murine model was utilized using human specific anti-endoglin siRNA delivered within a chitosan nanoparticle. Chitosan (CH) is a natural nanoparticle that has been previously demonstrated to result in efficient delivery of siRNA to tumor after IV administration, with subsequent protein downregulation and gene-specific modulation.[16, 20-22] Because the siRNA delivered is specific to the human endoglin mRNA, any observed effect would be expected to be due to targeting the tumor cells, rather than the vasculature, which would require murine-specific siRNA. ES2 and HeyA8MDR cells were injected IP, and treatment was started 1 week later with a) control siRNA-CH alone, b) control siRNA-CH plus carboplatin, c) anti-endoglin siRNA-CH alone, or d) anti-endoglin siRNA-CH plus carboplatin. Carboplatin was used instead of cisplatin because of its preferable side-effect profile *in vivo*, which has led to its choice as standard of care in ovarian cancer patients. Tumors demonstrated reduced growth both with endoglin downregulation alone and in combination with platinum. In the ES2 model (Figure 4A), mice

treated with carboplatin had similar tumor burden to control (p=0.555), an expected result due to the highly platinum-resistant nature of the ES2 cell line, which is derived from a patient with clear cell carcinoma. Mice treated with anti-endoglin siRNA alone had a significantly reduced tumor weight, by 35.6% (p=0.014). Combined END-siRNA-CH with carboplatin was more effective that either agent alone, with a 57.7% reduction in tumor weight compared to control (p<0.001). Furthermore, combination therapy was more effective than siRNA-endoglin-CH alone, with an additional 34.3% reduction (p=0.033) In the HeyA8MDR model (Figure 4B), mice treated with carboplatin, endoglin-siRNA-CH, or combination therapy had significantly less tumor weight when compared to control (34% reduction p=0.027, 41.2% reduction p=0.002, and 61.2% reduction p<0.01, respectively). Those treated with carboplatin and control siRNA-CH had similar tumor burden reduction as those treated with endoglin-siRNA-CH (p=0.628). Combination therapy was again more effective than either single-agent carboplatin (additional 40.6% reduction, p=0.069), or endoglin-siRNA alone (34%, p=0.048). In the resected tumors, reduced expression of endoglin was confirmed with immunohistochemistry, in both groups of tumors treated with endoglin-siRNA-CH. Representative sections are pictured (Figure 4C). With both models, there was not a significant difference in mouse weight in any group. The distribution of tumor was also similar in all groups, suggesting there was not a significant effect on particular site of growth, adhesion, or migration.

Endoglin downregulation induces DNA damage and apoptosis *in vivo*. Our *in vitro* findings suggest a role of DNA damage and apoptosis following endoglin downregulation. To validate these findings *in vivo*, tumors from each treatment group described above were examined for proliferation, apoptosis, and induction of DNA damage. PCNA IHC was performed and revealed

no significant differences in percentage of PCNA positive cells, with approximately half of cells being positive in each treatment group (Figure 5A). A lack of effect on progression through the cell cycle and proliferation may explain why combination with taxanes was not synergistic with endoglin downregulation *in vitro*. TUNEL assay was performed to evaluate to detect differences in apoptosis between treatment groups. Control, carboplatin and anti-endoglin siRNA groups were not significantly different. However, the cohort receiving combination therapy had a significantly higher percent of apoptotic cells when compared to control ($p<.001$, Figure 5B). This increase, though statistically significant, is relatively small, which may be due to clearance of dead cells over the course of the 4-week experiment. To determine if DNA damage was still noted in the tumors collected at completion of therapy, fluorescent IHC was performed to evaluate for γ-H2AX as an indicator of *in vivo* DSB. A significantly higher amount of DNA damage was detected in both treatment groups receiving anti-endoglin treatment than either control or single-agent carboplatin treatment (Figure 5C). Additionally, 53BP1 is a mediator of DNA damage response and a tumor suppressor whose accumulation on damaged chromatin promotes DNA repair and enhances DNA damage response signaling. A significantly higher number of 53BP1-positive cells was noted in both cohorts that received anti-endoglin treatment when compared to either control or single-agent platinum (Figure 5D). These data are consistent with *in vitro* studies demonstrating that endoglin downregulation alone leads to DNA damage and apoptosis.

Discussion

Endoglin is overexpressed in solid tumor vasculature and is a reliable marker of angiogenesis.[5] Multiple anti-angiogenic therapies have been studied in ovarian cancer, and anti-

endoglin therapy has been proposed for several cancers in which increased endothelial endoglin expression has been noted.[23] However, to date, few studies address the expression of endoglin on tumor cells and its potential role in cancer progression. Building off our previous findings that Endoglin is increase in recurrent samples when compared to matched primary tumors[11], we have demonstrated that endoglin expression is highly expressed in many ovarian cancer cell lines, and that downregulation results in induction of cell death through induction of DNA damage and a synergistic killing effect with platinum agents both *in vitro* and *in vivo*. These novel findings demonstrate that therapeutics targeting endoglin may affect both the vasculature and malignant cells within the tumor microenvironment.

The primary canonical role of endoglin is as a co-receptor for TGF-beta.[24-26] As such, its expression on endothelial cells is primarily on the cell membrane.[27] However, we interestingly found endoglin expression in ovarian cancer cells was predominantly cytoplasmic, and clustered together in the perinuclear region of the cell. This would suggest that endoglin either has a separate TGF-beta-independent function dependent on nuclear proximity, or trafficking to the cell membrane is an important component of its regulation. Only a small (5-6%), but well-defined population had surface expression. This distinct population would be consistent with a cancer stem cell-like population, as has been previously described in endoglin-positive renal cell carcinoma[18]. Endoglin-positive meningioma cells have similar increased tumorigenicity and capacity to differentiate into adipocytes and osteocytes.[28]

Henriksen et al. evaluated endoglin expression in primary ovarian cancer cells and found that high tumor cell endoglin staining correlated with short overall survival.[29] Another group has shown that cells from cultured ascites that progressed towards a mesenchymal phenotype were high in endoglin.[30] We identified endoglin as a potential target for therapeutics through a screen

of stem cell pathways overexpressed in recurrent ovarian cancer samples. Among members of the TGF-β, Notch, Wnt, and Hedgehog pathways, endoglin was most significantly and consistently overexpressed in recurrent ovarian cancer samples when compared to their matched primaries, suggesting a role in chemoresistance.[11] We specifically examined stem cell pathways to address the question of whether the cancer stem cell population may be responsible for surviving initial chemotherapy. Endoglin has previously been implicated in stem cell biology, having originally been described on hematopoietic progenitor cells[31], and later demonstrated to identify precursor cells capable of tissue-specific differentiation[32-33].

It makes sense that cells with prolonged survival, such as stem/progenitor cells, would reply on pathways to mediate DNA damage. Because of the association noted with increased endoglin expression in platinum (and taxane)-resistant recurrent ovarian cancers,[11] and the contribution of enhanced DNA repair for platinum resistance,[19] we further examined the contribution of endoglin to DNA repair. We have found a previously unknown contribution of endoglin to expression of numerous DNA repair genes. These encompass several subtypes of DNA repair, predominantly double stranded break repair (BARD1, H2AFX, NBN), but also nucleotide excision repair (SIRT1, NTHL1), and cell cycle arrest (DDIT3, PPP1R15A), which may be a reactionary process in order to accomplish DNA repair. Recently BARD1 has been implicated in ovarian cancer pathogenesis for its interaction with BRCA1 and 2. BARD1 and BRCA1 interact with each other through their amino terminal RING finger domains. This interaction is required for BRCA1 stability, as well as for nuclear localization. The BRCA1-BARD1 complex serves as an E3 ubiquitin ligase, which has been noted to have critical activity in both the cell cycle check point through H2AX, NPM and γ-tubulin and in DNA fragmentation.[34-35] Additionally, patients with mutations of both BARD1 and BRCA2 have a

substantially increased risk for development of both breast and ovarian cancer. While BARD 1 has been found to interact and co-localize with BRCA1 at the spindle poles in early mitosis, it also interacts with BRCA2 at late mitosis in the midbody. Therefore BARD1 has been found to sequentially link the function of these[36] two proteins. In our analysis, BARD1 expression was reduced by 50-75% and H2AX expression was reduced 35-50% following endoglin knockdown. endoglin-mediated downregulation of BARD1 and its subsequent effects on BRCA1 and 2 and H2AX may therefore explain why we found substantial decreased cell viability, DNA damage and increased apoptosis.[34]

Silent Information Regulator Type 1 (SIRT1) is a nicotinamide adenine dinucleotide-dependent class III histone deacetylase (HDAC). SIRT1 has is associated with longevity and has been found to act primarily by inhibiting cellular senescence. SIRT1 is up-regulated in tumor cell lines and human tumors, and may be involved in tumorigenesis.[36] It has also been found to be over-expressed in chemoresistant tumors of cancer patients. SIRT1 inhibition leads to decrease in MDR1 expression and increase in drug sensitivity in ovarian cancer cell lines.[37] Our research suggests that Endogin knockdown was associated with a 30-50% reduction in SIRT1. This inhibition may help account for the increased platinum sensitivity we found with endoglin downregulation.

In regards to therapeutic development in cancer patients, delivery of siRNA constructs has the potential to offer long duration of target inhibition as well as reduced toxicity compared other approaches.[16, 20, 38-44] However, development of a delivery modality for siRNA constructs remains the rate-limiting step in translational research. Early delivery modalities included delivery of "naked" siRNA. Later attempts included high-pressure siRNA injections and intratumoral injections, neither of which has demonstrated substantial success. The development

of chitosan encapsulation and nanoliposomes to deliver siRNA has become widely accepted in translational studies and is and promising as a therapeutic modality as modifications to enhance in vivo delivery progress.[22] SiRNA mediated therapeutics are being used in ongoing trials with patients with macular degeneration, AIDS, malignant melanoma, acute renal failure, hepatitis B, and now in cancer patients, where phase I trials are in development. One particular advantage of siRNA-based therapeutics over conventional treatment modalities would apply to endoglin-based targeting. If indeed the cytoplasmic portion of endoglin is important to chemoresistance, downregulation of production at the mRNA level may be more effective than antibody-based targeting currently aimed at inhibiting angiogenesis.[45-46]

Because of the rarity of endoglin expression in normal tissues, anti-endoglin therapy has the potential to offer tumor-directed therapy in addition to anti-angiogenic therapy. Anti-endoglin therapy is being explored as a therapeutic in several cancers as an anti-angiogenic agent. In ovarian cancer, endoglin-targeted therapies may offer the additional advantage of targeting tumor cells overexpressing endoglin, including platinum-resistant tumors. Its effects on BRCA1 and 2 and H2AX through BARD1 downregulation, and its association with SIRT1 downregulation contribute to DNA damage repair and enhancement of platinum sensitivity. Our data strongly suggest that endoglin-targeted therapy has the potential to improve platinum sensitivity through induction of DNA damage and should be actively pursued as a potential therapy in the treatment of ovarian cancer.

REFERENCES

1. Siegel R, Naishadham D, Jemal A. Cancer statistics, 2012. CA: A Cancer Journal for Clinicians. 2012;62(1):10-29.
2. Perez-Gomez E, Del Castillo G, Juan Francisco S, Lopez-Novoa JM, Bernabeu C, Quintanilla M. The role of the TGF-beta coreceptor endoglin in cancer. ScientificWorldJournal. 2010;10:2367-84.
3. Marioni G, Staffieri A, Manzato E, Ralli G, Lionello M, Giacomelli L, et al. A higher CD105-assessed microvessel density and worse prognosis in elderly patients with laryngeal carcinoma. Arch Otolaryngol Head Neck Surg. 2011 Feb;137(2):175-80.
4. Barbara NP, Wrana JL, Letarte M. Endoglin is an accessory protein that interacts with the signaling receptor complex of multiple members of the transforming growth factor-beta superfamily. J Biol Chem. 1999 Jan 8;274(2):584-94.
5. Dallas NA, Samuel S, Xia L, Fan F, Gray MJ, Lim SJ, et al. Endoglin (CD105): a marker of tumor vasculature and potential target for therapy. Clin Cancer Res. 2008 Apr 1;14(7):1931-7.
6. Fonsatti E, Altomonte M, Arslan P, Maio M. Endoglin (CD105): a target for anti-angiogenetic cancer therapy. Curr Drug Targets. 2003 May;4(4):291-6.
7. Gromova P, Rubin BP, Thys A, Cullus P, Erneux C, Vanderwinden JM. ENDOGLIN/CD105 is expressed in KIT positive cells in the gut and in gastrointestinal stromal tumors. J Cell Mol Med. 2011 Mar 24.
8. Davidson B, Stavnes HT, Forsund M, Berner A, Staff AC. CD105 (Endoglin) expression in breast carcinoma effusions is a marker of poor survival. Breast. 2010 Dec;19(6):493-8.
9. Bock AJ, Tuft Stavnes H, Kaern J, Berner A, Staff AC, Davidson B. Endoglin (CD105) expression in ovarian serous carcinoma effusions is related to chemotherapy status. Tumour Biol. 2011 Feb 26.
10. Taskiran C, Erdem O, Onan A, Arisoy O, Acar A, Vural C, et al. The prognostic value of endoglin (CD105) expression in ovarian carcinoma. Int J Gynecol Cancer. 2006 Sep-Oct;16(5):1789-93.
11. Steg AD, Bevis KS, Katre AA, Ziebarth A, Dobbin ZC, Alvarez RD, et al. Stem cell pathways contribute to clinical chemoresistance in ovarian cancer. Clin Cancer Res. 2012 Feb 1;18(3):869-81.
12. Wang H, Yang ES, Jiang J, Nowsheen S, Xia F. DNA damage-induced cytotoxicity is dissociated from BRCA1's DNA repair function but is dependent on its cytosolic accumulation. Cancer Res. 2010 Aug 1;70(15):6258-67.
13. Yang ES, Wang H, Jiang G, Nowsheen S, Fu A, Hallahan DE, et al. Lithium-mediated protection of hippocampal cells involves enhancement of DNA-PK-dependent repair in mice. J Clin Invest. 2009 May;119(5):1124-35.
14. SABiosciences. DNA Damage Signaling Pathway PCR Array. 2011 [cited; Available from: http://www.sabiosciences.com/rt_pcr_product/HTML/PAHS-029Z.html
15. Steg A, Wang W, Blanquicett C, Grunda JM, Eltoum IA, Wang K, et al. Multiple gene expression analyses in paraffin-embedded tissues by TaqMan low-density array: Application to hedgehog and Wnt pathway analysis in ovarian endometrioid adenocarcinoma. J Mol Diagn. 2006 Feb;8(1):76-83.

16. Han HD, Mangala LS, Lee JW, Shahzad MM, Kim HS, Shen D, et al. Targeted gene silencing using RGD-labeled chitosan nanoparticles. Clin Cancer Res. 2010 Aug 1;16(15):3910-22.
17. Lu C, Han HD, Mangala LS, Ali-Fehmi R, Newton CS, Ozbun L, et al. Regulation of tumor angiogenesis by EZH2. Cancer Cell. 2010 Aug 9;18(2):185-97.
18. Bussolati B, Bruno S, Grange C, Ferrando U, Camussi G. Identification of a tumor-initiating stem cell population in human renal carcinomas. FASEB J. 2008 Oct;22(10):3696-705.
19. Shahzad MM, Lopez-Berestein G, Sood AK. Novel strategies for reversing platinum resistance. Drug Resist Updat. 2009 Dec;12(6):148-52.
20. Steg AD, Katre AA, Goodman BW, Han HD, Nick AM, Stone RL, et al. Targeting the Notch Ligand Jagged1 in Both Tumor Cells and Stroma in Ovarian Cancer. Clin Cancer Res. 2011 Jul 13.
21. Nick AM, Stone RL, Armaiz-Pena G, Ozpolat B, Tekedereli I, Graybill WS, et al. Silencing of p130cas in ovarian carcinoma: a novel mechanism for tumor cell death. J Natl Cancer Inst. 2011 Nov 2;103(21):1596-612.
22. Pecot CV, Calin GA, Coleman RL, Lopez-Berestein G, Sood AK. RNA interference in the clinic: challenges and future directions. Nat Rev Cancer. 2011 Jan;11(1):59-67.
23. ten Dijke P, Goumans MJ, Pardali E. Endoglin in angiogenesis and vascular diseases. Angiogenesis. 2008;11(1):79-89.
24. Koleva RI, Conley BA, Romero D, Riley KS, Marto JA, Lux A, et al. Endoglin structure and function: Determinants of endoglin phosphorylation by transforming growth factor-beta receptors. J Biol Chem. 2006 Sep 1;281(35):25110-23.
25. Rodriguez-Barbero A, Obreo J, Alvarez-Munoz P, Pandiella A, Bernabeu C, Lopez-Novoa JM. Endoglin modulation of TGF-beta1-induced collagen synthesis is dependent on ERK1/2 MAPK activation. Cell Physiol Biochem. 2006;18(1-3):135-42.
26. She X, Matsuno F, Harada N, Tsai H, Seon BK. Synergy between anti-endoglin (CD105) monoclonal antibodies and TGF-beta in suppression of growth of human endothelial cells. Int J Cancer. 2004 Jan 10;108(2):251-7.
27. Yoshitomi H, Kobayashi S, Ohtsuka M, Kimura F, Shimizu H, Yoshidome H, et al. Specific expression of endoglin (CD105) in endothelial cells of intratumoral blood and lymphatic vessels in pancreatic cancer. Pancreas. 2008 Oct;37(3):275-81.
28. Hu D, Wang X, Mao Y, Zhou L. Identification of CD105 (endoglin)-positive stem-like cells in rhabdoid meningioma. J Neurooncol. 2012 Feb;106(3):505-17.
29. Henriksen R, Gobl A, Wilander E, Oberg K, Miyazono K, Funa K. Expression and prognostic significance of TGF-beta isotypes, latent TGF-beta 1 binding protein, TGF-beta type I and type II receptors, and endoglin in normal ovary and ovarian neoplasms. Lab Invest. 1995 Aug;73(2):213-20.
30. Ho CM, Chang SF, Hsiao CC, Chien TY, Shih DT. Isolation and characterization of stromal progenitor cells from ascites of patients with epithelial ovarian adenocarcinoma. J Biomed Sci. 2012;19:23.
31. Pierelli L, Bonanno G, Rutella S, Marone M, Scambia G, Leone G. CD105 (endoglin) expression on hematopoietic stem/progenitor cells. Leuk Lymphoma. 2001 Nov-Dec;42(6):1195-206.
32. Aslan H, Zilberman Y, Kandel L, Liebergall M, Oskouian RJ, Gazit D, et al. Osteogenic differentiation of noncultured immunoisolated bone marrow-derived CD105+ cells. Stem Cells. 2006 Jul;24(7):1728-37.

33. Jiang T, Liu W, Lv X, Sun H, Zhang L, Liu Y, et al. Potent in vitro chondrogenesis of CD105 enriched human adipose-derived stem cells. Biomaterials. 2010 May;31(13):3564-71.
34. Irminger-Finger I. BARD1, a possible biomarker for breast and ovarian cancer. Gynecol Oncol. 2010 May;117(2):211-5.
35. Irminger-Finger I, Busquets S, Calabrio F, Lopez-Soriano FJ, Argiles JM. BARD1 content correlates with increased DNA fragmentation associated with muscle wasting in tumour-bearing rats. Oncol Rep. 2006 Jun;15(6):1425-8.
36. Jang KY, Kim KS, Hwang SH, Kwon KS, Kim KR, Park HS, et al. Expression and prognostic significance of SIRT1 in ovarian epithelial tumours. Pathology. 2009;41(4):366-71.
37. Chu F, Chou PM, Zheng X, Mirkin BL, Rebbaa A. Control of multidrug resistance gene mdr1 and cancer resistance to chemotherapy by the longevity gene sirt1. Cancer Res. 2005 Nov 15;65(22):10183-7.
38. Salva E, Kabasakal L, Eren F, Ozkan N, Cakalagaoglu F, Akbuga J. Local delivery of chitosan/VEGF siRNA nanoplexes reduces angiogenesis and growth of breast cancer in vivo. Nucleic Acid Ther. 2012 Feb;22(1):40-8.
39. Han HD, Mora EM, Roh JW, Nishimura M, Lee SJ, Stone RL, et al. Chitosan hydrogel for localized gene silencing. Cancer Biol Ther. 2011 May 1;11(9):839-45.
40. Rudzinski WE, Aminabhavi TM. Chitosan as a carrier for targeted delivery of small interfering RNA. Int J Pharm. 2010 Oct 31;399(1-2):1-11.
41. Mao S, Sun W, Kissel T. Chitosan-based formulations for delivery of DNA and siRNA. Adv Drug Deliv Rev. 2010 Jan 31;62(1):12-27.
42. Feng S, Agoulnik IU, Truong A, Li Z, Creighton CJ, Kaftanovskaya EM, et al. Suppression of relaxin receptor RXFP1 decreases prostate cancer growth and metastasis. Endocr Relat Cancer. 2010;17(4):1021-33.
43. Dass CR, Choong PF. The use of chitosan formulations in cancer therapy. J Microencapsul. 2008 Jun;25(4):275-9.
44. Howard KA, Rahbek UL, Liu X, Damgaard CK, Glud SZ, Andersen MO, et al. RNA interference in vitro and in vivo using a novel chitosan/siRNA nanoparticle system. Mol Ther. 2006 Oct;14(4):476-84.
45. Rosen LS, Hurwitz HI, Wong MK, Goldman J, Mendelson DS, Figg WD, et al. A Phase I First-in-Human Study of TRC105 (Anti-Endoglin Antibody) in Patients with Advanced Cancer. Clin Cancer Res. 2012 Sep 1;18(17):4820-9.
46. Tsujie M, Tsujie T, Toi H, Uneda S, Shiozaki K, Tsai H, et al. Anti-tumor activity of an anti-endoglin monoclonal antibody is enhanced in immunocompetent mice. Int J Cancer. 2008 May 15;122(10):2266-73.

FIGURE LEGENDS

FIGURE 1. A) Endoglin expression in multiple ovarian cancer cell lines, as measured by Western blot. B) As assessed by IHC, endoglin expression is predominantly cytoplasmic, though some cells with strong membranous staining are noted (arrows). C) A small but distinct endoglin-positive population is seen by flow cytometry. D) Endoglin was effectively downregulated with siRNA. By TUNEL assay, Annexin V/PI co-fluorescence demonstrate a decrease in viable cells, and an increase in both early and late apoptosis, both alone and in combination with cisplatin. E) Cells treated with increasing doses of cisplatin after endoglin downregulation were also assessed by MTT, with the OD570 reflecting the absorbance produced by viable cells. Endoglin downregulation resulted in a significant reduction in cell viability, and increased cisplatin chemosensitivity about 4-fold in ES2 model and 2-fold in HeyA8MDR. Lines denoting the calculated IC50 for control and endoglin-siRNA treatment are shown (grey lines).

FIGURE 2. ES2 cells were evaluated for DNA damage after endoglin targeting. SiRNA-mediated endoglin downregulation induces significant persistent DNA damage, as indicated by alkaline comet assay mean tail moment (A), and visually at 24 hours (B, Original magnification, ×100). This is not a result of immediate apoptosis, as demonstrated by a predominance of large nuclei despite a prominent comet tail (C). Downregulation also induces activation of γ-H2AX foci, a specific measure of double-stranded DNA damage (D). The combination of endoglin downregulation and cisplatin on induction of γ-H2AX foci was greater than either agent alone. Error bars represent SEM.

FIGURE 3. A) ES2 and HeyA8MDR cells were exposed to endoglin-targeting siRNA or control siRNA, mRNA extracted 48 hours later, and subjected to quantitative PCR for selected genes. Each collection was performed in triplicate, and the mean change over housekeeping gene presented. Significant decreases were noted in H2AFX, BARD1, NBN, NTHL1, and SIRT1. Induction of DDIT3 and PPP1R15A was also significant. B) BARD1 mRNA was assessed by qPCR in a triad of progressively platinum-resistant A780 cell lines, and noted to be significantly increased in A2780cp55 at baseline, and in A2780ip2 and A2780cp20 with exposure to carboplatin. C) The copper transporter ATP7B was also modestly, but significantly, reduced with endoglin downregulation.

FIGURE 4. An orthotopic murine model using ES2 and HeyA8MDR cell lines was employed to evaluate treatment with control siRNA-CH alone, control siRNA-CH with carboplatin, anti-endoglin siRNA-CH alone, or anti-endoglin siRNA-CH plus carboplatin. A) In the ES2 model, carboplatin was ineffective, as expected given the platinum-resistant nature of the ES2 cell line. Mice treated with anti-endoglin siRNA-CH alone and combined with carboplatin demonstrated less tumor burden when compared to control or carboplatin alone. Those treated with both anti-endoglin siRNA-CH and carboplatin also demonstrated reduced tumor burden when compared to those endoglin-siRNA-CH alone ($p=0.03$). B) In the HeyA8MDR model, tumors were smaller in mice treated with carboplatin or anti-endoglin siRNA-CH alone, and again combination therapy was more effective than either agent alone ($p<0.05$). C) By qualitative assessment with IHC, endoglin expression was reduced in the tumors treated with endoglin-siRNA-CH therapy.

FIGURE 5. Tumors from each treatment group in our orthotopic mouse model were collected and analyzed by PCNA immunohistochemistry, TUNEL assay, γ-H2AX IHC and 53BP1 IHC. A) There were no significant differences in PCNA IHC, with approximately half of cells being positive. B) There was a significant increase in apoptosis in the cohort receiving combination therapy when compared to control as demonstrated by TUNEL assay. C) Fluorescent IHC was performed to evaluate for γ-H2AX as an indicator of DNA damage. There was a significantly higher amount of DNA damage in both treatment groups receiving anti-endoglin treatment when compared to control or single-agent carboplatin. D) Lastly, 53BP1 is a key protein in the DNA damage checkpoint that was evaluated by IHC. A significantly higher amount of 53BP1 was noted in both cohorts that received anti-endoglin treatment when compared to either control or single-agent carboplatin.

Figure 1.

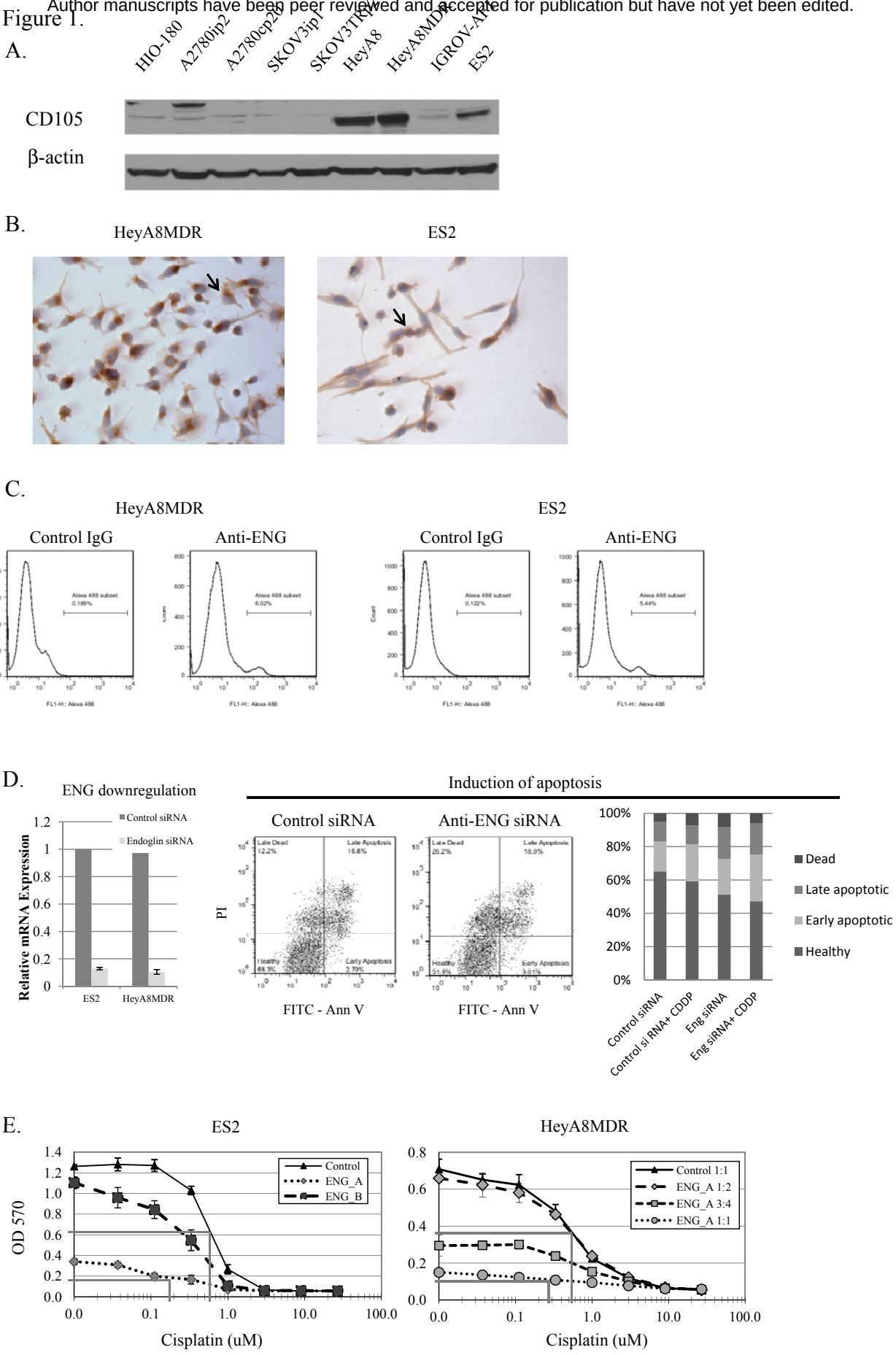

Figure 2.

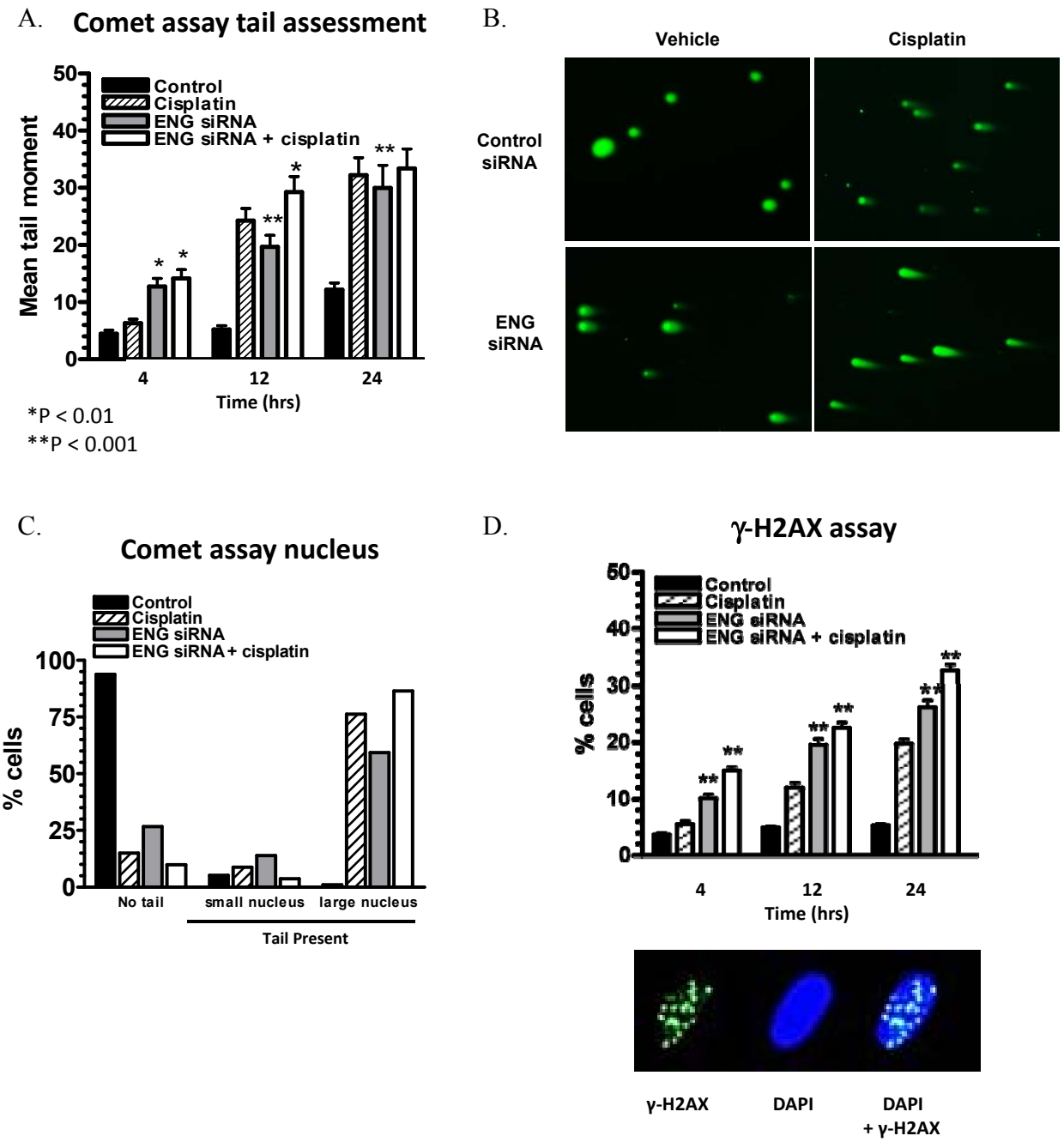

Figure 3.

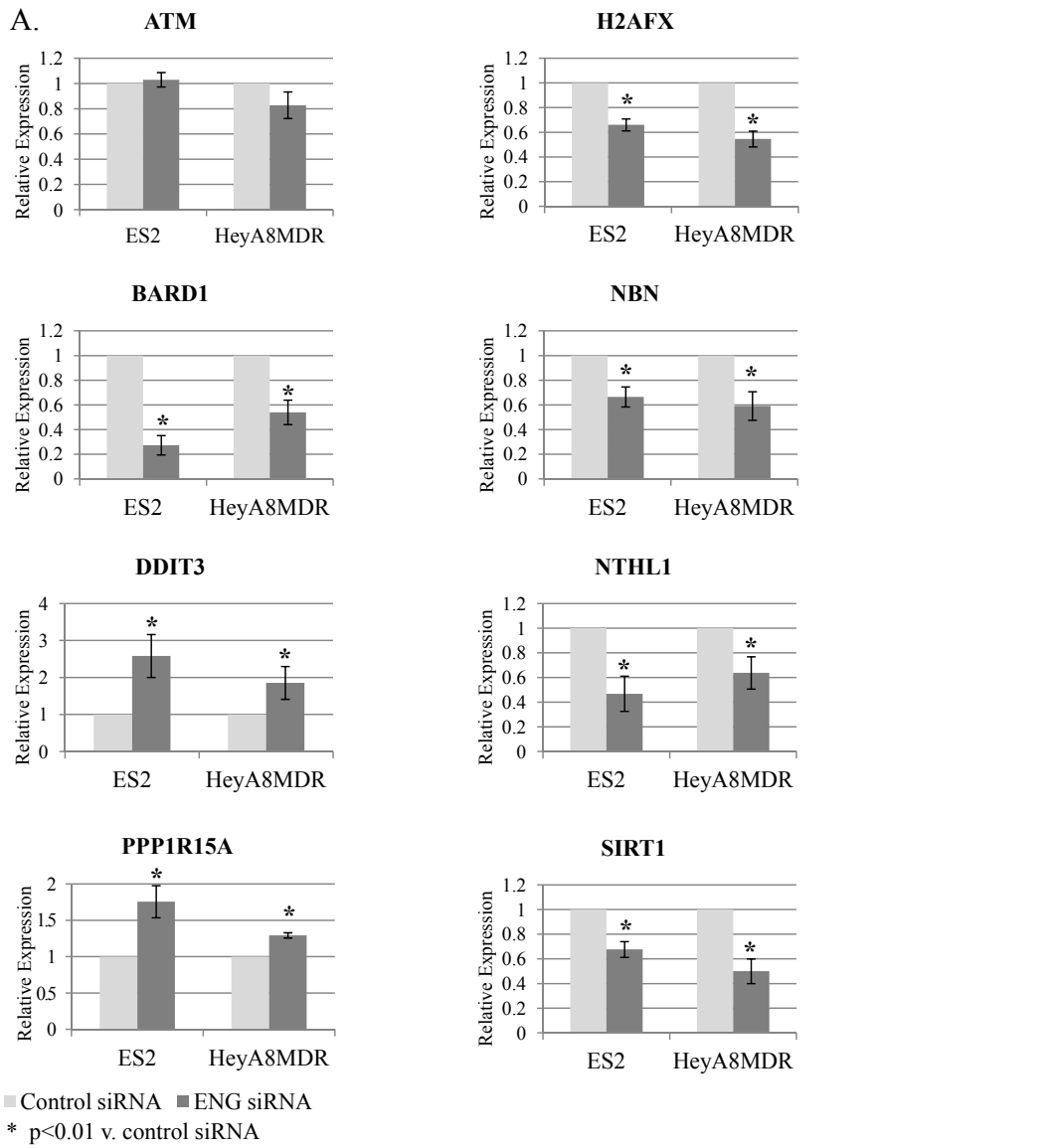

Figure 4.

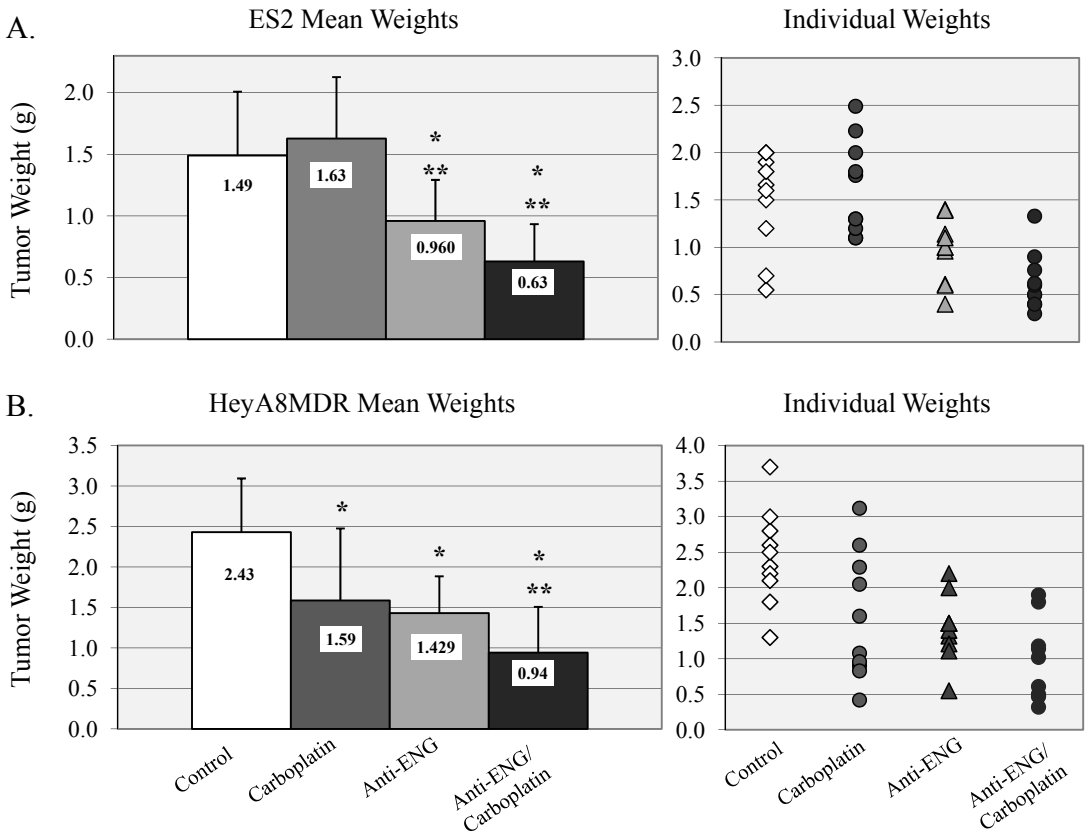

* - p<0.05 v. control
** - p< 0.05 v. carboplatin

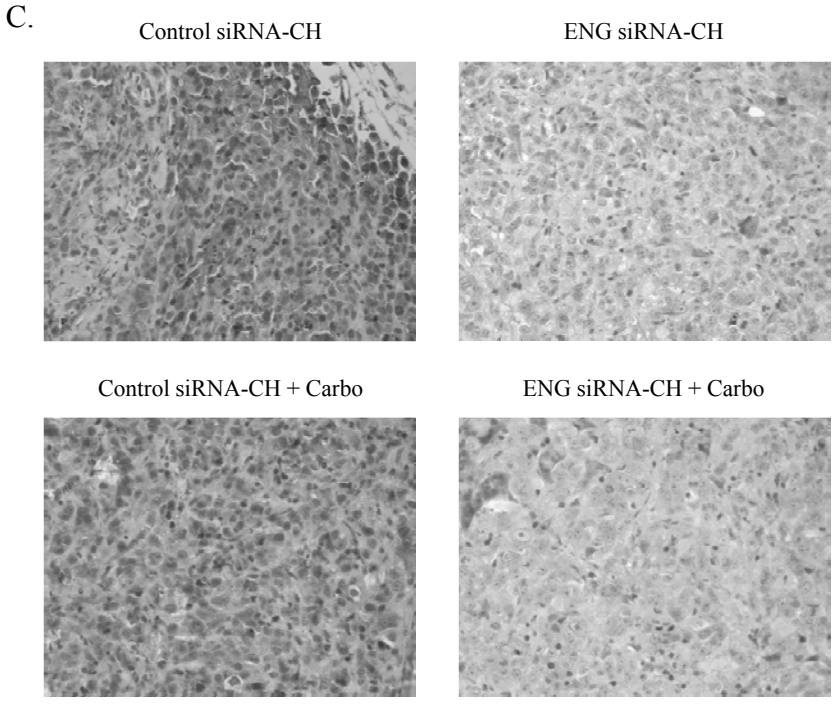

Author Manuscript Published OnlineFirst on November 12, 2012; DOI:10.1158/1078-0432.CCR-12-1045
Author manuscripts have been peer reviewed and accepted for publication but have not yet been edited.

Figure 5.

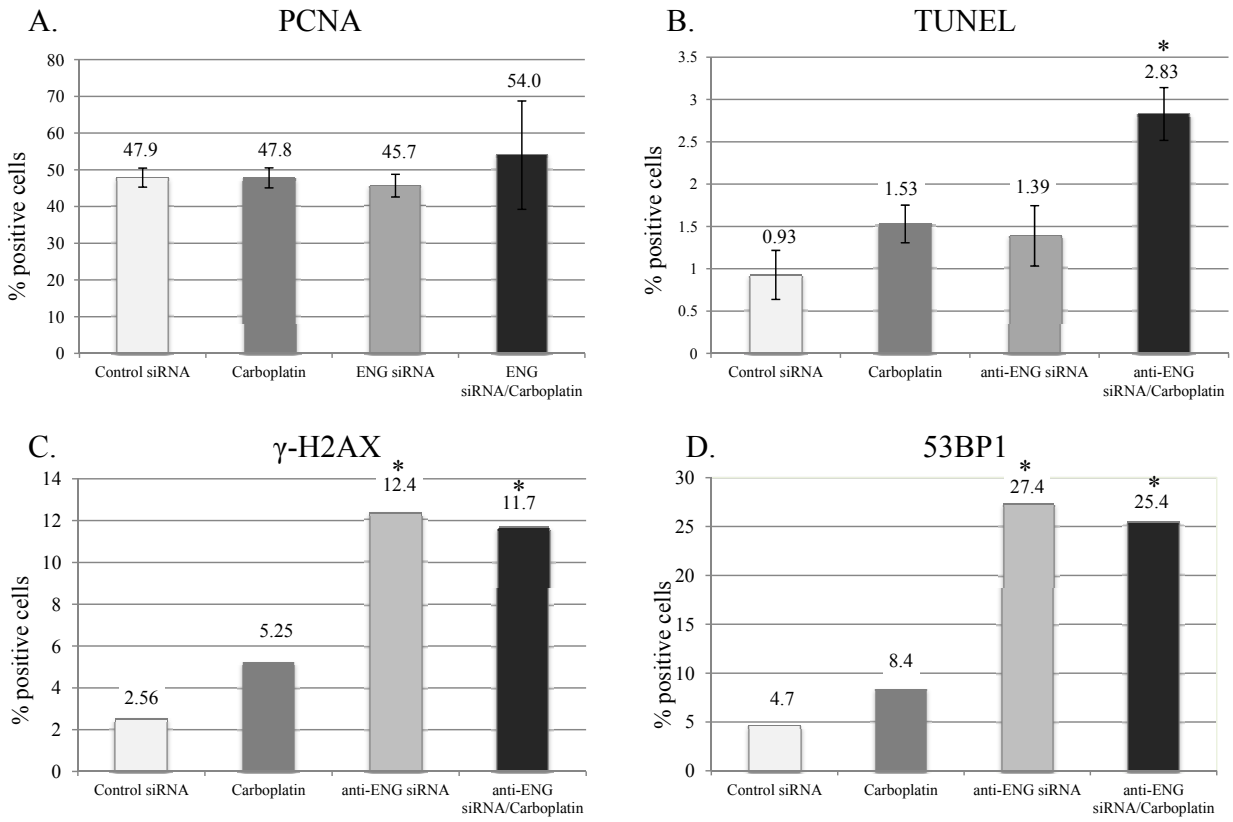

* $P < 0.01$ compared to control

Preclinical Development

Molecular Cancer Therapeutics

Smoothened Antagonists Reverse Taxane Resistance in Ovarian Cancer

Adam D. Steg, Ashwini A. Katre, Kerri S. Bevis, Angela Ziebarth, Zachary C. Dobbin, Monjri M. Shah, Ronald D. Alvarez, and Charles N. Landen

Abstract

The hedgehog (HH) pathway has been implicated in the formation and maintenance of a variety of malignancies, including ovarian cancer; however, it is unknown whether HH signaling is involved in ovarian cancer chemoresistance. The goal of this study was to determine the effects of antagonizing the HH receptor, Smoothened (Smo), on chemotherapy response in ovarian cancer. Expression of HH pathway members was assessed in three pairs of parental and chemotherapy-resistant ovarian cancer cell lines (A2780ip2/A2780cp20, SKOV3ip1/SKOV3TRip2, HeyA8/HeyA8MDR) using quantitative PCR and Western blot analysis. Cell lines were exposed to increasing concentrations of two different Smo antagonists (cyclopamine, LDE225) alone and in combination with carboplatin or paclitaxel. Selective knockdown of Smo, Gli1, or Gli2 was achieved using siRNA constructs. Cell viability was assessed by MTT assay. A2780cp20 and SKOV3TRip2 orthotopic xenografts were treated with vehicle, LDE225, paclitaxel, or combination therapy. Chemoresistant cell lines showed higher expression (>2-fold, $P < 0.05$) of HH signaling components compared with their respective parental lines. Smo antagonists sensitized chemotherapy-resistant cell lines to paclitaxel, but not to carboplatin. LDE225 treatment also increased sensitivity of ALDH-positive cells to paclitaxel. A2780cp20 and SKOV3TRip2 xenografts treated with combined LDE225 and paclitaxel had significantly less tumor burden than those treated with vehicle or either agent alone. Increased taxane sensitivity seems to be mediated by a decrease in P-glycoprotein (MDR1) expression. Selective knockdown of Smo, Gli1, or Gli2 all increased taxane sensitivity. Smo antagonists reverse taxane resistance in chemoresistant ovarian cancer models, suggesting combined anti-HH and chemotherapies could provide a useful therapeutic strategy for ovarian cancer. *Mol Cancer Ther; 1–11. ©2012 AACR.*

Introduction

Ovarian cancer is the leading cause of death from a gynecologic malignancy. Although ovarian cancer is among the most chemosensitive malignancies at the time of initial treatment (surgery and taxane/platinum-based chemotherapy), most patients will develop tumor recurrence and succumb to chemoresistant disease (1). Evaluation of multiple chemotherapy agents in several combinations in the last 20 years has yielded modest improvements in progression-free survival, but no increase in durable cures. This clinical course suggests that a population of tumor cells has either inherent or acquired resistance to chemotherapy that allows survival with initial therapy and ultimately leads to recurrence. Targeting the cellular pathways involved in this resistance may provide new treatment modalities for ovarian cancer.

The Hedgehog (HH) pathway plays an important role in cell growth and differentiation during embryonic development (2). There are 3 known mammalian HH ligands—Sonic, Indian, and Desert. These ligands are secreted peptides that bind to the transmembrane Patched (Ptch) receptor. In the absence of HH ligand, Ptch serves as a negative regulator of Smoothened (Smo), a G-protein–coupled receptor. In the presence of HH ligand, Ptch repression of Smo is abolished, leading to downstream activation of the Gli family of transcription factors (Gli1, refs. 2, 3). Gli transcription factors translocate from the cytoplasm to the nucleus, where they bind DNA and activate transcription of HH target genes, including *PTCH1* and *GLI1*, the expression of which are frequently measured to evaluate the presence or absence of HH pathway activity (3, 4). Gli homologues have distinct, but overlapping functions; Gli1 serves only as a transcriptional activator, whereas Gli2 and Gli3 are capable of both activating and repressing HH gene transcription.

Recent reports have implicated HH signaling in multiple malignancies (5, 6), including ovarian cancer (7–9), and suggest this pathway may be especially important in maintaining the subpopulation of cancer cells with stem

Authors' Affiliation: Department of Obstetrics and Gynecology, University of Alabama at Birmingham, Birmingham, Alabama

Corresponding Author: Charles N. Landen, Department of Obstetrics and Gynecology, The University of Alabama at Birmingham, 1825 University Boulevard, 505 Shelby Building, Birmingham, AL 35294. Phone: 205-934-0473; Fax: 205-934-0474; E-mail: clanden@uab.edu

doi: 10.1158/1535-7163.MCT-11-1058

cell properties (10, 11) as well as conferring resistance to chemotherapies (12, 13). Inhibition of the HH signaling pathway, therefore, has become a desirable therapeutic strategy for the treatment of various cancers. Cyclopamine, a steroidal alkaloid derived from the lily plant *Veratrum californicum*, was the first compound identified that inactivates HH signaling by antagonizing Smo function (14–16). Since this discovery, pharmaceutical companies have synthesized more selective Smo antagonists, including NVP-LDE225 (17), which is currently being investigated in clinical trials (11).

The effects of Smo antagonists, both alone and in combination with chemotherapies, remains an active area of study in cancer research. Examination of combination effects is potentially important, given the hypothesized role of stem cell pathways in chemoresistance. However, the mechanisms by which HH inhibition might sensitize cells to chemotherapy, and whether such an approach would be effective in ovarian cancer, are not known. In our study, we sought to determine the effects of Smo antagonists on the viability of ovarian cancer cells, both alone and in combination with chemotherapy. We show that Smo antagonists have activity alone, but more dramatically can reverse taxane resistance in ovarian cancer, both *in vitro* and *in vivo*, through modulation of the multidrug resistance mediator, P-glycoprotein (MDR1). These findings provide new insight into HH signaling, its contribution to an aggressive subpopulation of cells, and new opportunities for clinical development.

Materials and Methods

Reagents and cell culture

Cyclopamine was purchased from Toronto Research Chemicals and dissolved in 95% ethanol to create a 10 mmol/L stock solution. NVP-LDE225 (LDE225) was kindly provided by Novartis Pharma AG and dissolved in dimethyl sulfoxide (DMSO) to create a 10 mmol/L stock solution. The ovarian cancer cell lines A2780ip2, A2780cp20, HeyA8, HeyA8MDR, SKOV3ip1, and SKOV3TRip2 (18–23) were maintained in RPMI-1640 medium supplemented with 10% FBS (Hyclone). A2780cp20 (platinum- and taxane-resistant), HeyA8MDR (taxane-resistant), and SKOV3TRip2 (taxane-resistant, a kind gift of Dr Michael Seiden; ref. 24) were generated by sequential exposure to increasing concentrations of chemotherapy (25). HeyA8MDR and SKOV3TRip2 were maintained with the addition of 150 ng/mL of paclitaxel. All cell lines were routinely screened for *Mycoplasma* species (GenProbe detection kit; Fisher) with experiments done at 70% to 80% confluent cultures. Purity of cell lines was confirmed with STR genomic analysis, and only cells less than 20 passages from stocks were used in experiments.

RNA extraction and reverse transcription

Total RNA was isolated from ovarian cancer cell lines using TRIzol reagent (Invitrogen) per manufacturer's instructions. RNA was then DNase treated and purified using the RNeasy Mini Kit (QIAGEN). RNA was eluted in 50 μL of RNase-free water and stored at −80°C. The concentration of all RNA samples was quantified by spectrophotometric absorbance at 260/280 nm using an Eppendorf BioPhotometer plus. Before cDNA synthesis, all RNA samples were diluted to 20 ng/μL using RNase-free water. cDNA was prepared using the High Capacity cDNA Reverse Transcription Kit (Applied Biosystems). The resulting cDNA samples were analyzed using quantitative PCR (qPCR).

Quantitative PCR

Primer and probe sets for *Desert HH* (Hs0036806_m1), *GLI1* (Hs00171790_m1), *GLI2* (Hs00257977_m1), *Indian HH* (Hs00745531_s1), *MDR1* (Hs00184500_m1), *PTCH1* (Hs00181117_m1), *SMO* (Hs00170665_m1), *Sonic HH* (Hs), and *RPLP0* (Hs99999902_m1; housekeeping gene) were obtained from Applied Biosystems and used according to manufacturer's instructions. PCR amplification was conducted on an ABI Prism 7900HT sequence detection system and gene expression was calculated using the comparative C_T method as previously described (26). Briefly, this technique uses the formula $2^{-\Delta\Delta C}{}_T$ to calculate the expression of target genes normalized to a calibrator. The cycling threshold (C_T) indicates the cycle number at which the amount of amplified target reaches a fixed threshold. C_T values range from 0 to 40 (the latter representing the default upper limit PCR cycle number that defines failure to detect a signal).

Western blot analysis

Cultured cell lysates were collected in modified radioimmunoprecipitation assay lysis buffer with protease inhibitor cocktail (Roche) and subjected to immunoblot analysis by standard techniques (25) using anti-Gli1 antibody (Cell Signaling Technology) at 1:1,000 dilution overnight at 4°C, anti-Smo antibody (LifeSpan Biosciences) at 1:1,000 dilution overnight at 4°C, or anti-β-actin antibody (AC-15, Sigma-Aldrich) at 1:20,000 dilution for 1 hour at room temperature (RT), which was used to monitor equal sample loading. After washing, blots were incubated with goat anti-rabbit (for Gli1 and Smo) or goat anti-mouse (for β-actin) secondary antibodies (Bio-Rad) conjugated with horseradish peroxidase. Visualization was done by the enhanced chemiluminescence method (Pierce Thermo Scientific).

siRNA transfection

To examine downregulation of Smo, Gli1, or Gli2 individually with siRNA, cells were exposed to control siRNA (target sequence: 5′-UUCUCCGAACGUGUCACGU-3′, Sigma-Aldrich), one of 2 tested Smo-targeting constructs (siRNA1: 5′-GAGGAGUCAUGACUCUGUUCUCCAU-3′ or siRNA2: 5′-UGACCUCAAUGAGCCCUCAGCU-GAU-3′; Invitrogen), one of 2 tested Gli1-targeting constructs (siRNA1: 5′-CUACUGAUACUCUGGGAUA-3′ or siRNA2: 5′-GCAAAUAGGGCUUCACAUA-3′;

Sigma-Aldrich), or one of 2 tested Gli2-targeting constructs (siRNA1: 5′-GACAUGAGCUCCAUGCUCA-3′ or siRNA2: 5′-CGAUUGACAUGCGACACCA-3′; Sigma-Aldrich) at a 1:3 siRNA (μg) to Lipofectamine 2000 (μL) ratio. Lipofectamine and siRNA were incubated for 20 minutes at RT, added to cells in serum-free RPMI to incubate for up to 8 hours, followed by 10% FBS/RMPI thereafter. Transfected cells were grown at 37°C for 48 to 72 hours and then harvested for qPCR or Western blot analysis.

Assessment of cell viability and cell-cycle analysis

To a 96-well plate, 2,000 cells/well were exposed to increasing concentrations of cyclopamine or LDE225, alone or in combination with carboplatin or paclitaxel, in triplicate. Viability was assessed with 0.15% MTT (Sigma-Aldrich). For effects of siRNA-mediated downregulation on paclitaxel IC_{50}, cells were first transfected with siRNA (5 μg) for 24 hours in 6-well plates, then trypsinized and replated at 2,000 cells per well, followed by addition of chemotherapy after attachment. IC_{50} of the agent of interest was determined by finding the dose at which the drug had 50% of its effect, calculated by the equation $[(OD450_{MAX} - OD450_{MIN})/2) + OD450_{MIN}]$. For cell-cycle analysis, cells were treated with vehicle alone, paclitaxel alone, LDE225 alone, or combined LDE225 and paclitaxel for 72 hours, trypsinized, and fixed in 100% ethanol overnight. Cells were then centrifuged, washed in PBS, and resuspended in PBS containing 0.1% Triton X-100 (v/v), 200 μg/mL DNase-free RNase A, and 20 μg/mL propidium iodide (PI). PI fluorescence was assessed by flow cytometry and the percentage of cells in sub-G_0, G_0–G_1, S-, and G_2–M phases was calculated by the cell-cycle analysis module for Flow Cytometry Analysis Software (FlowJo v.7.6.1).

ALDEFLUOR assay

Active aldehyde dehydrogenase (ALDH) was identified with the ALDEFLUOR assay according to manufacturer's instructions (StemCell Technologies). The ALDH-positive population was defined by cells with increased FITC signal absent in DEAB-treated cells, as previously described (27). ALDEFLUOR-positive and -negative populations from SKOV3Trip2 cells were sorted with a FACS Aria II flow cytometer (BD Biosciences), and collected cells were seeded onto a 96-well plate at a concentration of 2,000 cells/well. After overnight attachment, cells were then exposed to either DMSO or 5 μmol/L LDE225, alone or in combination with increasing concentrations of paclitaxel. Viability was assessed with 0.15% MTT (Sigma-Aldrich).

Orthotopic ovarian cancer model

For orthotopic therapy experiments using ovarian cancer cell lines, female athymic nude mice (NCr-nu) were purchased from the National Cancer Institute (Frederick, MD, USA) after Institution Animal Care and Use Committee approval of protocols, and cared for in accordance with guidelines of the American Association for Accreditation of Laboratory Animal Care. For all *in vivo* experiments, trypsinized cells were resuspended in 10% FBS-containing RPMI, washed with PBS, and suspended in serum-free HBSS at a concentration of 5×10^6 cells/mL, and 1×10^6 cells (A2780cp20 or SKOV3TRip2) were injected IP in 200 μL into 40 mice per experiment. After 1 week, mice ($n = 10$ per group) were randomized to treatment with (a) vehicle alone (0.5% methyl cellulose/0.5% Tween 80 in sterile water), (b) vehicle plus paclitaxel 75 μg, (c) LDE225 alone (60 mg/kg), or (d) combined LDE225 and paclitaxel. Vehicle and LDE225 were administered by gavage once daily and paclitaxel was administered i.p. weekly. Mice were treated for 4 weeks (A2780cp20) or 6 weeks (SKOV3TRip2, which grow more slowly) before sacrifice and tumor collection. All tumors were excised and weighed in total.

Statistical analysis

Comparisons of gene expression, cell viability, PI fluorescence, and mean tumor weight were analyzed using a 2-tailed Student *t* test, if assumptions of data normality were met. Those represented by alternate distribution were examined using a nonparametric Mann–Whitney *U* test. Differences between groups were considered statistically significant at $P < 0.05$. Error bars represent standard deviation unless otherwise stated. Number of mice per group ($n = 10$) was chosen as directed by a power analysis to detect a 50% decrease in tumor growth with β error of 0.2.

Results

Expression of HH pathway members in chemosensitive and chemoresistant ovarian cancer cell lines

We first examined mRNA expression of HH ligands [Sonic (*SHH*), Indian (*IHH*), Desert (*DHH*)], receptors (*PTCH1*, *SMO*), and transcription factors (*GLI1*, *GLI2*) in 3 pairs of parental and chemoresistant ovarian cancer cell lines: A2780ip2/A2780cp20 (20-fold increased cisplatin resistance and 10-fold increased taxane resistance), HeyA8/HeyA8MDR (500-fold taxane resistant), and SKOV3ip1/SKOV3TRip2 (1000-fold taxane resistant). As shown in Fig. 1A, mRNA levels of *SHH* were significantly higher in A2780cp20 (17.4-fold, $P < 0.05$) and SKOV3-TRip2 (2.4-fold, $P < 0.05$) cells compared with parental. *IHH* was also higher (3.5-fold, $P < 0.05$) in SKOV3TRip2 cells with *DHH* expression remaining unchanged or decreased in chemoresistant cell lines compared with parental. mRNA levels of *PTCH1* were significantly higher (2.1-fold, $P < 0.05$) in SKOV3TRip2 compared with parental SKOV3ip1 cells; however, no significant changes in *SMO* expression were observed between chemoresistant and chemosensitive cell lines (Fig. 1B). Protein expression of Smo was confirmed in all cell lines tested and did not always correlate with expression at the mRNA level (Fig. 1C). *GLI1* mRNA expression was significantly

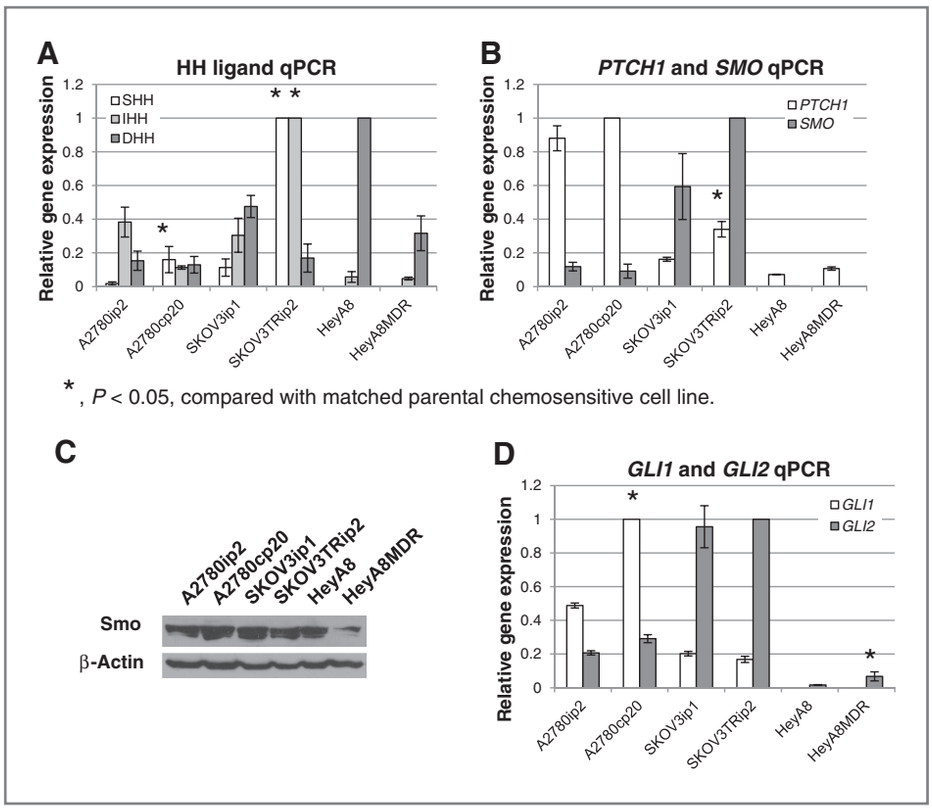

Figure 1. Expression of HH signaling components in chemosensitive and chemoresistant ovarian cancer cell lines. Gene expression was calculated relative to the sample/cell line with the highest expression of a particular gene. A, mRNA expression of HH ligands, Sonic (*SHH*), Indian (*IHH*), and Desert (*DHH*). B, mRNA expression of HH receptors, *PTCH1* and *SMO*. C, protein expression of Smo was also measured using Western blot analysis. β-Actin was used as a loading control. D, mRNA expression of HH transcription factors, *GLI1* and *GLI2*. Data are representative of 3 independent experiments. *, $P < 0.05$, compared with parental chemosensitive cell line.

higher (2.0-fold, $P < 0.05$) in A2780cp20 compared with parental A2780ip2 cells and *GLI2* mRNA expression was significantly higher (4.1-fold, $P < 0.05$) in HeyA8MDR compared with parental HeyA8 cells, although at very low levels in both (Fig. 1D). These results show that HH signaling is often higher in chemoresistant matched ovarian cancer cell lines.

Smo antagonists diminish cell viability and HH gene expression in ovarian cancer cell lines

Having observed Smo expression (both mRNA and protein) in both chemosensitive and chemoresistant ovarian cancer cell lines, we next examined response to the Smo antagonists cyclopamine and LDE225 among these cell lines. The chemical structure of LDE225 is shown in Fig. 2A. As shown in Table 1, cyclopamine IC_{50}s varied from 7.5 μmol/L (A2780ip2) to 19 μmol/L (SKOV3TRip2) and LDE225 IC_{50}s varied from 7.5 μmol/L (A2780cp20) to 24 μmol/L (SKOV3ip1). Interestingly, chemoresistant cell lines were more sensitive (up to 2.25-fold, $P < 0.05$) to LDE225 compared with their chemosensitive counterparts. Chemoresistant cell lines were also more sensitive to LDE225 than cyclopamine. To confirm that decreased cell viability was associated with diminished HH pathway activity, A2780cp20 cells were exposed to increasing concentrations of LDE225 (1, 5, and 10 μmol/L) for 72 hours and gene expression of HH target genes *PTCH1*, *GLI1*, and *GLI2* was analyzed by qPCR. A dose-dependent decrease in the expression of all 3 genes was observed with a maximum reduction of 39%, 43%, and 32% ($P < 0.05$), respectively, after exposure to 10 μmol/L LDE225 (Fig. 2B). Protein expression of the HH transcriptional activator Gli1 was also reduced in a dose-dependent manner after LDE225 treatment (Fig. 2C). Taken together, these data show the efficacy and HH-specific activity of LDE225 in multiple chemoresistant cell lines.

Smo antagonism reverses taxane resistance in chemoresistant ovarian cancer cell lines both *in vitro* and *in vivo*

Having observed increased expression of HH signaling components and response to Smo antagonists in chemoresistant ovarian cancer cell lines, we sought to determine whether targeting the HH pathway could increase sensitivity to carboplatin and paclitaxel, chemotherapy agents most commonly used in the treatment of ovarian cancer. Neither cyclopamine nor LDE225 affected response to carboplatin among the chemoresistant cell lines examined (data not shown). However, as shown in Table 1, both Smo antagonists significantly increased the sensitivity of all 3 chemoresistant cell lines to paclitaxel (by up to 27- and 20-fold, respectively; $P < 0.05$). Increased sensitivity to paclitaxel after combination with cyclopamine or LDE225 even occurred at low doses that were not effective alone (5 μmol/L cyclopamine, Fig. 3A and 1 μmol/L

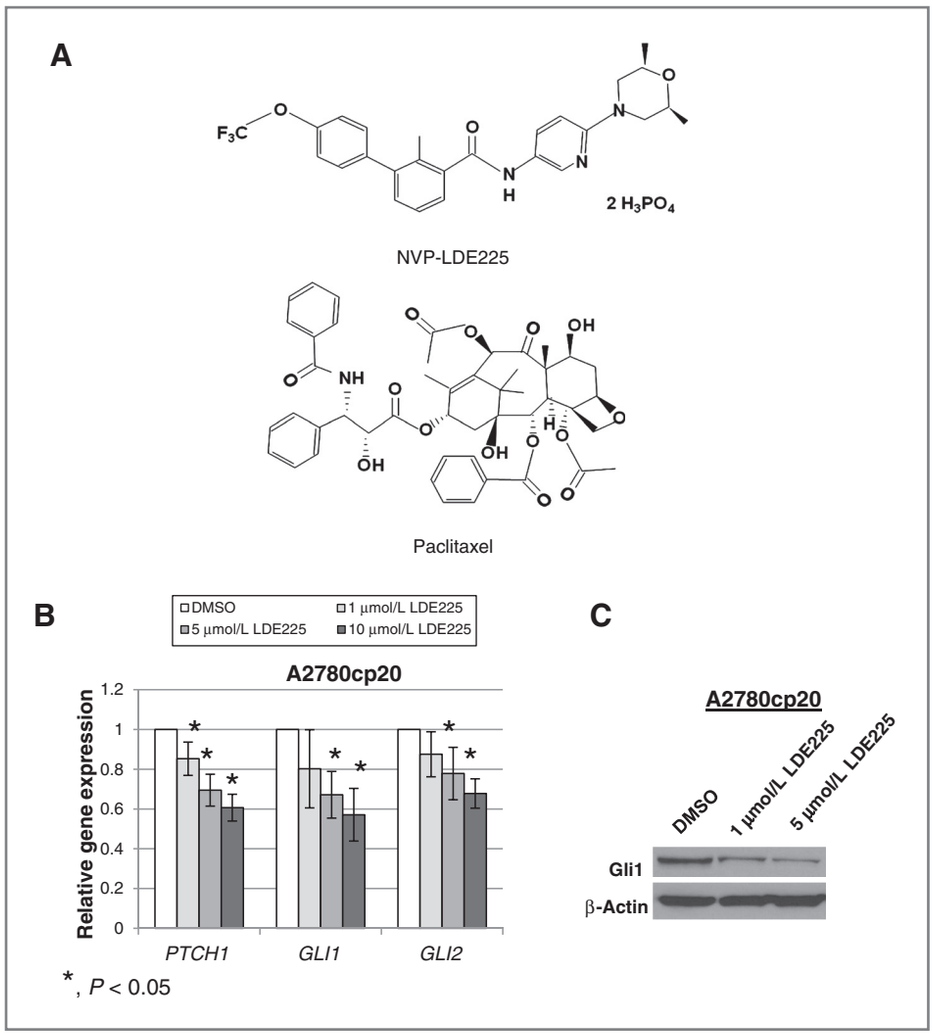

Figure 2. LDE225 reduces HH pathway activity in chemoresistant ovarian cancer cells. A, chemical structures of NVP-LDE225 and paclitaxel. B, gene expression of *PTCH1*, *GLI1*, and *GLI2* was examined in A2780cp20 cells after exposure to increasing concentrations of LDE225 using qPCR. *, $P < 0.05$, compared with DMSO vehicle control. C, protein expression of Gli1 in A2780cp20 cells after exposure to increasing concentrations of LDE225 was measured using Western blot analysis to confirm mRNA results. β-Actin was used as a loading control. Data are representative of 3 independent experiments.

LDE225, Fig. 3B). To determine the mechanism by which Smo antagonism combined with paclitaxel affects cell growth, we carried out cell-cycle analysis on A2780cp20 cells that were treated with DMSO alone (vehicle control), paclitaxel alone (30 nmol/L), LDE225 alone (5 μmol/L), or combined paclitaxel and LDE225 for 72 hours. As shown in Fig. 3C, combination treatment resulted in a greater accumulation of cells in the sub-G_0/apoptotic, S-, and G_2–M phases compared with control or either treatment alone. These data suggest that LDE225 enhances cell-cycle

Table 1. Ovarian cancer cell line response to Smo antagonists, alone and in combination with paclitaxel

	Mean IC_{50}, μmol/L		Mean paclitaxel IC_{50}, nmol/L			
Cell line	**Cyclopamine**	**LDE225**	**Control**	**w/Cyclopamine (5 μmol/L)**	**w/LDE225 (5 μmol/L)**	***P***
A2780ip2	7.5	12	4	1.5	2.6	NS
A2780cp20	10	7.5	30	1.3	1.5	<0.05
SKOV3ip1	14	24	6	3	5.5	NS
SKOV3TRip2	19	12	400	15	120	<0.05
HeyA8	12	18	7	4.2	6.5	NS
HeyA8MDR	13	8	650	50	115	<0.05

Abbreviation: NS, not significant.

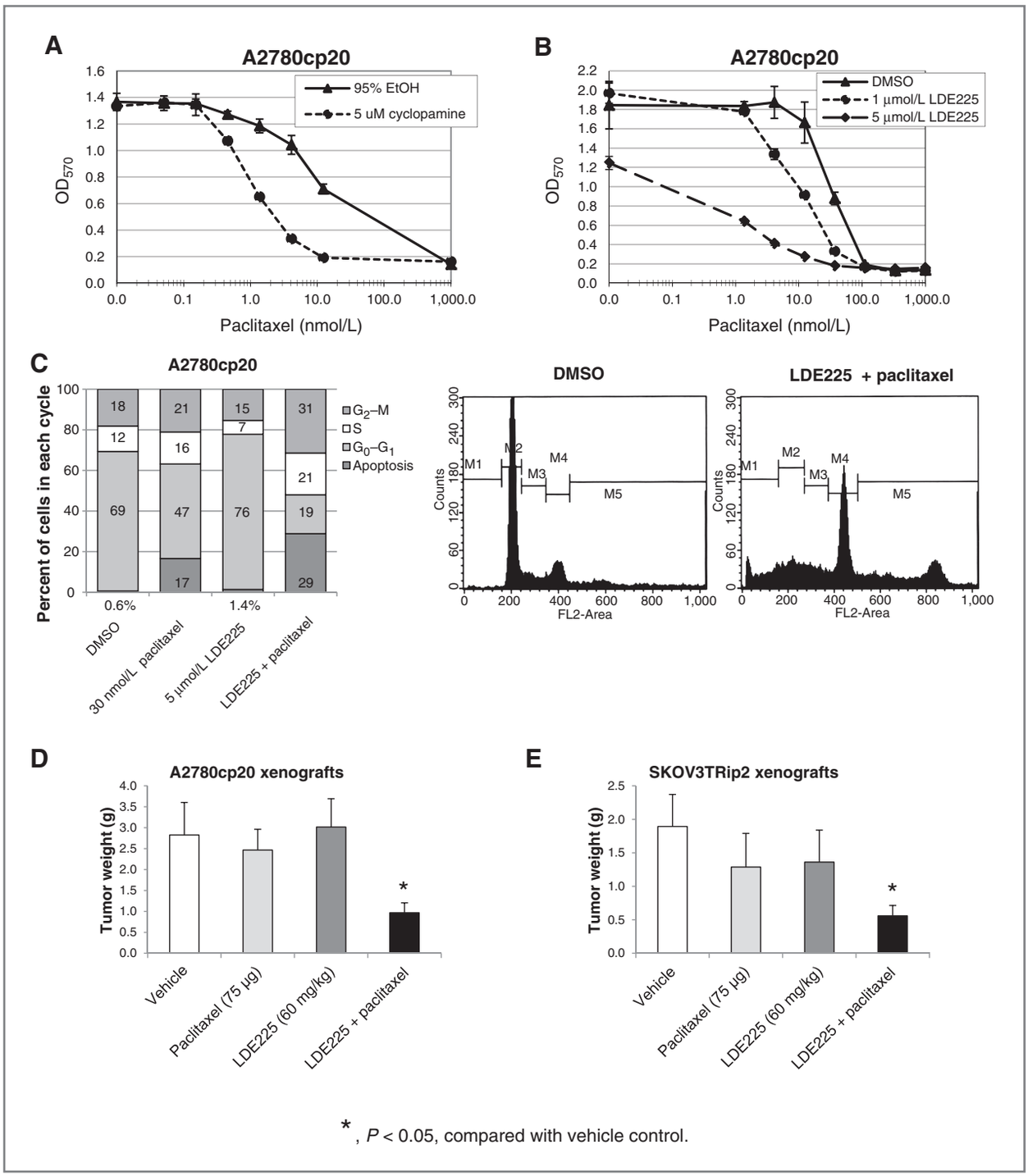

Figure 3. Smo antagonism reverses taxane resistance in chemoresistant ovarian cancer cell lines both *in vitro* and *in vivo*. A, A2780cp20 cells were exposed to either 95% ethanol (EtOH, vehicle control) or cyclopamine (5 μmol/L) in combination with increasing concentrations of paclitaxel. Cell viability was determined by MTT assay. B, A2780cp20 cells were exposed to either DMSO (vehicle control) or LDE225 (1 and 5 μmol/L) in combination with increasing concentrations of paclitaxel. Cell viability was determined by MTT assay. C, cell-cycle analysis was conducted on A2780cp20 cells treated with DMSO alone, paclitaxel alone, LDE225 alone, or combined paclitaxel and LDE225 using propidium iodide (PI) staining. Representative histograms of DMSO- and combination-treated cells are shown on the right. Data are representative of 3 independent experiments. D, mice injected intraperitoneally with A2780cp20 cells were treated with vehicle alone, paclitaxel alone, LDE225 alone, or combined paclitaxel + LDE225. E, mice injected intraperitoneally with SKOV3TRip2 cells were treated with either vehicle alone, paclitaxel alone, LDE225 alone, or combined paclitaxel + LDE225. For both xenograft models, mice treated with the combination paclitaxel + LDE225 showed a significant reduction in tumor weight compared with treatment with vehicle alone. Mean tumor weights with standard error are presented. *, $P < 0.05$, compared with vehicle control.

arrest and cell death induced by the microtubule-stabilizing effects of paclitaxel.

To determine if LDE225 can similarly reverse taxane resistance *in vivo*, an orthotopic mouse model using chemoresistant cell lines was used. Nude mice were injected intraperitoneally with either A2780cp20 or SKOV3TRip2 cells and randomized to 4 treatment groups: (a) vehicle alone, (b) paclitaxel alone (75 μg weekly), (c) LDE225 alone (60 mg/kg daily), or (d) combined paclitaxel and LDE225. When control mice started to become moribund with tumor burden, all mice were sacrificed and total tumor weights recorded. In the A2780cp20 model (Fig. 3D), there was no significant reduction in tumor growth with either paclitaxel or LDE225 alone. However, the combination of paclitaxel and LDE225 resulted in significantly reduced tumor weight, by 65.7% compared with vehicle alone ($P = 0.028$). This represented a 60.7% reduction compared with paclitaxel alone ($P = 0.014$) and a 68% reduction compared with LDE225 alone ($P = 0.010$), again showing synergy of paclitaxel and LDE225. Similar results were observed in SKOV3TRip2 xenografts (Fig. 3E). Neither paclitaxel nor LDE225 alone had a statistically significant impact on tumor growth, whereas combination treatment significantly reduced tumor weight, by 70.4% compared with vehicle alone ($P = 0.015$). This represented a 56.6% reduction compared with paclitaxel alone ($P = 0.18$) and a 58.8% reduction compared with LDE225 alone ($P = 0.13$), although neither was statistically significant.

LDE225 sensitizes chemoresistant ovarian cancer cells to paclitaxel by downregulating MDR1 expression and sensitizes both ALDH-negative and -positive ovarian cancer cells to paclitaxel

The primary mediator of taxane resistance in general, and in the chemoresistant cell lines examined in this study (27), is the expression of the drug efflux protein, P-glycoprotein (ABCB1/MDR1). To identify the mechanism underlying taxane sensitization after Smo antagonism, we next examined whether LDE225 could modulate *MDR1* gene expression. In A2780cp20 cells exposed to LDE225 alone, paclitaxel alone, and combined LDE225 + paclitaxel for 72 hours, it was observed that LDE225 decreased *MDR1* expression (by up to 49.2%, $P < 0.05$), whereas paclitaxel actually led to a compensatory *increase* in *MDR1* expression (2.88-fold, $P < 0.05$) compared with vehicle control (Fig. 4A). This compensatory increase in *MDR1* was alleviated by LDE225 in a dose-dependent manner (up to a 59.9% decrease, $P < 0.05$), showing that this compound increases sensitivity to paclitaxel, at least in part, by downregulating *MDR1*. Similar results were observed in SKOV3TRip2 cells (Fig. 4B); LDE225 decreased *MDR1* expression both alone (by up to 36.4%, $P < 0.05$ compared with vehicle control) and in combination with paclitaxel (by up to 50.8%, $P < 0.05$ compared with paclitaxel alone). In this cell line, a compensatory increase in *MDR1* was not observed with paclitaxel alone, likely because *MDR1* is already expressed at extremely high levels (140-fold more than in A2780cp20) in this 1,000-fold taxane-resistant cell line (27). To determine if similar modulation of *MDR1* occurs *in vivo*, RNA isolated from A2780cp20 tumors (from Fig. 3D) was examined. In agreement with the *in vitro* data, LDE225 alone significantly reduced *MDR1* expression (by 35.2%, $P < 0.05$) and paclitaxel alone significantly increased *MDR1* expression (2.55-fold, $P < 0.05$) compared with vehicle control (Fig. 4C). In addition, combination treatment significantly reduced *MDR1* expression compared with paclitaxel alone (by 48.8%, $P < 0.05$), blunting this compensatory rise.

In addition to our examination of MDR1 expression after LDE225 treatment, we also examined βIII-tubulin and stathmin, proteins that have been associated with microtubule regulation and resistance to taxanes (28). It was found that neither of these proteins was affected by LDE225 treatment *in vitro* (as determined by Western blot analysis, data not shown). Taken together, these data support a mechanism whereby LDE225 causes the downregulation of *MDR1* expression, which then leads to increased uptake of paclitaxel within chemoresistant cells, rather than potentiating the microtubule stabilizing effect of this compound.

We have previously shown that ALDH activity is associated with enhanced tumorigenicity and chemoresistance in ovarian cancer, and may define one of potentially many cancer cell populations with stem cell-like features (27, 29). To determine whether cancer stem cells (CSCs) might play a role in taxane sensitization after LDE225 treatment, we collected ALDH-negative and -positive cell populations from the SKOV3TRip2 cell line, and exposed them to combined LDE225 and paclitaxel. As shown in Fig. 4D, it was found that ALDH-negative and -positive SKOV3TRip2 cells showed a similar decrease in viability after LDE225 treatment alone (21.4% vs. 16.8%, respectively), compared with DMSO control. In addition, sensitivity to paclitaxel (as determined by IC_{50}) was similarly increased after combination treatment in ALDH-negative and -positive cells (5.1-fold vs. 4.0-fold change in IC_{50}, respectively). These results indicate that the more tumorigenic ALDH-positive cells are just as susceptible to LDE225 treatment as ALDH-negative cells, and that HH inhibition can sensitize both populations to taxane therapy. Whether other putative CSC populations such as CD133, CD44, and the side population, with which there is some (but not complete) crossover with the ALDH population (30), can also be sensitized to taxanes will be the subject of future investigations.

Knockdown of Smo diminishes HH pathway activity, reduces viability, and reverses taxane resistance in ovarian cancer cells

To determine whether LDE225 reverses taxane resistance through inhibition of Smo alone or off-target effects, we selectively targeted HH pathway members using siRNAs and observed effects on HH pathway activity and paclitaxel response. As shown in Fig. 5A, knockdown

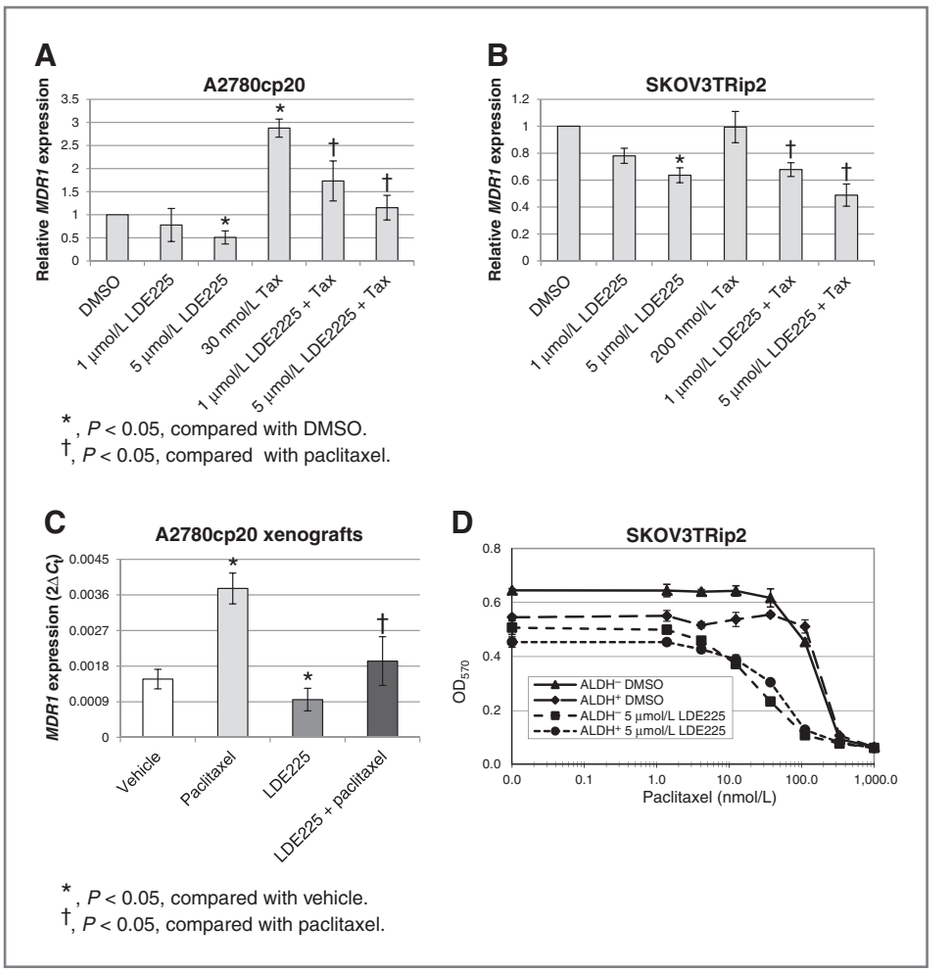

Figure 4. LDE225 sensitizes chemoresistant ovarian cancer cells to paclitaxel by downregulating MDR1 expression and sensitizes both ALDH-negative and -positive ovarian cancer cells to paclitaxel. A, A2780cp20 cells were exposed to DMSO, LDE225 (1 or 5 μmol/L), paclitaxel (Tax, 30 nmol/L), or combined LDE225 + paclitaxel for 72 hours and examined for *MDR1* gene expression. *, $P < 0.05$, compared with DMSO; †, $P < 0.05$, compared with paclitaxel alone. B, SKOV3TRip2 cells were exposed to DMSO, LDE225 (1 or 5 μmol/L), paclitaxel (Tax, 200 nmol/L), or combined LDE225 + paclitaxel for 72 hours and examined for *MDR1* gene expression. *, $P < 0.05$, compared with DMSO; †, $P < 0.05$, compared with paclitaxel alone. Data are representative of 3 independent experiments. C, A2780cp20 xenografts ($n = 5$ per group) treated with vehicle alone, paclitaxel alone, LDE225 alone, or combined LDE225 + paclitaxel were resected after 4 weeks of therapy and examined for *MDR1* gene expression. Mean expression with SE are presented. *, $P < 0.05$, compared with vehicle; †, $P < 0.05$, compared with paclitaxel alone. D, SKOV3TRip2 cells were sorted into aldehyde dehydrogenase–negative (ALDH−) and -positive (ALDH+) populations, using the ALDEFLUOR assay, and then exposed to either DMSO or 5 μmol/L LDE225, both alone and in combination with increasing concentrations of paclitaxel. Cell viability was determined by MTT assay.

of Smo was achieved both at the mRNA and protein level. As expected, this downregulation led to a significant decrease in HH target genes *PTCH1* (66.6%, $P < 0.01$), *GLI1* (86.5%, $P < 0.01$), and *GLI2* (62.0%, $P < 0.01$). Individual knockdown of HH mediators Smo, Gli1, or Gli2 using 2 distinct siRNA constructs for each gene led to increased sensitivity to paclitaxel (Fig. 5B–D). In particular, Smo knockdown decreased paclitaxel IC_{50} by up to 11.7-fold; Gli1 knockdown, up to 3.5-fold; and Gli2 knockdown, up to 5.9-fold. In agreement with cyclopamine and LDE225 biologic effects, knockdown of Smo, Gli1, or Gli2 alone significantly decreased cell viability (by up to 73.5%, 57.6%, and 26.5%, respectively, $P < 0.01$) compared with control siRNA. Collectively, these data suggest that HH signaling promotes ovarian cancer cell survival and mediates taxane resistance.

Discussion

In this study, we found that HH pathway signaling components are overexpressed in chemoresistant ovarian cancer cells. Moreover, targeting the HH pathway decreased ovarian cancer cell viability and sensitized chemoresistant ovarian cancer cells to paclitaxel therapy through decreased *MDR1* expression. The participation of HH signaling in ovarian cancer cell survival and chemotherapy resistance makes it an attractive target for therapy, especially because most patients with ovarian

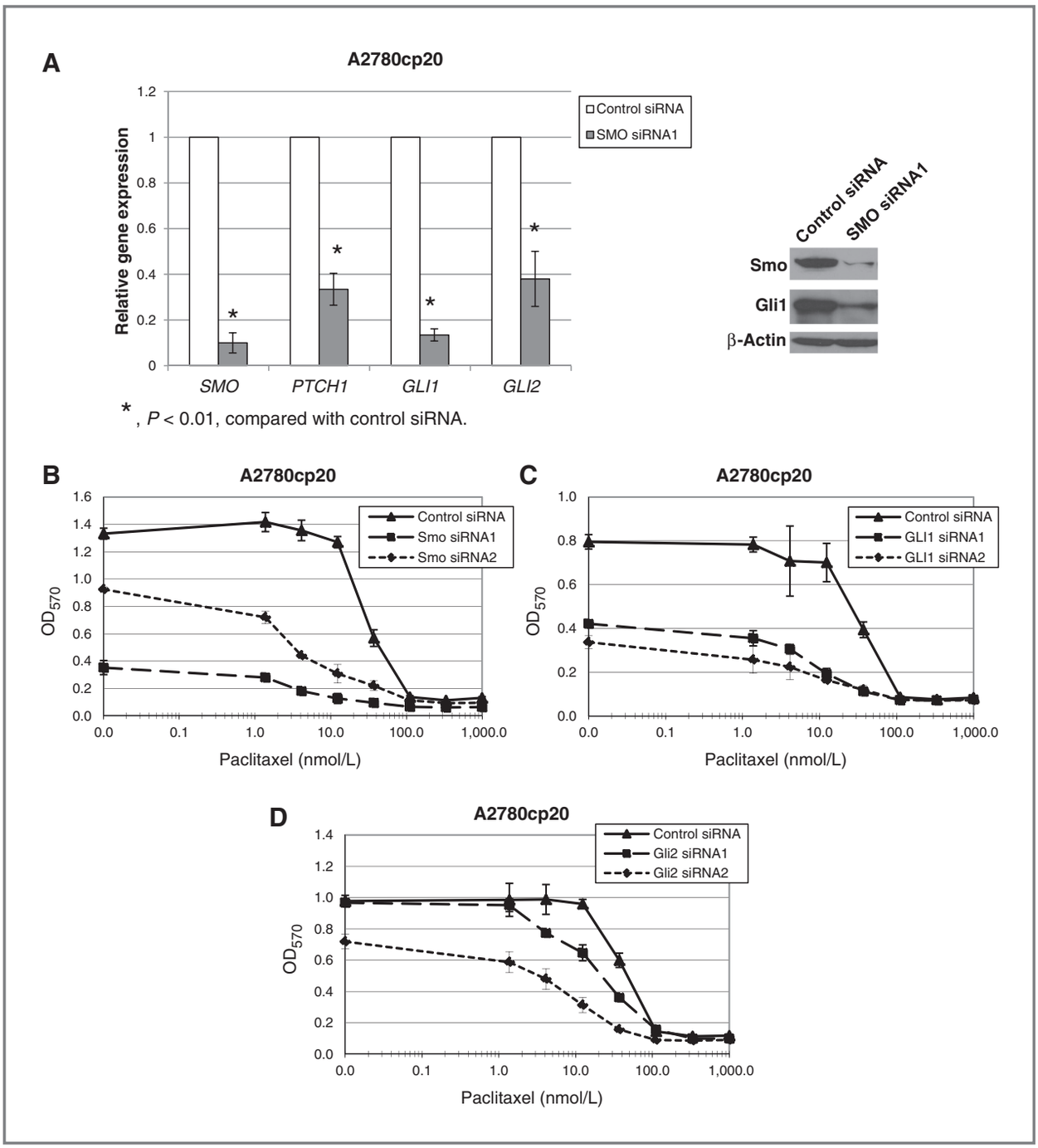

Figure 5. Knockdown of Smo diminishes HH pathway activity, reduces viability, and reverses taxane resistance in ovarian cancer cells. A, A2780cp20 cells were exposed to either control or Smo siRNA for 72 hours and examined for mRNA expression of HH pathway mediators *SMO*, *PTCH1*, *GLI1*, and *GLI2*. *, $P < 0.01$, compared with control siRNA. Protein expression of Smo and Gli (inset) was also measured using Western blot analysis to confirm mRNA results. β-Actin was used as a loading control. A2780cp20 cells were transfected with either control siRNA or 2 distinct siRNA constructs designed against Smo (B), Gli1 (C), or Gli2 (D) and exposed to increasing concentrations of paclitaxel. Cell viability was determined by MTT assay. Data are representative of 3 independent experiments.

cancer develop tumor recurrence and succumb to chemoresistant disease.

Currently, it has not been shown what role HH signaling might play in mediating ovarian cancer chemoresistance, a persistent obstacle in the treatment of this disease. Although the clinical behavior of ovarian cancer suggests that most cancer cells are initially sensitive to chemotherapy, they subsequently either develop resistance or

contain a population of cells that are inherently resistant. The latter hypothesis is consistent with what has become known as tumor initiating cells or CSCs. These CSCs are commonly believed to have enhanced tumorigenicity, differentiation capacity, and resistance to chemotherapy in comparison with non-CSCs. It is because of these features that CSCs have been examined for molecular pathways and markers that could be targeted for therapeutic purposes. Recent studies have suggested that developmental pathways, including HH, play important roles in the maintenance of CSCs (10/11) and that inhibiting these pathways may provide enhanced chemosensitivity when combined with traditional chemotherapies. In our study, we sought to define a role for HH signaling in ovarian cancer chemoresistance. Both *in vitro* and *in vivo*, we observed significant sensitization to paclitaxel after Smo antagonism (LDE225) in taxane-resistant ovarian cancer cells. This sensitization was also present in ALDH-positive cells, a subpopulation of cancer cells with enhanced tumorigenicity and chemoresistance. The mechanism underlying this sensitization seems to involve downregulation of P-glycoprotein (ABCB1/MDR1), a well-characterized mediator of multidrug resistance. By downregulating *MDR1* expression, uptake of paclitaxel by cancer cells would be increased, resulting in a greater response to the chemotherapeutic agent. This mechanism would explain why Smo antagonists did not sensitize chemoresistant cells to carboplatin, because this compound is not a substrate for the P-glycoprotein drug efflux pump. In addition, this model of HH inhibition and chemosensitization agrees with a previous study done by Sims-Mourtada and colleagues, in which it was showed that cyclopamine sensitized prostate cancer cells to a variety of chemotherapy agents *in vitro* (including the taxane docetaxel), through modulation of MDR1 expression (12). The observation that Smo antagonism did not sensitize cells to platinum therapy highlights the specificity of this effect.

Previous studies have showed aberrant expression of the HH pathway in primary specimens of ovarian cancer compared with normal ovarian epithelium (7–9), including a study that found elevated Gli1 expression is associated with decreased survival (9). These studies have also showed decreased ovarian cancer cell growth/viability after treatment with the Smo antagonist cyclopamine, results that our study supports. We have previously shown that *GLI1* and *GLI2* mRNA levels were significantly higher in cancer cells isolated from persistent/chemoresistant tumors compared with those isolated from matched primary tumors (29). Smo expression was also increased (3.7-fold) in persistent tumors; however, this increase was not statistically significant. Patients from whom persistent tumors were obtained had failed both taxane and platinum chemotherapies, making it difficult to determine whether this increase in HH pathway genes is a taxane-specific effect. The *in vitro* data presented in this study, however, would suggest that Smo, as well as Gli1 and Gli2, are associated with taxane resistance. In our initial experiments examining the effects of targeting HH alone, either with Smo antagonists or RNAi, ovarian cancer cell viability was significantly decreased *in vitro*, indicating that the HH pathway is important for ovarian cancer survival. However, this effect did not seem to translate to our xenograft models, in which the Smo antagonist LDE225 had no significant impact on tumor growth when used alone, even in models with relatively high Gli1 expression. These findings suggest that survival pathways are activated in the murine tumor microenvironment that allows resistance to HH antagonist monotherapy. Given the recognized importance of crosstalk between the tumor stromal cells and malignant cells in the HH pathway (6), and the failure of this model to target both murine and human compartments, more efficacy may be noted with monotherapy in humans.

Collectively, the data presented in this study show that increased expression of HH signaling components is associated with taxane resistance, which can be overcome by targeting multiple effectors of the HH signaling pathway. With the ability to identify subsets of patients with cancer with HH pathway overexpression, antagonism of HH signaling in combination with taxane therapy could ultimately provide a useful therapeutic strategy for recurrent, chemoresistant ovarian cancer.

Disclosure of Potential Conflicts of Interest

No potential conflicts of interest were disclosed.

Authors' Contributions

Conception and design: A.D. Steg, C.N. Landen
Development of methodology: A.D. Steg, C.N. Landen
Acquisition of data (provided animals, acquired and managed patients, provided facilities, etc.): A.D. Steg, A.A. Katre, K.S. Bevis, A. Ziebarth, Z. C. Dobbin, M.M. Shah, C.N. Landen
Analysis and interpretation of data (e.g., statistical analysis, biostatistics, computational analysis): A.D. Steg, C.N. Landen
Writing, review, and/or revision of the manuscript: A.D. Steg, A. Ziebarth, R.D. Alvarez, C.N. Landen
Administrative, technical, or material support (i.e., reporting or organizing data, constructing databases): A.A. Katre, Z.C. Dobbin, C.N. Landen
Study supervision: C.N. Landen

Acknowledgments

NVP-LDE225 was kindly provided by Novartis Pharma AG.

Grant Support

This work was supported by the University of Alabama at Birmingham Center for Clinical and Translational Science (5UL1RR025777, C.N. Landen), the Reproductive Scientist Development Program through the Ovarian Cancer Research Fund and the NIH (K12 HD00849, C.N. Landen), and the Gynecologic Cancer Foundation and the Department of Defense Ovarian Cancer Research Academy (OC093443, C.N. Landen).

The costs of publication of this article were defrayed in part by the payment of page charges. This article must therefore be hereby marked *advertisement* in accordance with 18 U.S.C. Section 1734 solely to indicate this fact.

Received December 28, 2011; revised April 3, 2012; accepted April 18, 2012; published OnlineFirst May 2, 2012.

References

1. Bhoola S, Hoskins WJ. Diagnosis and management of epithelial ovarian cancer. Obstet Gynecol 2006;107:1399–410.
2. Hooper JE, Scott MP. Communicating with Hedgehogs. Nat Rev 2005;6:306–17.
3. Ruiz i Altaba A, Mas C, Stecca B. The Gli code: an information nexus regulating cell fate, stemness and cancer. Trends Cell Biol 2007;17: 438–47.
4. Stecca B, Ruiz IAA. Context-dependent regulation of the GLI code in cancer by HEDGEHOG and non-HEDGEHOG signals. J Mol Cell Biol 2010;2:84–95.
5. Pasca di Magliano M, Hebrok M. Hedgehog signalling in cancer formation and maintenance. Nat Rev Cancer 2003;3:903–11.
6. Theunissen JW, de Sauvage FJ. Paracrine Hedgehog signaling in cancer. Cancer Res 2009;69:6007–10.
7. Chen X, Horiuchi A, Kikuchi N, Osada R, Yoshida J, Shiozawa T, et al. Hedgehog signal pathway is activated in ovarian carcinomas, correlating with cell proliferation: it's inhibition leads to growth suppression and apoptosis. Cancer Sci 2007;98:68–76.
8. Bhattacharya R, Kwon J, Ali B, Wang E, Patra S, Shridhar V, et al. Role of hedgehog signaling in ovarian cancer. Clin Cancer Res 2008;14: 7659–66.
9. Liao X, Siu MK, Au CW, Wong ES, Chan HY, Ip PP, et al. Aberrant activation of hedgehog signaling pathway in ovarian cancers: effect on prognosis, cell invasion and differentiation. Carcinogenesis 2009;30: 131–40.
10. Ruiz i Altaba A. Therapeutic inhibition of Hedgehog-GLI signaling in cancer: epithelial, stromal, or stem cell targets? Cancer Cell 2008;14: 281–3.
11. Merchant AA, Matsui W. Targeting Hedgehog—a cancer stem cell pathway. Clin Cancer Res 2010;16:3130–40.
12. Sims-Mourtada J, Izzo JG, Ajani J, Chao KS. Sonic Hedgehog promotes multiple drug resistance by regulation of drug transport. Oncogene 2007;26:5674–9.
13. Singh RR, Kunkalla K, Qu C, Schlette E, Neelapu SS, Samaniego F, et al. ABCG2 is a direct transcriptional target of hedgehog signaling and involved in stroma-induced drug tolerance in diffuse large B-cell lymphoma. Oncogene 2011;30:4874–86.
14. Binns W, James LF, Shupe JL, Everett G. A congenital Cyclopian-type malformation in lambs induced by maternal ingestion of a range plant, *Veratrum californicum*. Am J Vet Res 1963;24:1164–75.
15. Cooper MK, Porter JA, Young KE, Beachy PA. Teratogen-mediated inhibition of target tissue response to Shh signaling. Science 1998;280:1603–7.
16. Chen JK, Taipale J, Cooper MK, Beachy PA. Inhibition of Hedgehog signaling by direct binding of cyclopamine to Smoothened. Gen Dev 2002;16:2743–8.
17. Buonamici S, Williams J, Morrissey M, Wang A, Guo R, Vattay A, et al. Interfering with resistance to smoothened antagonists by inhibition of the PI3K pathway in medulloblastoma. Sci Transl Med 2010;2:51ra70.
18. Louie KG, Behrens BC, Kinsella TJ, Hamilton TC, Grotzinger KR, McKoy WM, et al. Radiation survival parameters of antineoplastic drug-sensitive and -resistant human ovarian cancer cell lines and their modification by buthionine sulfoximine. Cancer Res 1985;45: 2110–5.
19. Landen CN, Kim TJ, Lin YG, Merritt WM, Kamat AA, Han LY, et al. Tumor-selective response to antibody-mediated targeting of alphavbeta3 integrin in ovarian cancer. Neoplasia 2008;10:1259–67.
20. Halder J, Kamat AA, Landen CN Jr, Han LY, Lutgendorf SK, Lin YG, et al. Focal adhesion kinase targeting using *in vivo* short interfering RNA delivery in neutral liposomes for ovarian carcinoma therapy. Clin Cancer Res 2006;12:4916–24.
21. Buick RN, Pullano R, Trent JM. Comparative properties of five human ovarian adenocarcinoma cell lines. Cancer Res 1985;45:3668–76.
22. Moore DH, Allison B, Look KY, Sutton GP, Bigsby RM. Collagenase expression in ovarian cancer cell lines. Gynecol Oncol 1997;65:78–82.
23. Yu D, Wolf JK, Scanlon M, Price JE, Hung MC. Enhanced c-erbB-2/neu expression in human ovarian cancer cells correlates with more severe malignancy that can be suppressed by E1A. Cancer Res 1993;53: 891–8.
24. Duan Z, Feller AJ, Toh HC, Makastorsis T, Seiden MV. TRAG-3, a novel gene, isolated from a taxol-resistant ovarian carcinoma cell line. Gene 1999;229:75–81.
25. Landen CN Jr, Lu C, Han LY, Coffman KT, Bruckheimer E, Halder J, et al. Efficacy and antivascular effects of EphA2 reduction with an agonistic antibody in ovarian cancer. J Natl Cancer Inst 2006;98:1558–70.
26. Steg A, Wang W, Blanquicett C, Grunda JM, Eltoum IA, Wang K, et al. Multiple gene expression analyses in paraffin-embedded tissues by TaqMan low-density array: application to hedgehog and Wnt pathway analysis in ovarian endometrioid adenocarcinoma. J Mol Diagn 2006;8:76–83.
27. Landen CN Jr, Goodman B, Katre AA, Steg AD, Nick AM, Stone RL, et al. Targeting aldehyde dehydrogenase cancer stem cells in ovarian cancer. Mol Cancer Ther 2010;9:3186–99.
28. Kavallaris M. Microtubules and resistance to tubulin-binding agents. Nat Rev Cancer 2010;10:194–204.
29. Steg AD, Bevis KS, Katre AA, Ziebarth A, Dobbin ZC, Alvarez RD, et al. Stem cell pathways contribute to clinical chemoresistance in ovarian cancer. Clin Cancer Res 2012;18:869–81.
30. Silva IA, Bai S, McLean K, Yang K, Griffith K, Thomas D, et al. Aldehyde dehydrogenase in combination with CD133 defines angiogenic ovarian cancer stem cells that portend poor patient survival. Cancer Res 2011;71:3991–4001.

ONCOLOGY

The role of the fallopian tube in the origin of ovarian cancer

Britt K. Erickson, MD; Michael G. Conner, MD; Charles N. Landen Jr, MD

Advanced cases of epithelial ovarian, primary peritoneal, and primary tubal malignancies have a relatively poor prognosis and collectively remain the most deadly of all gynecologic malignancies. Although traditionally thought of as one disease process, ongoing research suggests that there is not 1 single site or cell type from which these cancers arise. A majority of the serous tumors appear to originate from dysplastic lesions in the distal fallopian tube. Therefore, what we have traditionally considered "ovarian" cancer may in fact be tubal in origin. In this article, we will review epithelial ovarian cancer classification and genetics, theories regarding cells of origin with a focus on tubal intraepithelial carcinoma, and implications for prevention and screening.

Key words: ovarian carcinogenesis, TP53 mutation, tubal intraepithelial carcinoma

At the core of understanding any malignancy is determining exactly where the tumor originates. Determination of the cells of origin helps researchers better understand carcinogenesis and subsequently has implications for diagnosing, classifying, treating, and preventing malignancies.

For many epithelial malignancies, the cell of origin is well defined with precursor lesions easily identified. For example, adenocarcinoma of the colon originates in dysplastic lesions within the colonic mucosa, and cervical cancer originates from human papillomavirus (HPV)-infected cells in the cervical transformation zone.[1,2] In contrast to these tumor types, the origins of epithelial ovarian cancer (EOC) are not clearly defined. Moreover, primary peritoneal cancer and primary tubal cancer are typically grouped with EOC despite apparently distinct anatomic locations.

Many theories have been proposed as to the cells of origin and mechanisms of carcinogenesis of ovarian cancer. Traditionally based on epidemiologic studies and pathologic observation, these theories largely assumed that EOC was one disease process. As technology has improved and more sophisticated molecular techniques have developed, we now understand EOC to be a complex and heterogeneous disease process.

Just as endometriosis has been implicated in the development of some endometrioid ovarian adenocarcinomas,[3] emerging data suggest that the fallopian tube may play a critical role in the origin of what has traditionally been classified as serous ovarian cancer. In this review we will discuss proposed mechanisms of "ovarian" carcinogenesis focusing on the emerging role of the fallopian tube in the development of ovarian cancer.

Ovarian cancer classification and genetics

Ovarian cancer is the most lethal gynecologic malignancy. In 2013, it is estimated there will be >22,000 new diagnoses and >14,000 deaths from the disease.[4] Although many improvements have been made in surgical techniques and adjuvant treatment, the prognosis of ovarian cancer is poor, with a 5-year survival rate of only 45%.[5] The majority of ovarian cancer is diagnosed in advanced stages, in part because no screening test exists to detect preinvasive or early-stage disease.

Traditionally, EOC is divided into its histologic subtypes: serous, mucinous, endometrioid, clear cell, transitional cell, or any combination of these (mixed). Serous histology is the most common, representing 70% of EOC.[6] Serous tumors are aggressive tumors that usually present at an advanced stage, and although they commonly respond to surgery and platinum-based chemotherapy, they usually recur.

With improved molecular techniques, it has recently been shown that almost all of these serous tumors harbor TP53 mutations.[7] In fact, serous EOC has the highest frequency of TP53 mutations of any solid cancer.[7] These high-grade, clinically aggressive TP53-mutated serous cancers are now often termed "type 2" EOC.[8] In contrast to type 2 tumors, type 1 tumors often present at earlier stages, have a more indolent clinical course, and rarely have TP53 mutations. Instead, they carry other genetic mutations suggesting distinct pathways of carcinogenesis including phosphatase and tensin homolog (PTEN), v-Ki-ras2 Kirsten rat sarcoma viral oncogene homology (KRAS), and v-raf murine sarcoma viral oncogene homolog B1 (BRAF).[9,10] Although the terminology suggests that low-grade and high-grade EOC may be a spectrum of disease, it is now believed that these represent 2 distinct pathologic entities with different origins, mutations, behavior, and clinical course.[11,12]

From the Divisions of Gynecologic Oncology (Drs Erickson and Landen) and Anatomic Pathology (Dr Conner), University of Alabama at Birmingham, Birmingham, AL.

Received Feb. 14, 2013; revised April 2, 2013; accepted April 8, 2013.

Supported in part by T32-CA091078 (Dr Erickson), and by the University of Alabama at Birmingham Center for Clinical and Translational Science (5UL1RR025777); the Reproductive Scientist Development Program through the Ovarian Cancer Research Fund and the National Institutes of Health (K12 HD00849); and the Department of Defense Ovarian Cancer Research Academy (OC093443) (Dr Landen).

The authors report no conflict of interest.

Reprints: Charles N. Landen Jr, MD, Division of Gynecologic Oncology, University of Alabama at Birmingham, 176F Suite 10250, 619 19 St. S., Birmingham, AL 35294. clanden@uabmc.edu.

0002-9378/$36.00

http://dx.doi.org/10.1016/j.ajog.2013.04.019

Cellular composition of the ovary

The ovary is derived from multiple embryonic structures including the coelomic epithelium, the subcoelomic mesoderm, and the primordial germ cells from the yolk sac endoderm. The rest of the female genital tract, including the fallopian tubes, uterus, cervix, and upper vagina, are derived from the Müllerian ducts. These distinctly different developmental pathways are highlighted by the fact that in patients with müllerian agenesis, the ovaries are usually functional and intact.

As a result of its complex embryologic development, the ovary is composed of various cell types that serve specific structural, hormonal, or reproductive functions. Additionally, each cell type can develop into a distinctly different neoplasm. For example, granulosa cell tumors and fibrothecomas develop from stromal cells, and teratomas and yolk sac tumors originate from germ cells. EOC is frequently thought of in the same manner. However, the ovary does not actually contain a well-differentiated epithelium. Instead, the ovary is covered with a single-cell mesothelial layer, termed the "ovarian surface epithelium" (OSE). This layer derives from the coelomic epithelium, not the Müllerian ducts, and also covers the serosa of the fallopian tubes, uterus, and peritoneal cavity. The cells of the OSE are distinct from other differentiated epithelial layers from a molecular standpoint as well. OSE does not express cancer antigen 125 (CA125) or E-cadherin, which are markers of mature, differentiated epithelium.[13] Instead, OSE expresses the mesenchymal markers vimentin and N-cadherin.[14]

So then, why are these malignancies termed "epithelial," if no true well-differentiated ovarian epithelium exists? On pathologic assessment, these cancers are composed of elements that resemble, both in histology and genetic mutations, Müllerian-derived epithelium of the female genital tract. Specifically, serous tumors resemble the cells found in the tubal epithelium, mucinous tumors resemble the mucin-producing glandular cells of the endocervix, and endometrioid tumors resemble the structure of the endometrium.[15]

Theories of origin of EOC

Early attempts to characterize ovarian carcinogenesis noted a clear relationship between ovulation and risk for ovarian cancer. In 1971, Fathalla[16] first described the incessant ovulation hypothesis. In these studies performed on hens, a high rate of metastatic ovarian adenocarcinoma was noted in the hens that were forced to produce an excessive number of eggs without any breaks in ovulation. It was theorized that OSE cells are damaged during the process of ovulation and then internalized to form cortical inclusion cysts.[16] It was postulated that these cysts then undergo metaplasia to become differentiated Müllerian-like epithelium, eventually becoming dysplastic, and ultimately leading to ovarian carcinoma.[17] This transformation may result from constant exposure to growth factors secreted into the cyst that normally would be lost into the peritoneal cavity when secreted by cells on the ovarian surface.

This theory is further supported by epidemiologic evidence in human beings showing an association between ovulation and an increased risk for ovarian cancer.[18] Women who have breaks in ovulation due to pregnancy and breastfeeding have lower risk of disease.[19,20] Moreover, women who take oral contraceptive pills (OCPs), and therefore have fewer ovulatory cycles, reduce their risk of ovarian cancer by almost 50%.[21,22]

Not all epidemiologic evidence supports the hypothesis that incessant ovulation is the culprit for tumor initiation. For example, women with polycystic ovarian syndrome, who by default ovulate infrequently, are at increased risk for EOC.[23] Although it was initially proposed that OCP use decreased the risk of ovarian cancer by decreasing the number of ovulatory cycles, it appears that the protective effect of OCPs is similar in progesterone-only formulations, which usually do not inhibit ovulation.[24]

Due in some part to the weaknesses identified in the incessant ovulation hypothesis, another theory was proposed regarding how OSE transforms into malignancy. The gonadotropin hypothesis theorizes that overstimulation of OSE via follicle stimulating hormone (FSH) and luteinizing hormone (LH) receptors leads to proliferation and risk for malignant transformation.[25] Pregnant women and women taking OCPs also maintain lower levels of gonadotropins, potentially explaining their decreased risk of EOC. This could also explain the increased risk of EOC in nulliparous women, women with polycystic ovary syndrome, and women with other types of primary infertility who also have increased gonadotropin production. The increased production of gonadotropins in perimenopausal women may also account for the increase in incidence of EOC presenting approximately 10 years after menopause. However, despite these theories, serum FSH and LH levels have not correlated with risk of disease in either premenopausal or postmenopausal women.[26,27] Moreover, although animal studies have shown that gonadotropin exposure promotes tumor growth, no study has been able to convincingly demonstrate malignant transformation of OSE or cortical inclusion cysts with gonadotropin exposure.[9]

Although these and other theories have been proposed to describe how the ovarian mesothelium could undergo metaplasia and dysplasia,[28,29] perhaps the greatest gap in understanding the process of ovarian carcinogenesis from OSE is the identification of a true precursor lesion of high-grade carcinoma within the ovary. Although benign ovarian cystadenomas can progress into a borderline tumor (and later a low-grade malignancy), the progression of low-grade to high-grade serous carcinoma is exceedingly rare.[30] Ovarian endometriosis has been identified within endometrioid and some mixed histology ovarian cancers, however it does not seem to be causative in serous tumors.[31]

In search of a cell of origin

As the complexity and heterogeneity of the origins of ovarian cancer became apparent, it was clear that there is likely not 1 single location or etiology for all types of EOC. For example, endometriosis became more definitively linked to many cases of endometrioid and clear cell EOC. Mucinous tumors were recognized

as often coming from appendiceal or other gastrointestinal origins. Thus the search to identify a precursor lesion of high-grade serous carcinoma intensified.

In 2001, Piek et al[32] reported close examination of tubal segments removed from women undergoing a risk-reducing bilateral salpingo-oophorectomy (BSO). These women had either breast cancer gene (BRCA) mutations or a strong family history of ovarian cancer. Of 12 pathologic specimens examined, 6 had areas of cellular dysplasia noted in the tubal epithelium and 5 additional specimens had hyperplastic lesions. These hyperplastic and dysplastic lesions histologically resembled high-grade serous ovarian cancer, but without invasion.

When larger cohorts of patients with BRCA mutations were studied with thin sectioning and careful analysis of the fallopian tube, it was noted that about 1-5% of patients already had an early tubal malignancy at the time of their risk-reducing surgery.[33,34] The majority of these malignancies had an early intraepithelial component and they all were located in the distal fimbriated end of the fallopian tube. As a result of the detection of occult malignancies and dysplastic lesions, it appeared that these patients had a higher risk for serous carcinoma derived from the fallopian tube, not the ovary.[35] Fallopian tube carcinoma thus became part of the spectrum of BRCA-associated diseases.[32,35]

In 2003, in a letter to the editor, Piek et al[36] synthesized these data and proposed a new hypothesis regarding the relationship between tubal and ovarian serous carcinoma. They hypothesized that most hereditary serous carcinomas originate from the epithelium of the fallopian tube. These tubal epithelial cells are then spilled onto the surface of the ovary and therefore create the appearance of ovarian origin.

Regions of dysplasia within tubal epithelium were termed "tubal intraepithelial carcinoma" (TIC) and in most cases, these areas demonstrated high levels of p53 accumulation (Figure). As noted previously, TP53 mutations are present in almost 100% of type 2 high-grade serous ovarian cancers. The majority of TP53 mutations lead to the production of a nonfunctional p53 protein that accumulates in the cytoplasm of tumor cells. Thus, positive p53 staining is a surrogate for TP53 mutational status. Subsequent studies in patients with BRCA mutations have shown that even "benign" areas of distal tubal epithelium overexpress p53. These areas are termed "p53 signatures"[37] and may represent an even earlier precursor lesion than TIC in the development of high-grade serous carcinomas. The fact that TIC often stains p53 positive and contains such a signature further suggests premalignant changes at the molecular level.[32,38]

FIGURE
Tubal intraepithelial carcinoma

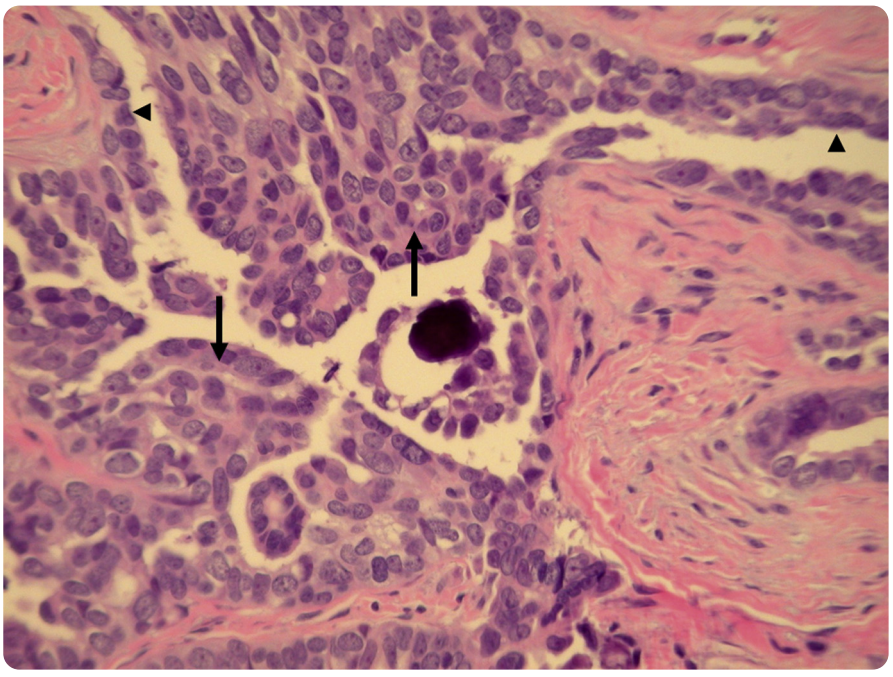

Section of fallopian tube exhibiting tubal intraepithelial carcinoma (*arrows*) and adjacent normal tubal epithelium (*arrowheads*). Note lack of stromal invasion (×200).

Erickson. Fallopian tube in ovarian cancer. Am J Obstet Gynecol 2013.

Beyond BRCA mutation carriers

These patterns of tumor origin were next studied outside of cohorts of BRCA mutation carriers. Kindelberger et al[39] examined the pathology of 55 women with advanced-stage cases of serous ovarian, tubal, or primary peritoneal carcinoma. Tubal specimens were subjected to careful thin sectioning of the fimbriae as well as p53 immunostaining. Surprisingly, 75% of all cases of pelvic serous carcinomas contained areas of TIC. Specifically, 5 of 5 cases of tubal carcinomas contained TIC, 4 of 6 peritoneal carcinomas, and 20 of 30 ovarian carcinomas. The majority (93%) of TIC was identified in the distal tubal fimbriae. In the cases where TIC was identified in a patient with ovarian carcinoma, most ovarian tumors were both bilateral and also intraparenchymal.

These areas of TIC were dissected and subject to p53 immunostaining and specific TP53 mutational analysis. Thousands of distinct TP53 mutations have been described in human cancers and thus a tumor's TP53 mutation can serve as its unique label.[40] In all 5 cases subject to TP53 mutational analysis, the exact same TP53 mutation that was identified in the TIC was identified in the metastatic ovarian tumor, supporting their clonality. Therefore, although the distal fallopian tube cannot be implicated universally in the development of carcinoma, as was suggested in

BRCA mutation carriers, its frequent involvement in what has typically been termed "ovarian" cancer has changed our understanding of the cells of origin of EOC and has prompted further research.

In another large pathological assessment of 52 cases of EOC, Przybycin et al[41] noted a TIC frequency rate of 59% in patients with serous tumors. They also noted that there was no TIC identified in mucinous, endometrioid, or carcinosarcoma histologies.[41] Thus TIC seems to be uniquely associated with the development of serous histology EOC. Kuhn et al[42] further showed the clonality of TIC and the metastatic counterparts in a study that examined the histology of 29 patients with both TIC and high-grade serous tumors. In all, 93% of the paired specimens had identical TP53 mutations in the TIC and metastatic tumor, providing further evidence that these areas of TIC are the precursor lesions for the metastatic tumor.

Unifying the hypotheses

It is clear that TIC is not present in every case of high-grade serous ovarian cancer. Therefore, a dual pathway model for the carcinogenesis of high-grade pelvic serous tumors has been proposed. As evidenced by studies identifying the clonal relationship between TIC and metastatic tumor, the majority of serous tumors likely originate in the distal fallopian tube. These small areas of dysplasia eventually become malignant and, due to their location, metastasize to the ovaries and surrounding pelvic structures. They may also present as fallopian tube cancers or primary peritoneal cancer if there is no significant involvement of the ovary. The remaining cases of serous EOC may have truly ovarian origins. Müllerian epithelium, present on the ovary through either metaplasia of the ovarian mesothelium or ectopic Müllerian tissue (eg, endometriosis and endosalpingiosis) could progress to dysplastic epithelium and eventually lead to malignant transformation.

The role of the fallopian tube in other histologic types of EOC is also being investigated. Based on the areas of papillary tubal hyperplasia noted in patients with low-grade serous tumors, it is hypothesized that these ovarian and extraovarian tumors may also have precursor lesions in the fallopian tube.[43] Moreover, with further study of the ovarian mesothelium and ovarian inclusion cysts, it appears that even inclusion cysts may have fallopian tube origins.[43]

Implications for prevention

Effective cancer screening programs typically require identification of either a precursor lesion or an early-stage malignancy. This is demonstrated most notably in colon, cervix, and breast cancer screening. Unfortunately, without a clear precursor lesion or biomarker, ovarian cancer screening has thus far been unsuccessful in identifying preinvasive or early-stage disease. A large trial studying ultrasonography and serum CA125 for ovarian cancer screening in asymptomatic women was unable to demonstrate efficacy in detecting early-stage disease.[44] Modifications to this approach may demonstrate efficacy, either by following CA125 over time rather than at a single point,[45] or by triaging patients to ultrasound only if the CA125 is consistently elevated.[46] Because the majority of EOC precursor lesions are not harbored within the ovary, it is not surprising that adnexal imaging is of limited utility.

Although no method of TIC detection has been established short of surgical resection, the future holds promise for novel methods of EOC screening and prevention. Models have predicted that TIC and early-stage disease are likely present for at least 4 years before becoming widely metastatic.[47] With improved understanding of TIC and its role in carcinogenesis, there may be opportunities for developing screening methods and biomarker identification.[48-51]

Due to the role of the fallopian tube in EOC, approaches to gynecologic surgery have already begun to shift. Risk-reducing surgery for patients with BRCA mutations currently includes complete excision of the ovaries and fallopian tubes with serial sectioning. With careful excision and close evaluation, rates of occult preinvasive or invasive tubal malignancies in this population may be as high at 10%.[52]

Surgical implications may extend beyond prophylactic surgery for high-risk patients. In the United States, >600,000 hysterectomies are performed each year and about 55% of hysterectomies are accompanied by BSO.[53] There has been considerable debate about the risks and benefits of performing a BSO at the time of hysterectomy. On one hand, the risk of EOC is reduced, but this comes at the expense of the potential risks of cardiovascular disease, osteoporosis, and even cognitive impairment seen with early surgical menopause.[54] In a large analysis of >20,000 patients from the Nurses' Health Study, all-cause mortality as well as cancer mortality both increased in women who received a BSO.[55] This was due primarily to increases in heart disease and stroke. The authors concluded that with an expected lifespan of 35 years after surgery, for every 9 BSOs performed there was 1 additional early death.[55]

With the risks associated with BSO at the time of hysterectomy for benign disease, it is becoming more apparent that it may be clinically prudent to leave the ovaries in place for prolonged hormone exposure. However, because the postreproductive fallopian tube serves little biologic purpose, it may be sensible to perform *only* a salpingectomy at the time of surgery. Although no prospective data support this practice, it follows rationally that this has the potential to reduce the risk of serous carcinoma with little or no increased morbidity.[56] Given that an estimated 80-90% of BRCA-related "ovarian" cancers originate in the fallopian tube, consideration might also be given to performing a risk-reducing salpingectomy in especially young patients.[57]

It has long been noted that bilateral tubal ligation confers some protection toward developing ovarian cancer. Specifically, in a metaanalysis of 13 studies, there was a 34% risk reduction in the development of endometrioid and serous EOC.[58] Proposed mechanisms include effects on ovarian function and mechanical barriers against ascending vaginal carcinogens and ascending proximal tubal or endometrial cells.[59]

Due to their localization at the fimbriated end of the fallopian tube, it is unlikely that tubal ligation surgically removes areas of TIC, however this has not yet been rigorously evaluated.

Finally, there may be opportunities to sample the fallopian tube for preinvasive disease. Kinde et al[60] reported that TP53 mutations can be detected in cervical cytology specimens in 40% of ovarian cancers. Protocols are being evaluated whereby the fallopian epithelial cells are brushed away hysteroscopically for cytologic analysis.

Conclusion

Epithelial ovarian, primary peritoneal, and primary tubal malignancies are a complex and heterogeneous group of tumors that remain the most deadly of all gynecologic malignancies. Ongoing research has confirmed that there is not 1 single site or cell type from which these cancers arise. A majority of serous carcinomas appear to have preinvasive lesions in the distal fallopian tube. This recent finding has shifted the paradigm of ovarian cancer carcinogenesis. Complete bilateral salpingectomy as a risk-reducing strategy in patients with BRCA mutations is an approach worthy of further investigation and it may be reasonable to consider salpingectomy for all patients undergoing hysterectomy for benign disease. As we move forward, new research directed specifically at TIC may provide insight into carcinogenesis, and molecular studies may someday allow for more effective screening strategies. ■

REFERENCES

1. Winawer SJ, Zauber AG, Fletcher RH, et al. Guidelines for colonoscopy surveillance after polypectomy: a consensus update by the US Multi-Society Task Force on Colorectal Cancer and the American Cancer Society. CA Cancer J Clin 2006;56:143-59; quiz 184-5.

2. Pudney J, Quayle AJ, Anderson DJ. Immunological microenvironments in the human vagina and cervix: mediators of cellular immunity are concentrated in the cervical transformation zone. Biol Reprod 2005;73:1253-63.

3. Jiang X, Morland SJ, Hitchcock A, et al. Allelotyping of endometriosis with adjacent ovarian carcinoma reveals evidence of a common lineage. Cancer Res 1998;58:1707-12.

4. Siegel R, Naishadham D, Jemal A. Cancer statistics, 2013. CA Cancer J Clin 2013;63:11-30.

5. Siegel R, Ward E, Brawley O, et al. Cancer statistics, 2011: the impact of eliminating socioeconomic and racial disparities on premature cancer deaths. CA Cancer J Clin 2011;61:212-36.

6. McCluggage WG. Morphological subtypes of ovarian carcinoma: a review with emphasis on new developments and pathogenesis. Pathology 2011;43:420-32.

7. Ahmed AA, Etemadmoghadam D, Temple J, et al. Driver mutations in TP53 are ubiquitous in high grade serous carcinoma of the ovary. J Pathol 2010;221:49-56.

8. Shih IeM, Kurman RJ. Ovarian tumorigenesis: a proposed model based on morphological and molecular genetic analysis. Am J Pathol 2004;164:1511-8.

9. Landen CN Jr, Birrer MJ, Sood AK. Early events in the pathogenesis of epithelial ovarian cancer. J Clin Oncol 2008;26:995-1005.

10. O'Neill CJ, Deavers MT, Malpica A, et al. An immunohistochemical comparison between low-grade and high-grade ovarian serous carcinomas: significantly higher expression of p53, MIB1, BCL2, HER-2/neu, and C-KIT in high-grade neoplasms. Am J Surg Pathol 2005;29:1034-41.

11. Singer G, Shih IeM, Truskinovsky A, et al. Mutational analysis of K-ras segregates ovarian serous carcinomas into two types: invasive MPSC (low-grade tumor) and conventional serous carcinoma (high-grade tumor). Int J Gynecol Pathol 2003;22:37-41.

12. Singer G, Stohr R, Cope L, et al. Patterns of p53 mutations separate ovarian serous borderline tumors and low- and high-grade carcinomas and provide support for a new model of ovarian carcinogenesis: a mutational analysis with immunohistochemical correlation. Am J Surg Pathol 2005;29:218-24.

13. Sundfeldt K, Piontkewitz Y, Ivarsson K, et al. E-cadherin expression in human epithelial ovarian cancer and normal ovary. Int J Cancer 1997;74:275-80.

14. Blaustein A. Peritoneal mesothelium and ovarian surface cells—shared characteristics. Int J Gynecol Pathol 1984;3:361-75.

15. Marquez RT, Baggerly KA, Patterson AP, et al. Patterns of gene expression in different histotypes of epithelial ovarian cancer correlate with those in normal fallopian tube, endometrium, and colon. Clin Cancer Res 2005;11:6116-26.

16. Fathalla MF. Incessant ovulation—a factor in ovarian neoplasia? Lancet 1971;2:163.

17. Auersperg N, Wong AS, Choi KC, et al. Ovarian surface epithelium: biology, endocrinology, and pathology. Endocr Rev 2001;22:255-88.

18. Casagrande JT, Louie EW, Pike MC, et al. "Incessant ovulation" and ovarian cancer. Lancet 1979;2:170-3.

19. Soegaard M, Jensen A, Hogdall E, et al. Different risk factor profiles for mucinous and nonmucinous ovarian cancer: results from the Danish MALOVA study. Cancer Epidemiol Biomarkers Prev 2007;16:1160-6.

20. Rosenblatt KA, Thomas DB. Lactation and the risk of epithelial ovarian cancer: the WHO collaborative study of neoplasia and steroid contraceptives. Int J Epidemiol 1993;22:192-7.

21. Cramer DW, Hutchison GB, Welch WR, et al. Factors affecting the association of oral contraceptives and ovarian cancer. N Engl J Med 1982;307:1047-51.

22. Epithelial ovarian cancer and combined oral contraceptives: the WHO collaborative study of neoplasia and steroid contraceptives. Int J Epidemiol 1989;18:538-45.

23. Schildkraut JM, Schwingl PJ, Bastos E, et al. Epithelial ovarian cancer risk among women with polycystic ovary syndrome. Obstet Gynecol 1996;88:554-9.

24. Rosenberg L, Palmer JR, Zauber AG, et al. A case-control study of oral contraceptive use and invasive epithelial ovarian cancer. Am J Epidemiol 1994;139:654-61.

25. Cramer DW, Welch WR. Determinants of ovarian cancer risk, II: inferences regarding pathogenesis. J Natl Cancer Inst 1983;71:717-21.

26. Arslan AA, Zeleniuch-Jacquotte A, Lundin E, et al. Serum follicle-stimulating hormone and risk of epithelial ovarian cancer in postmenopausal women. Cancer Epidemiol Biomarkers Prev 2003;12:1531-5.

27. Helzlsouer KJ, Alberg AJ, Gordon GB, et al. Serum gonadotropins and steroid hormones and the development of ovarian cancer. JAMA 1995;274:1926-30.

28. Risch HA. Hormonal etiology of epithelial ovarian cancer, with a hypothesis concerning the role of androgens and progesterone. J Natl Cancer Inst 1998;90:1774-86.

29. Ness RB, Cottreau C. Possible role of ovarian epithelial inflammation in ovarian cancer. J Natl Cancer Inst 1999;91:1459-67.

30. Boyd C, McCluggage WG. Low-grade ovarian serous neoplasms (low-grade serous carcinoma and serous borderline tumor) associated with high-grade serous carcinoma or undifferentiated carcinoma: report of a series of cases of an unusual phenomenon. Am J Surg Pathol 2012;36:368-75.

31. Oral E, Ilvan S, Tustas E, et al. Prevalence of endometriosis in malignant epithelial ovary tumors. Eur J Obstet Gynecol Reprod Biol 2003;109:97-101.

32. Piek JM, van Diest PJ, Zweemer RP, et al. Dysplastic changes in prophylactically removed fallopian tubes of women predisposed to developing ovarian cancer. J Pathol 2001;195:451-6.

33. Callahan MJ, Crum CP, Medeiros F, et al. Primary fallopian tube malignancies in BRCA-positive women undergoing surgery for ovarian cancer risk reduction. J Clin Oncol 2007;25:3985-90.

34. Cass I, Holschneider C, Datta N, et al. BRCA-mutation-associated fallopian tube

carcinoma: a distinct clinical phenotype? Obstet Gynecol 2005;106:1327-34.

35. Leeper K, Garcia R, Swisher E, et al. Pathologic findings in prophylactic oophorectomy specimens in high-risk women. Gynecol Oncol 2002;87:52-6.

36. Piek JM, Verheijen RH, Kenemans P, et al. BRCA1/2-related ovarian cancers are of tubal origin: a hypothesis. Gynecol Oncol 2003;90:491.

37. Lee Y, Miron A, Drapkin R, et al. A candidate precursor to serous carcinoma that originates in the distal fallopian tube. J Pathol 2007;211:26-35.

38. Lee Y, Medeiros F, Kindelberger D, et al. Advances in the recognition of tubal intraepithelial carcinoma: applications to cancer screening and the pathogenesis of ovarian cancer. Adv Anat Pathol 2006;13:1-7.

39. Kindelberger DW, Lee Y, Miron A, et al. Intraepithelial carcinoma of the fimbria and pelvic serous carcinoma: evidence for a causal relationship. Am J Surg Pathol 2007;31:161-9.

40. Soussi T, Ishioka C, Claustres M, et al. Locus-specific mutation databases: pitfalls and good practice based on the p53 experience. Nat Rev Cancer 2006;6:83-90.

41. Przybycin CG, Kurman RJ, Ronnett BM, et al. Are all pelvic (nonuterine) serous carcinomas of tubal origin? Am J Surg Pathol 2010;34:1407-16.

42. Kuhn E, Kurman RJ, Vang R, et al. TP53 mutations in serous tubal intraepithelial carcinoma and concurrent pelvic high-grade serous carcinoma–evidence supporting the clonal relationship of the two lesions. J Pathol 2012;226:421-6.

43. Kurman RJ, Vang R, Junge J, et al. Papillary tubal hyperplasia: the putative precursor of ovarian atypical proliferative (borderline) serous tumors, noninvasive implants, and endosalpingiosis. Am J Surg Pathol 2011;35:1605-14.

44. Buys SS, Partridge E, Black A, et al. Effect of screening on ovarian cancer mortality: the prostate, lung, colorectal and ovarian (PLCO) cancer screening randomized controlled trial. JAMA 2011;305:2295-303.

45. Drescher CW, Shah C, Thorpe J, et al. Longitudinal screening algorithm that incorporates change over time in CA125 levels identifies ovarian cancer earlier than a single-threshold rule. J Clin Oncol 2013;31:387-92.

46. Menon U, Gentry-Maharaj A, Hallett R, et al. Sensitivity and specificity of multimodal and ultrasound screening for ovarian cancer, and stage distribution of detected cancers: results of the prevalence screen of the UK collaborative trial of ovarian cancer screening (UKCTOCS). Lancet Oncol 2009;10:327-40.

47. Brown PO, Palmer C. The preclinical natural history of serous ovarian cancer: defining the target for early detection. PLoS Med 2009;6:e1000114.

48. Kuhn E, Kurman RJ, Sehdev AS, et al. Ki-67 labeling index as an adjunct in the diagnosis of serous tubal intraepithelial carcinoma. Int J Gynecol Pathol 2012;31:416-22.

49. Kuhn E, Kurman RJ, Soslow RA, et al. The diagnostic and biological implications of laminin expression in serous tubal intraepithelial carcinoma. Am J Surg Pathol 2012;36:1826-34.

50. Crum CP, McKeon FD, Xian W. The oviduct and ovarian cancer: causality, clinical implications, and "targeted prevention." Clin Obstet Gynecol 2012;55:24-35

51. Chivukula M, Niemeier LA, Edwards R, et al. Carcinomas of distal fallopian tube and their association with tubal intraepithelial carcinoma: do they share a common "precursor" lesion? loss of heterozygosity and immunohistochemical analysis using PAX 2, WT-1, and P53 markers. ISRN Obstet Gynecol 2011;2011:858647.

52. Powell CB, Kenley E, Chen LM, et al. Risk-reducing salpingo-oophorectomy in BRCA mutation carriers: role of serial sectioning in the detection of occult malignancy. J Clin Oncol 2005;23:127-32.

53. Whiteman MK, Hillis SD, Jamieson DJ, et al. Inpatient hysterectomy surveillance in the United States, 2000-2004. Am J Obstet Gynecol 2008;198:34e1-7.

54. Shuster LT, Gostout BS, Grossardt BR, et al. Prophylactic oophorectomy in premenopausal women and long-term health. Menopause Int 2008;14:111-6.

55. Parker WH, Broder MS, Chang E, et al. Ovarian conservation at the time of hysterectomy and long-term health outcomes in the nurses' health study. Obstet Gynecol 2009;113:1027-37.

56. Dietl J, Wischhusen J, Hausler SF. The postreproductive fallopian tube: better removed? Hum Reprod 2011;26:2918-24.

57. Kwon JS, Tinker A, Pansegrau G, et al. Prophylactic salpingectomy and delayed oophorectomy as an alternative for BRCA mutation carriers. Obstet Gynecol 2013;121:14-24.

58. Cibula D, Widschwendter M, Majek O, et al. Tubal ligation and the risk of ovarian cancer: review and meta-analysis. Hum Reprod Update 2011;17:55-67.

59. Cibula D, Widschwendter M, Zikan M, et al. Underlying mechanisms of ovarian cancer risk reduction after tubal ligation. Acta Obstet Gynecol Scand 2011;90:559-63.

60. Kinde I, Bettegowda C, Wang Y, et al. Evaluation of DNA from the Papanicolaou test to detect ovarian and endometrial cancers. Sci Transl Med 2013;5:167ra4.